THESIS

APPLICATION AND EFFECTS OF METAL-BASED THERAPEUTICS ON CANCER CELL LINES IN TISSUE CULTURE

Submitted by

Kameron Leigh Klugh

Department of Chemistry

In partial fulfillment of the requirements

For the Degree of Master of Science

Colorado State University

Fort Collins, Colorado

Summer 2024

Master's Committee:

Advisor: Debbie Crans

Robert Paton
Carmen Menoni

ABSTRACT

APPLICATION AND EFFECTS OF METAL-BASED THERAPEUTICS ON CANCER CELL LINES IN TISSUE CULTURE

In recent years, metal-based drugs have emerged as significant players in the field of therapeutics, leveraging the unique properties of metals to enhance medical treatments. These compounds, incorporating transition metals such as vanadium and platinum, have shown remarkable efficacy in treating various conditions, most notably cancer. The ability of such metals to form complex structures with organic molecules allows for precise targeting and modulation of biological pathways, leading to improved drug efficacy and reduced side effects. Thus, this approach has opened new avenues for designing advanced therapeutics such as vanadium(V) Schiff base catecholate complexes for the treatment of cancer. This thesis aims to explore the potential of non-innocent Schiff base vanadium(V) catecholate complexes as promising agents against glioblastoma, an aggressive form of brain cancer. Two catecholate ligands, 3,5-di-isopropyl catechol and 3,4,6-tri-isopropyl catechol, were synthesized and coordinated to both known and novel vanadium(V) Schiff base scaffolds. Upon testing on glioblastoma T98g cell lines, two of the new complexes, namely [VO(3-tBuHSHED)(TIPCAT)] and [VO(3,5-tBuHSHED)(TIPCAT)], showed remarkable antiproliferative activity. Parallelly, the manuscript delves into the therapeutic applications of platinum-based drugs and how the resistance of platinum-based chemotherapeutics remains a significant challenge. This area of the manuscript identifies the newly discovered role of long non-coding RNAs in platinum-resistance in gastrointestinal cancer treatment. The interaction of these drugs with cellular RNA, in addition to DNA, contributes to this resistance. This manuscript examines the speciation of cisplatin and oxaliplatin, their interactions with DNA and RNA, and the resulting physiological responses of long

non-coding RNAs. It identifies aberrantly expressed lncRNAs in platinum-resistant gastrointestinal cancer cell lines, including those from oral cavity, esophageal, gastric, and colorectal cancers. Despite testing different cell lines, similar patterns of aberrant expression compared to normal cells suggest consistent changes in gene expression and cellular pathways. Understanding these changes may help develop new therapeutic strategies for gastrointestinal cancer patients. Together, the vanadium(V) complex investigations and the new insights into platinum-resistance underscore progress in the understanding of the molecular interactions of metal-based drugs, offering pathways to enhance their efficacy and overcome resistance in cancer therapy.

ACKNOWLEDGEMENTS

I would like to acknowledge the people that have made this work possible and provided support throughout this process. First, I am grateful for my advisor, Debbie Crans, for her mentorship, and to my committee, Rob Paton and Carmen Menoni for their direction and counsel.

I am deeply grateful for my coworkers and collaborators for their assistance in Chapter 1 of this document, namely Andrew Bates, Raley Patch, Emma Scurek, John Manganaro, Aviva Levina, Peter Lay, and Debbie Crans. I express similar gratitude for my collaborators on Chapter 2 of this document, namely V.A. Ferretti, K.A. Doucette, I.E. León, and Debbie Crans.

Of course, I would not have been able to come this far without the unwavering support of my friends and family. I am beyond grateful to have such wonderful people in my corner.

TABLE OF CONTENTS

THESIS INTRODUCTION

Applications of metal-based drugs are increasing as the need for diverse drugs and exploration of new chemical space is becoming important. My master's research focused on two different projects: an experimental chemical project synthesizing vanadium-based anticancer drugs, which is described in chapter 1, and a review focusing on the importance of chemistry and speciation of platinum-based drugs on genetic cellular changes induced by gastric cancers that have been treated with platinum-based drugs, as described in chapter 2.

Chapter 1 discusses the synthesis and characterization of vanadium(V) Schiff base catecholate complexes with isopropyl catechol ligands. This work has been an ongoing project of the Crans group; in the past few years, the group has focused on synthesizing a variety of antiproliferative vanadium(V) Schiff base complexes for the treatment of varying cancers. The complexes contain catecholate ligands that individuals in the group have functionalized with the aim of increasing hydrophobicity, efficacy, and stability of the complexes. My conceptual contribution to the project was to synthesize two isopropyl catechol ligands that would further be used to synthesize vanadium(V) Schiff base complexes that were tested on cell lines for cytotoxicity. The majority of the project was my own work, with help from lab mates and undergraduate students on characterization and certain syntheses. Appendix I includes the biology data not mentioned in the body of the thesis. Appendix II discusses a cobalt Schiff base complex that was synthesized to provide a comparison of a different metal to the vanadium Schiff base complexes.

Chapter 2 explores a more biological project which I undertook because of my focus in chemical biology and medicinal chemistry. It is a review exploring metal-based drugs and discussing how Pt-based drugs induce chemoresistance in gastric cancers with a focus on the effects of long non-coding RNA (lncRNA). The chapter is the contents of a review publication in Coordination Chemistry Reviews. I am the co-first author, and my work focused on converting a

draft by a former Crans group member into a publishable manuscript. Our collaborators focused on summarizing the expression of different lncRNAs. The work is important because it provides insight on how platinum-based drugs affect the cell and expands my knowledge in chemical biology beyond the effects of vanadium compounds. The project described in the first chapter of this thesis has the end goal of being used as chemotherapy, so any insight on the activity of metal-based drugs is useful to the overall project. As a review paper, this chapter takes a slightly different format than that of the first. The chapter is adapted with permissions and can be found published in Coordination Chemistry Reviews, doi: https://doi.org/10.1016/j.ccr.2024.215791

CHAPTER 1: SYNTHESIS AND CHARACTERIZATION OF BIOACTIVE VANADIUM(V) SCHIFF BASE COMPLEXES WITH ISOPROPYL CATECHOL LIGANDS

1.1 Introduction

The treatment of aggressive forms of cancer is a prevailing issue in the world of medicine today. Specifically, the treatment of glioblastoma, an aggressive form of brain cancer that currently has no cure, has been particularly difficult in recent years. The average survival after a diagnosis is typically 15-18 months with an overall five-year survival rate of 10% [1]. The primary issue with the treatment of this type of cancer is an inability of current treatment methods to effectively cross the blood-brain barrier (BBB). For example, the most effective chemotherapy treatments for other drugs, such as cisplatin, have shown little effect on the treatment of glioblastoma. Even when placed directly into the brain within standard delivery systems, the drug is limited by severe systemic toxicity and inefficient penetration of brain tumor tissue [2,3]. Thus, there is a dire need for the development of drugs that can combat the BBB issue and successfully treat cancers such as glioblastoma.

In recent decades, vanadium compounds have been investigated as therapeutic agents for the treatment of a number of human conditions including diabetes, cardiovascular disease, and cancer [4-7]. Most strikingly, this first-row transition metal has made its mark on disease treatment through anti-cancer applications of vanadium(V) coordination complex species [4–12] The complexes work through a plethora of biological mechanisms including signal transduction, phosphatase inhibition, protein transport, and their effects on reactive oxygen species [9,13–18]. Of these complexes, those of particular interest include hydrophobic non-innocent vanadium(V) complexes [19-21]. These complexes can evade the blood-brain barrier issue because hydrophobic complexes interact favorably with hydrophobic cell membranes [19–24] These complexes could be administered through intratumoral injections, a drug delivery mode that is

making headway in clinical trials [19,25]. Moreover, the complexes are favorable because they are designed to break down before diffusion or transport outside the tumor and into contact with healthy tissue [25–31].

Within the realm of vanadium(V) coordination complex species, of most notable activity is a class of species that include a Schiff base backbone and a non-innocent ligand scaffold. These complexes are in oxidation state V and are stabilized by a ternary ligand and coordinated to a redox-active catecholate ligand [32-34]. The complexes are non-innocent because they are redox-active and contain a ligand that can also undergo a redox reaction [32–34]. The Schiff base moiety of these complexes is integral because it makes the metal more active, controls reactivity, and is non-toxic after the scaffold breaks apart [35,36]. In recent studies, Schiff bases have been identified as having anti-cancer activity, so they are a prime choice as a backbone for anti-cancer complexes [19]. In sum, these vanadium(V) Schiff base catecholate complexes are good candidates for intratumoral injections because they are highly effective when given to the tumor but fall apart into non-toxic decomposition products (Fig. 1.1).

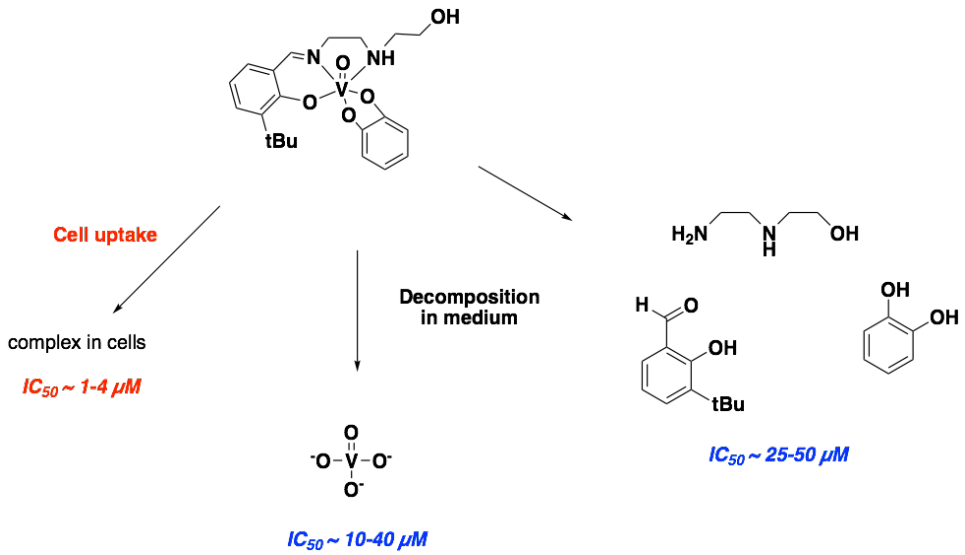

Fig. 1.1. Relative toxicity of a previously studied Vanadium(V) Schiff base complex, where IC_{50} value is a measure at of toxicity, with a low IC_{50} value correlates to high toxicity. The complex exhibits high toxicity when initially given to cells, yet its decomposition products exhibit low toxicity and are not harmful to surrounding healthy cells. These properties give vanadium(V) Schiff base complexes promise as intratumoral injections. *Figure adapted from Levina, et. Al.* [19].

This work intends to build off an ongoing project of the Crans group by identifying the efficacy, hydrophobicity, functionality, stability, and anti-proliferative properties of new vanadium(V) Schiff base catecholate complexes. Previous work has determined compounds that exhibit favorable efficacy in cell culture studies on T98g (human glioblastoma) cells. The compounds have increased hydrolytic stability and include hydrophobic catecholate ligands such as 3,5-di-*tert*-butyl catecholato. One of these compounds, [VO(HSHED)(DTB)] (where HSHED is N-(salicylideneaminato)-N′-(2-hydroxyethyl)-1,2-ethanediamine and DTB is 3,5-di-*tert*-butyl catechol) exhibited the greatest resistance to hydrolysis in cell culture medium ($t_{1/2}$ ~5 min) [37]. Furthermore, this complex exhibited an IC_{50} value of 1-2μm, a relatively low IC_{50} value, especially when compared to lead treatments such as cisplatin [37]. From these studies, we gained structural insight into what is most effective in these types of complexes. Specifically, hydrophobic groups in the form of alkyl substituents such as *tert*-butyl groups on the catecholate ligand grant

complex stability by increasing steric hindrance that protects the V core from hydrolysis. However, these complexes are precarious because their speciation makes it difficult to determine which isomers are responsible for their observed cytotoxicity and hydrolytic stability [38]. Thus, in more recent studies, evidence has pointed to increased efficacy and stability by replacing the HSHED moiety with pyridine-based Schiff bases, such as those containing N-(salicylideneaminato)-2-(2-aminomethylpyridine), abbreviated SALIMP (Fig. 1.2.) or those containing for N-(salicylideneaminato)-2-(2-aminoethylpyridine), abbreviated SALIEP [38]. The SALIMP complexes contain a 5-membered pyridine ring in the ternary Schiff base ligand, whereas the SALIEP complexes contain a 6-membered ring on the Schiff base backbone. These complexes are advantageous to study because the aromatic Schiff base limits the potential number of geometric isomers to two [38]. Of the SALIEP complexes, the one that exhibited the most activity was [VO(SALIEP)(DTB)], with moderate stability in cell culture media and high antiproliferative activity (IC_{50} < 10 μM at 72 hr treatment) in cancer cell lines vs normal cell lines [38]. Although the pyridine of the SALIEP complexes significantly improved hydrolytic stability, their level of cellular uptake could be improved. In light of this, in comparison to the SALIEP series, early studies with the SALIMP complexes report increased hydrolytic stability, increased cellular uptake, and high antiproliferative activity.

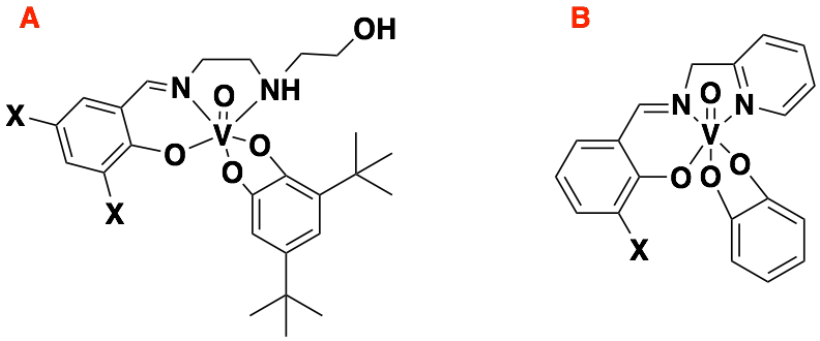

Fig. 1.2. Structure of the current lead compound A, [VO(HSHED)(DTB)] where X represents modification positions on the backbone. The most promising modifications include a *tert*-butyl substituent. Compound B, [VO(SALIMP)(CAT)] (where CAT is catechol), has been successful in recent studies, where X represents a backbone modification position.

Working off the promising results of previous studies, this work intends to combine both ideas of increasing steric effects on the catechol ligand and increasing hydrolytic stability and efficacy of the Schiff base scaffold. To begin, this work presents the synthesis and characterization of two catechols: 3,4,6-tri-isopropyl catechol (abbreviated TIPCAT in structure notation) and 3,5-di-isopropyl catechol (abbreviated DIPCAT in structure notation). Of key interest is the 3,4,6-tri-isopropyl catechol because it presents a novel substitution pattern, giving rise to a new mode of increased steric effects that contribute to hydrolytic stability. This substitution pattern on the catechol includes the 4- and 6- positions, ortho to the coordinating oxygen atoms and near the vanadium core, possibly granting complexes increased stability in aqueous media. These two catechols were coordinated to the most potent Schiff base scaffolds, [VO_2(3,5-tBuHSHED], [VO_2(3-tBuHSHED)], and a novel scaffold, [VO_2(3-OEtSALIMP)]. The known scaffolds were chosen due to their efficacy in previous studies, and the new scaffold was chosen to build off preliminary studies with SALIMP complexes by increasing the hydrophobicity using the pyridine Schiff base backbone and increasing stability using an ethoxy substituent [38]. Ultimately, the goal of both the Schiff base scaffolds and addition of 3,4,6-tri-isopropyl catechol is to increase hydrophobic bulk of the complexes to reduce potential of hydrolysis and increase complex stability

in cell culture media, which is a hydrolytic environment. In addition to the complexes of interest, a range of complexes were synthesized and characterized. They are reported in the experimental section of this manuscript, but not further discussed because the biological measurements have either not been completed or were not significantly relevant to the project. The complexes of interest were tested against a variety of cell lines, primarily T98g cells, human glioblastoma. Thus, this work explores the relationship between structure, cytotoxicity, and hydrophobicity of new complexes in comparison with previously reported V(V) Schiff base complexes.

1.2. Experimental

1.2.1. General Materials. Catechol, 2-propanol, sulfuric acid, 2-(2-aminomethyl)pyridine, 3-ethoxy salicylaldehyde, vanadyl acetylacetone, 3-*tert*-butyl salicylaldehyde, 3,5-di-*tert*-butyl salicylaldehyde, and all organic solvents were purchased from Sigma-Aldrich and used as-is.. Ultrapure Ar (AR UHP300) from Airgas was used to keep inert atmosphere conditions and for degassing solutions. Pre-sterilized media and sterile plasticware used in cell culture studies were purchased from Thermo Fisher Scientific Australia.

1.2.2. General Methods and Instrumentation. The hydrolytic stabililty of the complexes was studied by UV-vis spectroscopy (AvaLight UV-vis/NIR Light Source and AvaSpex-UL S2048 Fiber-Optic Spectrometer).

1.2.3. General Synthesis. [VO_2(3-tBuHSHED)], [VO_2(3,5-tBuHSHED)], [VO_2(Dea-HSHED)] were prepared as reported previously [39]

3,4,6-tri-isopropyl catechol Catechol (2.02g, 20.0 mmol) and 2-propanol (4.59 mL, 60.0 mmol) were stirred together under reflux until a temperature of 58°C was reached. Sulfuric acid (4.26mL, 80.0 mmol) was added dropwise and the reaction was allowed to reflux for 4 hours. The reaction mixture was neutralized with ice water (100mL) and sodium bicarbonate (s), and the organic

phase was extracted with 3x50mL ethyl acetate. The solvent was removed under reduced pressure and the crude product was purified via column chromatography in 10% ethyl acetate: hexanes to yield 1.18g (50%) of 3,4,6-tri-isopropyl catechol as a red solid. R_f=0.66 in 30% ethyl acetate:hexanes. ^{1}H NMR: (400 MHz, Chloroform-d) δ 6.64 (s, 1H), 5.32 (s, 1H), 4.72 (s, 1H), 3.42 – 3.32 (m, 1H), 3.17 (hept, J = 6.5 Hz, 1H), 3.05 (hept, J = 6.9 Hz, 1H), 1.39 (dd, J = 7.1, 0.8 Hz, 6H), 1.27 (dd, J = 6.9, 0.8 Hz, 6H), 1.21 (dd, J = 6.9, 0.8 Hz, 6H). V_{max}/cm^{-1}: 3369 (OH), 2959 (CH), 2928 (CH), 2868 (CH).

3,5-di-isopropyl catechol Catechol (2.02g, 20.0 mmol) and 2-propanol (4.59 mL, 60.0 mmol) were stirred together under reflux until a temperature of 58°C was reached. Sulfuric acid (4.26mL, 80.0 mmol) was added dropwise and the reaction was allowed to reflux for 4 hours. The reaction mixture was neutralized with ice water (100mL) and sodium bicarbonate (s), and the organic phase was extracted with ethyl acetate. The solvent was removed under evaporated pressure and the crude product was purified via column chromatography in 10% ethyl acetate: hexanes to yield 266mg (13%) of 3,5-di-isopropyl catechol as an orange solid. R_f=0.46 in 30% ethyl acetate:hexanes. ^{1}H NMR (400 MHz, Chloroform-*d*) δ 6.63 (d, *J* = 2.1 Hz, 1H), 6.60 (d, *J* = 2.1 Hz, 1H), 4.97 (s, 1H), 4.88 (s, 1H), 3.17 (sept, *J* = 6.9 Hz, 1H), 2.79 (sept, *J* = 7.0 Hz, 1H), 1.26 (d, *J* = 6.8 Hz, 6H), 1.20 (d, *J* = 6.9 Hz, 6H). V_{max}/cm^{-1}: 3282 (OH), 2957 (CH), 2924 (CH), 2868 (CH).

[VO(3-OEtSALIMP)(TIPCAT)] [VO(3-OEtSALIMP)(acac)] (0.42g, 1.00 mmol) and 3,4,6-tri-isopropyl catechol (0.24g, 1.00 mmol) were added to a Schlenk flask with degassed dichloromethane (100mL) under an argon atmosphere. The reaction was refluxed for 1 hour then allowed to cool to room temperature before stirring overnight. The reaction mixture was vacuum filtered, and the remaining residue was dissolved in a minimal amount of acetone and 100mL of

hexanes. The recrystallization mixture was stored overnight in the freezer. The product was isolated via vacuum filtration to yield 0.23g (41%) as a purple solid. ^{1}H NMR (400 MHz, Chloroform-*d*) δ 8.44 (s, 1H), 7.87 (t, *J* = 7.7 Hz, 1H), 7.46 (d, *J* = 8.0 Hz, 1H), 7.40 (t, *J* = 6.5 Hz, 1H), 7.07 (d, *J* = 7.8 Hz, 1H), 7.02 (d, *J* = 7.9 Hz, 2H), 6.63 (t, *J* = 7.8 Hz, 1H), 5.44 (d, *J* = 8.5 Hz, 2H), 4.21 – 3.99 (m, 3H), 1.45 (t, *J* = 7.0 Hz, 1H), 1.21 (t, *J* = 7.1 Hz, 4H), 1.15 (d, *J* = 6.9 Hz, 5H) ^{51}V NMR (105 MHz, DMSO-d_6) δ 424, 438. V_{max}/cm^{-1}: 3053 (coordinate amine), 2900 (CH), 941 (V=O).

[VO(3-OEtSALIMP)(DIPCAT)] [VO(3-OEtSALIMP)(DIPCAT)] was synthesized following the [VO(3-OEtSALIMP)(TIPCAT)] procedure to yield 0.39g (75%) as a purple solid. ^{1}H NMR (400 MHz, DMSO-d_6) δ 8.87 (s, 1H), 8.16 (d, *J* = 6.3 Hz, 1H), 8.12 (d, *J* = 7.7 Hz, 1H), 7.79 (d, *J* = 7.9 Hz, 1H), 7.64 (s, 1H), 7.23 – 7.17 (m, 1H), 7.09 (dd, *J* = 7.8, 1.6 Hz, 1H), 6.73 (t, *J* = 7.8 Hz, 1H), 6.02 (s, 1H), 5.86 (s, 1H), 5.67 (d, *J* = 19.9 Hz, 1H), 5.56 (t, *J* = 19.5 Hz, 2H), 3.96 (q, *J* = 6.8 Hz, 2H), 1.28 (s, 2H), 1.25 (d, *J* = 6.4 Hz, 2H), 1.20 (t, *J* = 7.0 Hz, 5H), 1.07 (s, 7H). ^{51}V NMR (105 MHz, DMSO-d_6) δ 372, 435. V_{max}/cm^{-1}: 3059 (coordinate amine), 2868 (CH), 938 (V=O).

[VO_2(3-tBuHSHED)] 3-tBu-salicylaldehyde (3.12 g, 18.8 mmol) was dissolved in degassed MeOH (50 ml) and added to a solution of N-(2-hydroxyethyl)ethylenediamine (1.9 mL, 18.8 mmol) in degassed MeOH (50 mL). The yellow reaction mixture was refluxed for 2 hours under an argon atmosphere. The mixture was cooled to room temperature and vanadyl sulfate hydrate (4.08 g, 22.6 mmol) dissolved in degassed DI water (20 mL) was added to the reaction slowly over 10 minutes, turning the reaction black. This mixture was allowed to stir for 3 hours under argon. After 3 hours, NaOH (1.51 g, 37.6 mmol) in DI water (30 mL) was added and the resulting mixture was allowed to stir open to air for 12 hours. The reaction was filtered and the resulting yellow-green solid was rinsed with cold methanol (2 x 25 mL) and dried under vacuum for 3 days to yield 4.5 g (72%). ^{1}H NMR (400 MHz, cdcl3) δ 8.19 (s, 1H), 7.51 (dd, J = 7.4, 1.6 Hz, 1H), 7.00 (dd, J = 7.9,

1.7 Hz, 1H), 6.76 (t, J = 7.6 Hz, 1H), 5.03 (s, 1H), 4.86 (t, J = 10.3 Hz, 1H), 4.19 (t, J = 13.3 Hz, 1H), 3.91 (d, J = 12.4 Hz, 1H), 3.77 (dd, J = 4.1, 4.8 Hz, 1H), 3.62 (s, 1H), 3.46 (s, 1H), 3.23 (s, 1H), 3.12 (s, 1H), 2.86 (dd, J = 13.3, 8.7 Hz, 1H), 1.41 (s, 9H). ^{51}V NMR (105 MHz, cdcl3) δ -543.69. λ_{max}/nm ($CHCl_3$): 287.

[VO(3-tBuHSHED)(TIPCAT)] 3,4,6-tri-isopropylcatechol (0.11g, 0.44 mmol) was added to a solution of [VO_2(3-tBuHSHED)] (0.15g, 0.44mmol) and stirred in acetone (50.0mL) for 24 hours under an argon atmosphere. The solvent was then removed under evaporated pressure. The crude substrate was redissolved in a minimal amount of acetone, diluted with pentane, cooled to -78°C, and vacuum filtered. The solvent was removed from the filtrate via evaporated pressure to yield 0.18g (81%) of [VO(3-tBuHSHED)(TIPCAT)] as a purple solid. ^{1}H NMR (400 MHz, DMSO-d_6) δ 8.68 (s, 1H), 8.58 (s, 1H), 7.44 – 7.35 (m, 1H), 7.31 (t, *J* = 8.7 Hz, 1H), 7.24 (q, *J* = 7.7, 6.4 Hz, 1H), 6.64 (q, *J* = 9.1, 7.7 Hz, 1H), 6.56 (t, *J* = 7.5 Hz, 1H), 5.97 (s, 1H), 5.89 (s, 1H), 5.51 (s, 1H), 4.88 – 4.81 (m, 1H), 4.79 (t, *J* = 5.3 Hz, 1H), 4.41 (s, 1H), 4.16 (t, *J* = 12.4 Hz, 1H), 4.07 – 3.89 (m, 2H), 3.82 (p, *J* = 8.3, 6.9 Hz, 1H), 3.73 – 3.61 (m, 1H), 3.59 – 3.44 (m, 2H), 3.13 (s, 1H), 3.11 – 2.95 (m, 2H), 2.88 (dd, *J* = 18.4, 9.1 Hz, 2H), 2.42 (d, *J* = 6.2 Hz, 1H), 1.42 – 1.26 (m, 4H), 1.22 – 0.96 (m, 18H), 0.86 (dd, *J* = 16.0, 6.6 Hz, 3H), 0.65 (d, *J* = 6.8 Hz, 1H). ^{51}V NMR (105 MHz, DMSO-d_6) δ 429, 404, 387. V_{max}/cm^{-1}: 3479 (OH), 3200 (coordinate amine), 2958 (CH), 2925 (CH), 2866 (CH), 921 (V=O).

[VO_2(3,5-tBuHSHED)] [VO_2(3,5-tBuHSHED)] was synthesized following the [VO_2(3-tBuHSHED] procedure to yield 3.7g (60%) as a yellow-green solid. ^{1}H NMR (400 MHz, Chloroform-*d*) δ 8.26 (s, 1H), 7.61 (d, *J* = 2.4 Hz, 1H), 7.04 (d, *J* = 2.5 Hz, 1H), 5.36 (s, 1H), 4.74 (s, 1H), 4.33 – 4.12 (m, 1H), 3.90 (d, *J* = 12.1 Hz, 2H), 3.75 (dd, *J* = 13.7, 4.7 Hz, 1H), 3.49 (d, *J* = 8.7 Hz, 1H), 3.25 (d, *J* = 11.1 Hz, 1H), 3.17 – 3.00 (m, 1H), 2.81 (tt, *J* = 15.4, 7.7 Hz, 1H), 1.44 (s, 9H), 1.33 (s, 10H).

[VO(3,5-tBuHSHED)(TIPCAT)] 3,4,6-tri-isopropylcatechol (0.12g, 0.50 mmol) was added to a solution of [VO_2(3,5-tBuHSHED)] (0.20g, 0.50 mmol) and stirred in acetone (50.0mL) for 24 hours under an argon atmosphere. The solvent was then removed under evaporated pressure. The crude substrate was redissolved in a minimal amount of acetone, diluted with pentane, and cooled to -78°C. The solvent was removed from the filtrate via evaporated pressure to yield 0.17g (68%) [VO(3,5-tBuHSHED)(TIPCAT)] as a purple solid. ^{1}H NMR (400 MHz, DMSO-d_6) δ 8.61 (s, 1H), 7.29 (s, 1H), 4.39 (s, 1H), 4.15 (s, 1H), 3.96 (d, *J* = 14.1 Hz, 1H), 3.79 (d, *J* = 5.4 Hz, 1H), 3.53 (dt, *J* = 24.9, 5.3 Hz, 1H), 3.18 – 3.10 (m, 1H), 3.10 – 2.94 (m, 1H), 2.84 (d, *J* = 13.1 Hz, 1H), 2.42 (s, 1H), 1.39 (s, 1H), 1.34 (d, *J* = 6.9 Hz, 1H), 1.25 (d, *J* = 12.0 Hz, 5H), 1.20 – 1.03 (m, 11H), 1.01 (d, *J* = 6.6 Hz, 1H), 0.87 (d, *J* = 7.7 Hz, 1H), 0.81 (d, *J* = 6.9 Hz, 1H), 0.60 (d, *J* = 6.7 Hz, 1H). ^{51}V NMR (105 MHz, DMSO-d_6) δ 399, 370, 358. V_{max}/cm^{-1}: 3264 (OH), 3100 (coordinate amine), 2956 (CH), 2867 (CH), 937 (V=O).

[VO(3-OEtSALIMP)(acac)] 2-(2-aminomethyl)pyridine (0.91mL, 8.85 mmol) and 3-hydroxy-3-ethoxy benzaldehyde (1.47g, 8.85 mmol) were added to a Schlenk flask with degassed ethanol (32.5mL) and refluxed under an argon atmosphere for 1 hour. In a separate flask, vanadyl acetylacetone (2.34g, 8.85 mmol) was dissolved in degassed ethanol (15.0mL). The initial reaction was cooled to room temperature, combined with the vanadyl acetylacetone solution, and allowed to reflux under an argon atmosphere for 1 hour. The reaction was cooled to room temperature, vacuum filtered, and washed with cold ethanol until the filtrate was colorless. The residue was washed with pentanes and dried to yield 2.95g (80%) of [VO(3-OEtSALIMP)(acac)] as a gold solid. ^{1}H NMR (400 MHz, Chloroform-*d*) δ 15.46 (s, 1H), 5.50 (s, 1H), 4.16 (d, *J* = 7.0 Hz, 1H), 3.72 (s, 1H), 2.24 (s, 1H), 2.05 (s, 7H), 1.44 (t, *J* = 7.0 Hz, 7H), 1.24 (t, *J* = 6.9 Hz, 3H). ^{51}V NMR (105 MHz, Chloroform-*d*) δ -524.

[VO(3-OEtSALIMP)(CAT)] [VO_2(3-OEtSALIMP)] (0.070g, 0.20mmol) and catechol (0.023g, 0.20 mmol) were added to a Schlenk flask with degassed dichloromethane (20mL) under an argon atmosphere. The reaction was refluxed for 1 hour, then allowed to cool to room temperature before stirring overnight. The reaction mixture was vacuum filtered, and the remaining residue was dissolved in a minimal amount of acetone and 100mL of hexanes. The recrystallization mixture was stored overnight in the freezer. The product was isolated via vacuum filtration to yield 18mg (21%) of [VO(3-OEtSALIMP)(CAT)] as a purple solid. ^{1}H NMR (400 MHz, Chloroform-*d*) δ 8.53 (s, 1H), 8.46 (d, *J* = 5.4 Hz, 1H), 7.90 (t, *J* = 7.6 Hz, 1H), 7.49 (d, *J* = 7.8 Hz, 1H), 7.43 (t, *J* = 6.7 Hz, 1H), 7.10 (d, *J* = 7.6 Hz, 1H), 7.06 (d, *J* = 8.0 Hz, 1H), 6.74 (t, *J* = 7.8 Hz, 2H), 5.45 (d, *J* = 18.7 Hz, 1H), 4.18 – 4.03 (m, 2H), 1.57 (s, 2H), 1.27 (t, *J* = 7.0 Hz, 3H). ^{51}V NMR (105 MHz, Chloroform-*d*)) δ 273.75. V_{max}/cm^{-1}: 3053 (coordinate amine), 2957 (CH), 937 (V=O).

[VO(3-OEtSALIMP(TBU)] [VO(3-OEtSALIMP)(acac)] (0.42g, 1.00 mmol) and 4-tertbutyl catechol (0.17g, 1.00 mmol) were added to a Schlenk flask with degassed dichloromethane (100mL) under an argon atmosphere. The reaction was refluxed for 1 hour then allowed to cool to room temperature before stirring overnight. The reaction mixture was vacuum filtered, and the remaining residue was dissolved in a minimal amount of acetone and 100mL of hexanes. The recrystallization mixture was stored overnight in the freezer. The product was isolated via vacuum filtration to yield 0.34g (70%) of [VO(3-OEtSALIMP)TBU)] as a purple solid. ^{1}H NMR (400 MHz, Chloroform-*d*) δ 8.49 (s, 1H), 8.43 (d, *J* = 5.5 Hz, 1H), 7.93 – 7.86 (m, 1H), 7.49 (d, *J* = 7.8 Hz, 1H), 7.47 – 7.41 (m, 1H), 7.08 (d, *J* = 7.6 Hz, 1H), 7.02 (d, *J* = 7.9 Hz, 1H), 6.69 (d, *J* = 7.7 Hz, 1H), 6.62 (d, *J* = 8.7 Hz, 1H), 6.28 (s, 1H), 5.58 – 5.40 (m, 2H), 4.18 – 3.98 (m, 2H), 1.26 (d, *J* = 7.4 Hz, 3H), 1.22 (d, *J* = 7.0 Hz, 3H), 1.19 (s, 5H).^{51}V NMR (105 MHz, Chloroform-*d*) δ 454, 426. V_{max}/cm^{-1}: 3057 (coordinate amine), 2954 (CH), 938 (V=O).

[VO(3-OEtSALIMP)(DTB)] [VO(3-OEtSALIMP)(DTB)] was synthesized following the [VO(3-OEtSALIMP)(TBU)] procedure to yield 0.37mg (69%) as a purple solid. ^{1}H NMR (400 MHz, Chloroform-*d*) δ 8.44 (s, 1H), 8.41 (d, *J* = 5.5 Hz, 1H), 7.88 (td, *J* = 7.7, 1.5 Hz, 1H), 7.47 (d, *J* = 7.9 Hz, 1H), 7.41 (t, *J* = 6.5 Hz, 1H), 7.08 (d, *J* = 7.6 Hz, 1H), 7.01 (dd, *J* = 8.0, 1.6 Hz, 1H), 6.64 (t, *J* = 7.7 Hz, 1H), 6.18 (s, 1H), 5.60 – 5.37 (m, 2H), 4.16 (s, 1H), 4.07 (q, *J* = 8.7, 7.8 Hz, 1H), 1.20 (d, *J* = 6.3 Hz, 9H), 0.99 – 0.80 (m, 1H). ^{51}V NMR (105 MHz, Chloroform-*d*) δ 588, 467. V_{max}/cm^{-1}: 3063 (coordinate amine), 2867 (CH), 940 (V=O).

[VO(dea-HSHED)(DIPCAT)] 3,5-di-isopropyl catechol (0.05g, 0.25 mmol) was added to a solution of [VO_2(dea-HSHED)] and stirred in degassed acetone (25.0mL) under an argon atmosphere for 24 hours. The crude product was isolated by vacuum filtration and excess solvent was removed under evaporated pressure. The crude product was then dissolved in a minimal amount of acetone, diluted with pentane, and cooled to -78°C. The solvent was removed from the filtrate via evaporated pressure to yield 0.06g (22%) of [VO(dea-HSHED)(DIPCAT)] as a purple solid.^{1}H NMR (400 MHz, Chloroform-*d*) δ 8.07 (s, 1H), 7.09 (d, *J* = 8.9 Hz, 1H), 6.25 (s, 1H), 6.21 – 6.04 (m, 3H), 4.11 (d, *J* = 15.0 Hz, 2H), 3.89 (s, 2H), 3.37 (t, *J* = 7.3 Hz, 5H), 2.86 (s, 1H), 1.38 – 1.21 (m, 9H), 1.23 – 1.07 (m, 12H), 0.92 – 0.82 (m, 4H).^{51}V NMR (105 MHz, Chloroform-*d*) δ 323.63.

1.2.4. NMR Spectroscopy. Complexes were characterized using ^{51}V NMR spectroscopy recorded on a Bruker model AVANCE Neo400 spectrometer equipped with a BBFO smart probe and an automated tuning module operated at 101 MHz, as reported previously[40,41] The ^{51}V NMR spectra were acquired with a spectral window of 86,200 Hz, 2048 scans, a 90° pulse, acquisition time of 0.08s, and a 0.01 s relaxation delay as reported previously [42–44] 1D ^{51}V NMR studies were referenced against [VO(HSHED)(DAD)] at -529 ppm. 1D and 2D ^{1}H NMR studies were carried out in organic solvents using a Bruker NEO400 spectrometer operating at

400 MHz at ambient temperature. Chemical shift values are referenced against tetramethyl silane (TMS) and reported in ppm. 1D ^{51}V NMR studies were recorded on a Bruker NEO spectrometer at 105.2 MHz at ambient temperature. Complexes were dissolved in CD_3CN, CD_3OD, or DMSO-d_6.

1.2.5. FTIR Spectroscopy. Spectra were recorded within the range of 600–4,000 cm−1 using a ThermoFisher Scientific Nicolet iS-50 FTIR spectrometer with ATR crystals (diamond, ZnSe and germanium). All samples were characterized on a diamond crystal and the aperture was set to 20. Spectra obtained were an average of 64 scans of the sample.

1.2.6. Cell Culture and Growth Conditions. Human glioblastoma multiforme cell lines (T98G) were purchased from American Type Culture Collection. The cells were cultured in Advanced DMEM, supplemented with L-glutamine (2.00mM) antibiotic-antimycotic mixture (100 U mL^{-1} penicillin, 100mg mL^{-1} streptomycin, and 0.25 mg mL^{-1} amphotericin B), and fetal calf serum (FCS; heat-inactivated; 2% vol). For proliferation and cytotoxicity experiments, cells were seeded in 96-well plates at an initial density of $1.50x10^3$ viable cells per well in 100 *u*L medium and left to attach overnight.

For all cell assays, freshly prepared stock solutions of V(V) complexes in 10.0mM DMSO were used. The solutions were further diluted so that all cell treatments contained 1.00% (vol) of DMSO, low enough to not affect cell growth during assays. Stock solutions of the treatment complexes were diluted with fully supplement cell culture media to the required final concentrations, and the resultant media were added to the cells within 1 min (for fresh solutions) or left in cell culture incubator (310 K, 5% CO_2) for 24 h prior to cell treatments (for aged solutions).

Each treatment was composed of six replicate wells with cells and two background wells without cells but containing the same compounds. After addition of treatment complexes, the plates were incubated for 72 h at 310 K and 5% CO_2, then MTT reagent [1-(4,5-dimethylthiazol-

2-yl)-3,5-diphenylformazan, Sigma M5655] was added (50 *u*L per well of freshly prepared 2.0mg/mL solution in complete medium), and incubation was continued for 4-6 h. Medium was then removed, the blue formazan crystals were dissolved in 0.10mL per well of DMSO, and the absorbance at 600nm was measured with a Victor V3 plate reader. The treatment complexes were applied in a series of nine two-fold dilutions, starting from 100+/- 20 *u*M V plus the vehicle control. The exact V concentrations in the assays were verified by ICP-MS measurements using samples of cell culture media and in calculations of the IC_{50} values. Origin 6.1 software (Microcal Origin, 199) was used for fitting of the experimental data and calculations and IC_{50} value determination. For all assays, consistent results were obtained in at least two independent experiments using passages of cells and varying stock solutions of the treatment complexes[40]

1.3. Results and Discussion

1.3.1. Design of Vanadium Schiff Base Complexes. Here we report the solution characterization and anticancer properties of derivatives of a new class of SALIMP Schiff base V-catecholate complexes with the addition of an ethoxy group on the SALIMP backbone. Additionally, we report the solution characterization and anticancer properties of known vanadium(V) Schiff base backbones with the addition of 3,4,6-tri-isopropyl catechol and 3,5-di-isopropyl catechol. The complexes were developed with the goal of modifying complex stability, hydrophobicity, and redox properties. Most notably, the design goal of the complexes with the 3,4,6-tri-isopropyl catechol was to further protect the vanadium core of the complexes from hydrolysis through adding substituents in the 3 and 6 position, which are closer to the vanadium core. This ligand, with substituents in these key positions, can further act as a “shield” for the vanadium core and contribute to increased hydrolytic stability. Thus, we can compare the complexes with the 3,4,6-tri-isopropyl catechol ligand to the previously reported lead compounds that contain ligands such as 3,5-di-*tert*-butyl catechol and in comparison to complexes with 3,5-di-isopropyl (Fig. 1.3.) [32]. In addition to complexes with the isopropyl catecholate ligands, a

range of compounds have been synthesized and characterized. The biological measurements are not completed, so these complexes are only referred to in the experimental section.

1.3.2. Design of Catechols. Our group has previously reported several catecholate ligands that

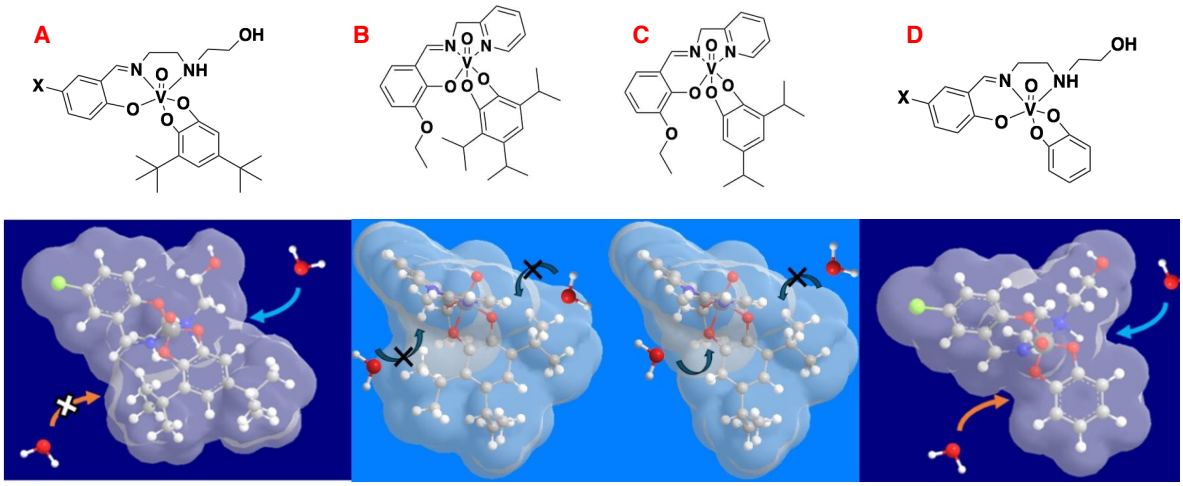

Fig 1.3. Hydrolytic stability model of B. [VO(3-OEtSALIMP)(TIPCAT)] and C. [VO(3-OEtSALIMP)(DIPCAT)] in comparison to previously studied complexes with activity. Complex A, [VO(X-HSHED)(TBU)], where X=Cl, is a known standard of comparison for high hydrolytic stability. Compound D is a comparison model with a catecholate ligand without substituents The model demonstrates that the 3,6-substituted catechol better protects the V core from hydrolysis, as opposed either a 3,5-substituted catechol which only offers protection in one position or a non-substituted catechol which offers no protection. *Figure adapted from Murakami, et. Al* [32].

have different effects on the hydrophobicity, efficacy, and stability of V(V) Schiff base complexes. We have found that increasing the steric bulk of the ligands increases the hydrolytic stability and cytotoxicity of the complexes [32]. Specifically, the most stable and active complexes contain a 3,5-di-*tert*-butyl catechol [45,46]. Moving on these principles, we aimed to design a tri-isopropyl catechol ligand that was more sterically hindered than the 3,5-di-*tert*-butyl catechol and had a novel substitution pattern for our use in these complexes (Fig.1.3.). The synthesis of this ligand co-produced 3,5-di-isopropyl-catechol, so the di-substituted ligand was used in additional syntheses for comparison (Fig.1.4.). The synthesis of the two isopropyl catechols have been

observed in the literature with different synthetic methods and in lower yields, so the yields observed here are a significant improvent [47]. In terms of steric hinderance, we expected to find that the di-substituted catechol would be produced in higher yields, but this is not what is observed. Due to the high equivalence of acid and the fact that an isopropyl substituent is less sterically hindered than substituents such as a *tert*-butyl group, we observe that the tri-substituted catechol is not only produced but is the major product. Herein, we report the solution characterization and anticancer properties of complexes containing these catechols. We found that in comparison to other 3,5-substituted catechol ligands previously synthesized, the 3,5-di-isopropyl catechol did not grant any significant improvements to complex activity. However, we discovered that the 3,4,6-tri-isopropyl catechol increased both the relative stability and efficacy when coordinated to previously synthesized V(V) Schiff base backbones and to the newly synthesized [$VO_2$3-OEtSALIMP] backbones.

1.3.3. Synthesis of V Catecholato Complexes. Four key structures of interest were synthesized

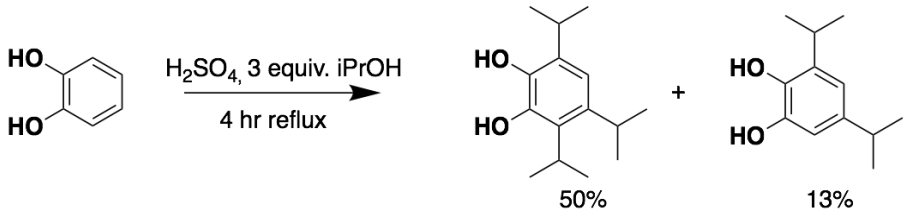

Fig. 1.4**.** Synthetic method for 3,4,6-tri-isopropyl catechol and 3,5-di-isopropyl catechol.

containing the two new isopropyl catecholate ligands (Fig. 1.5.). The [VO_2(3-tBuHSHED)] and [VO_2(3,5-tBuHSHED)] Schiff base V(V) precursor complexes were synthesized using similar procedures as reported in the literature [9,39]. The Schiff bases were first formed by a condensation reaction between 3-*tert*-butyl-2-hydroxybenzaldehyde, 3,5-di-*tert*-butyl-2-hydroxybenzaldehyde, or 4-(diethylamino)salicylaldehyde) (dependent on the reaction) with ethylene diamine. This was reacted in situ with vanadyl sulfate to form the vanadium Schiff base scaffold. The complexes were isolated after the addition of 2 equivalents of NaOH. The desired

catechol was reacted with vanadium Schiff base scaffold to form the desired complexes (Fig. 1.6.). Immediate color change from yellow to purple resulted after the addition of the catechols, due to charge-transfer from the catechol on to the complex. After stirring overnight, the solutions were reduced to dryness. The complexes were recrystallized from a solution of a minimal amount of acetone and hexanes (100mL), vacuum filtered, and isolated from reduced pressure with yields ranging from 70-80%.

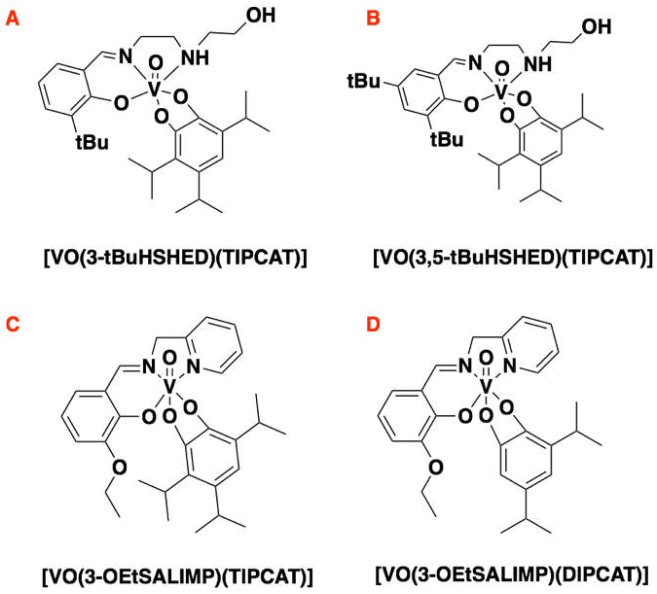

Fig. 1.5. Structures of interest containing 3,4,6-tri-isopropyl catechol and 3,5-di-isopropyl catechol ligands. Structures A and B were chosen based off known high biological activity previously reported by the Crans group [32]. Structures C and D were chosen to test the efficacy of a pyridine-based backbone with a hydrophobic substituent on the ring of the backbone.

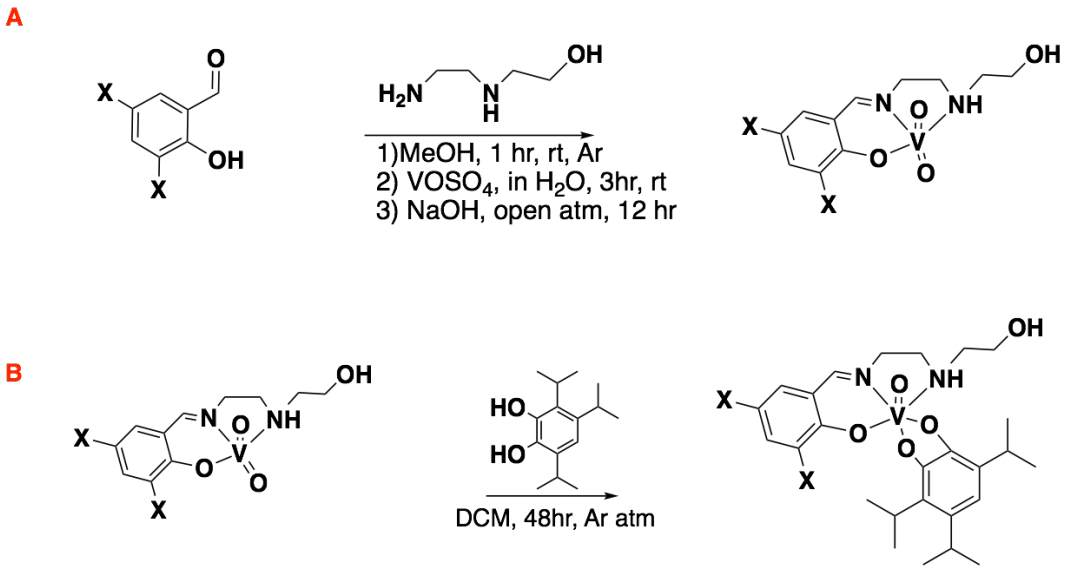

Fig. 1.6. A. Synthesis of [VO_2(X-HSHED)] (X=tBu) precursors according to modified procedures from literature [9]. B. Synthesis of [VO(X-HSHED)(TIPCAT)] (X=tBu) complexes modified from procedures from the literature [9]. The same procedures were used to synthesize complexes with DIPCAT ligands.

The [VO_2(3-OEtSALIMP)] condensation reaction was performed using a similar procedure from the previously reported [VO_2(SALIMP)] precursor (Fig. 1.7.[48]. The Schiff base was first formed by a condensation reaction between 3-ethoxy salicylaldehyde and 2-(2-aminomethyl)pyridine. This was reacted in situ with vanadium acetylacetone to form the V(IV) Schiff base scaffold. This complex was isolated via vacuum filtration and rinsed with cold methanol. The [VO(3-OEtSALIMP)(acac)] complex was reacted with the desired tri-isopropyl catechol or di-isopropyl catechol to form the complexes. Color change from gold to purple happened almost instantly. Following a 1hr reflux and after stirring overnight, the solutions were reduced to dryness and recrystallized from a solution of a minimal amount of acetone and hexanes (100mL). The complexes were vacuum filtered and isolated under reduced pressure with yields between 20-80%. The lower end of yields resulted from running the reactions starting from [VO_2(3-OEtSALIMP)], losing material in the oxidation process.

The complexes were characterized by UV-vis spectroscopy, IR spectroscopy, and multinuclear NMR spectroscopy as described below.

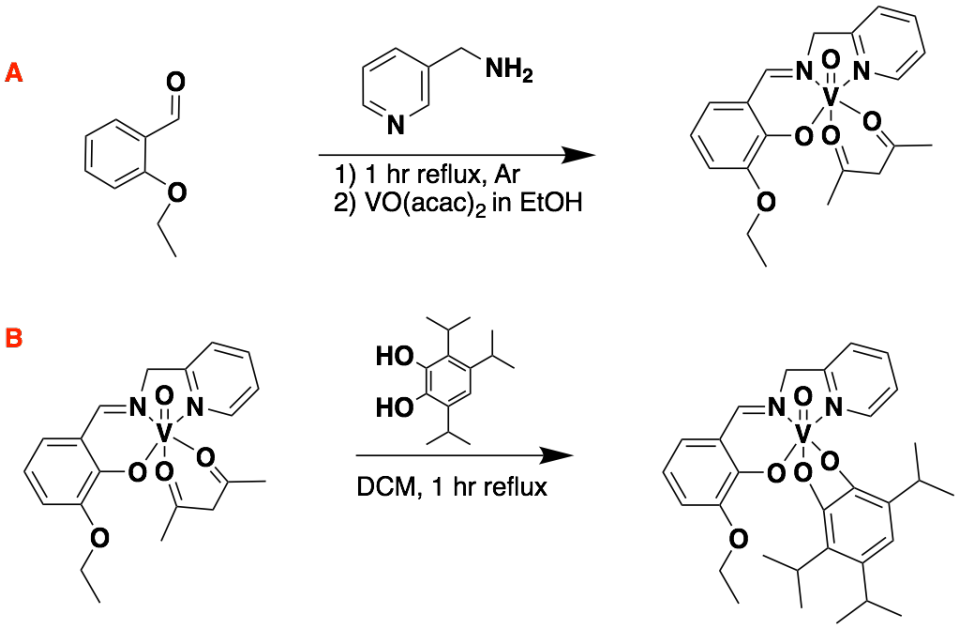

Fig.1.7. A. Synthesis of [VO(3-OEtSALIMP)(acac)] precursor according to modified procedures from the literature [18]. B. Synthesis of [VO(3-OEtSALIMP)(TIPCAT)] according to modified procedures from the literature [18]. The same procedures were used to synthesized complexes with DIPCAT ligands.

1.3.4. Characterization of Vanadium Schiff Base Complexes by FTIR Spectroscopy. FTIR data was collected for the compounds of interest to compliment NMR studies by identifying functional groups and providing a complete molecular picture. In each spectrum, a vibration with a sharp peak was observed between 921-945 cm^{-1} correlating to a vanadyl stretch (V=O), as reported in previous literature [49]. For [VO(3-OEtSALIMP)(DIPCAT)] and [VO(3-OEtSALMP)(TIPCAT)], a coordinate amine peak is observed between 3053-3063 cm^{-1}. This peak was observed near 3100 cm^{-1} in [VO(3-tBuHSHED)(TIPCAT)] and [VO(3,5-tBuHSHED)(TIPCAT]. In all spectra of the compounds of interest, we also observe multiple peaks correlating to alkane stretches around 2900 cm^{-1}.

1.3.5. Lipophilicity and *P* Values. Computational methods were used to determine the hydrophobicity of compounds using Chemicalize software by ChemAxon. The lipophilicity and partition coefficient (logP) of compounds is a critical indicator of membrane permeability and absorption and distribution of a drug [50–52]. Chemicalize has been successful in the analysis of organic compounds. However, the tool is designed for organic molecules and assumes that a covalent bond representation can approximate a coordinate bond in the V complexes. Given that all complexes share similar coordinate bonds, this approach should accurately reflect their relative hydrophobic differences (Table 1.1). The most hydrophobic complex identified is [VO(3,5-tBuHSHED)(TIPCAT)] and the least hydrophobic complex is [VO(3-OEtSALIMP)(DIPCAT)].

Table 1.1. Estimated logP values of [VO(3-tBuHSHED)(TIPCAT)], [VO(3,5-tBuHSHED)(TIPCAT)], [VO(3-OEtSALIMP)(TIPCAT)], and [VO(3-OEtSALIMP)(DIPCAT)] as estimated using Chemicalize software.

Complex	**LogP**
VO(3-tBuHSHED)(TIPCAT)]	**7.4**
[VO(3,5-tBuHSHED)(TIPCAT)]	**9.0**
[VO(3-OEtSALIMP)(TIPCAT)]	**7.6**
[VO(3-OEtSALIMP)(TIPCAT)]	**6.4**

*The calculations required the assumption that a covalent bond description can approximate a V-N coordinate bond in these metal complexes.

1.3.6. Characterization of Vanadium Schiff Base Complexes by ^{51}V and ^{1}H NMR Spectroscopies. ^{51}V NMR spectroscopy was used to confirm that the complexes formed and the VO_2 precursor was fully consumed. Each spectrum was run at a concentration of 10mM. In addition, the spectroscopy was used to demonstrate that isomers may form in solution at ambient temperature. The ^{51}V NMR spectra of solutions of substituted complexes showed more than one signal in either $CDCl_3$ or DMSO-d_6. These signals were not due to impurities or hydrolysis products, as confirmed by running studies in varying solvents. To demonstrate that the signals are a result of isomers, the spectra of 10mM solutions of [VO(3-tBuHSHED)(TIPCAT)] were compared (Fig. 1.8.). As compared to the spectrum in DMSO, the spectrum in $CDCl_3$ contains sharpened peaks, a shift downfield, and the presence of four isomers. Additionally, the spectrum

in $CDCl_3$ showed increased solubility. The change from three to four deshielded peaks between the two solvents indicates that the change in peak number is consistent with interconverting isomers on the NMR time scale rather than from impurities. Next, the broadened peaks in DMSO indicate rapid interconversion between isomers. The multiple isomer peaks are most likely due to the change in position of the catecholate ligand and the ethanol arm connected to the secondary amine. ^{1}H NMR spectra recorded in DMSO-d_6 and $CDCl_3$ support this interpretation (data not shown). Hydrolysis products are not observed in any of the solvents, as indicated by the absence of the [VO_2(3-tBuHSHED)] precursor peak, which is observed at -543 ppm in ^{51}V NMR.

Additionally, this is supported by formation of isomers in a previously reported series of vanadium(V) Schiff base catecholate complexes [32].

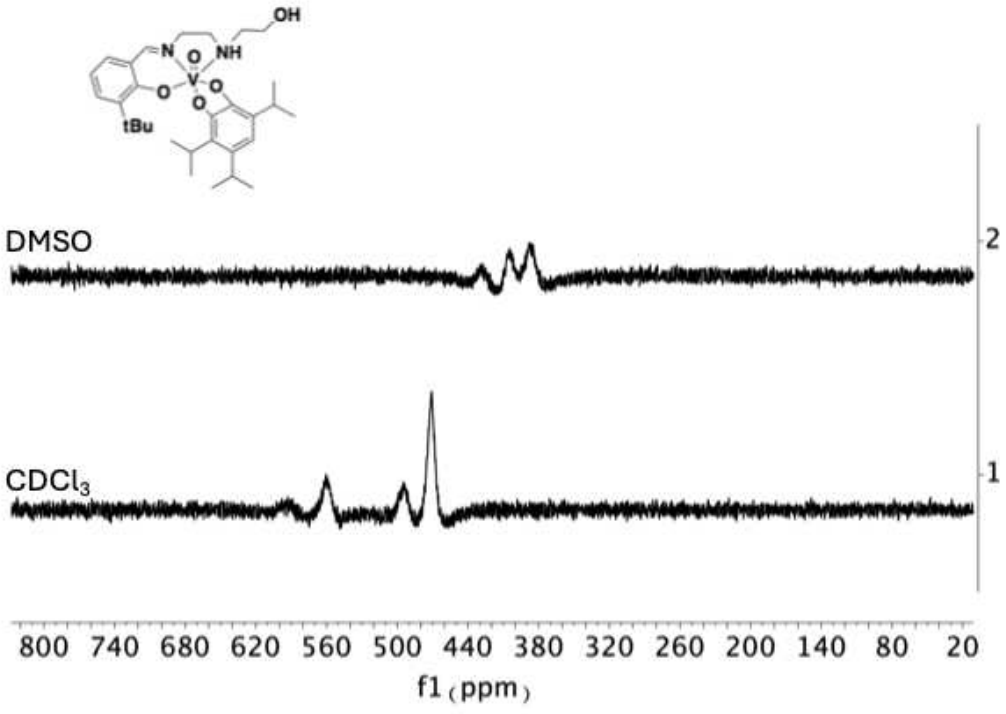

Fig. 1.8. Stacked spectra of [VO(3-tBuHSHED)(TIPCAT)] DMSO and $CDCl_3$, showing the interconversion of isomers in different solvent systems.

In some spectra, minimal amounts of the vanadium precursor were present in $CDCl_3$ at -537 or in DMSO-d_6 at -539. Specifically, the precursor was present in the ^{51}V NMR for [VO(3-OEtSALIMP)(CAT)] and [VO(3-OEtSALIMP)(TIPCAT)]. This can be explained by the complex falling apart in solution. Switching solvents or running samples within an hour of preparation decreases the intensity of the signal seen for the precursor.

For the compounds that showed multiple signals, the ratio and intensities of the different isomer peaks varied depending on the catechol coordinated to the given complex. All the Schiff bases and catechols described in this study have the potential to form isomeric complexes with different geometric isomers. For the pyridine containing Schiff bases, the spectra for [VO(3-OEtSALIMP)(TBU)] showed a major peak at 426 ppm and a minor peak at 454 ppm with a of 7:3 in $CDCl_3$, respectively. The spectra for [VO(3-OEtSALIMP)(DTB)] showed a major peak at 467 ppm and a minor peak at 588 ppm with a relative major to minor ratio of 9:1 in $CDCl_3$. The spectra for [VO(3-OEtSALIMP)(TIPCAT)] showed a major peak at 424 ppm and a minor peak at 438 ppm with a relative major to minor ratio of 5:1 in DMSO-d_6. The spectra for [VO(3-OEtSALIMO)(DIPCAT)] showed a major peak at 372 ppm and a minor peak at 435 ppm with a relative major to minor ratio of 9:1 in DMSO-d_6.

2D NMR spectra were run to determine connectivity and orientation of the complexes containing di-isopropyl catechol ligands and for complexes containing tri-isopropyl catechol ligands. [VO(3-OEtSALIMP)(DIPCAT)] was chosen as the complex containing the di-isopropyl catecholate ligand because of the unique structure of the ethoxy arm on the Schiff base backbone. For comparison, 2Ds were run on [VO(3-OEtSALIMP)(TIPCAT)].

The 2D spectra of [VO(3-OEtSALIMP)(DIPCAT)] (Fig. 1.9.), $^1H-^1H$ 2D NOESY, gave insight into the overall 3D structure of the molecule by showing through-space interactions up to 5 Å of length. Specifically, the $^1H-^1H$ 2D NOESY allowed the determination of the major isomer in solution. The key cross peak between H_b and H_o confirmed that one isopropyl group resided on the 3rd position of the catechol and was closest to the pyridine ring. In addition, the NOE

correlation between the catechol proton H_i and both H_n and H_p confirmed that H_i is positioned in between the two isopropyl groups on the catechol. The second catechol proton H_j only had a NOE correlation with H_n, which is expected since this catechol proton is positioned next to only one isopropyl group and closer to the Schiff base. Additional cross-peaks within the NOESY spectra confirmed the proton assignments on the Schiff base and pyridine ring. Specifically, H_a had correlations with both H_m and H_f which is to be expected. The assignments for the isopropyl groups proved to be difficult due to overlapping peaks in the ^{1}H NMR. In the future, running these spectra in a different solvent could allow for higher resolution and higher confidence in proton assignment in the alkane regions of the ^{1}H NMR (0.5-2 ppm).

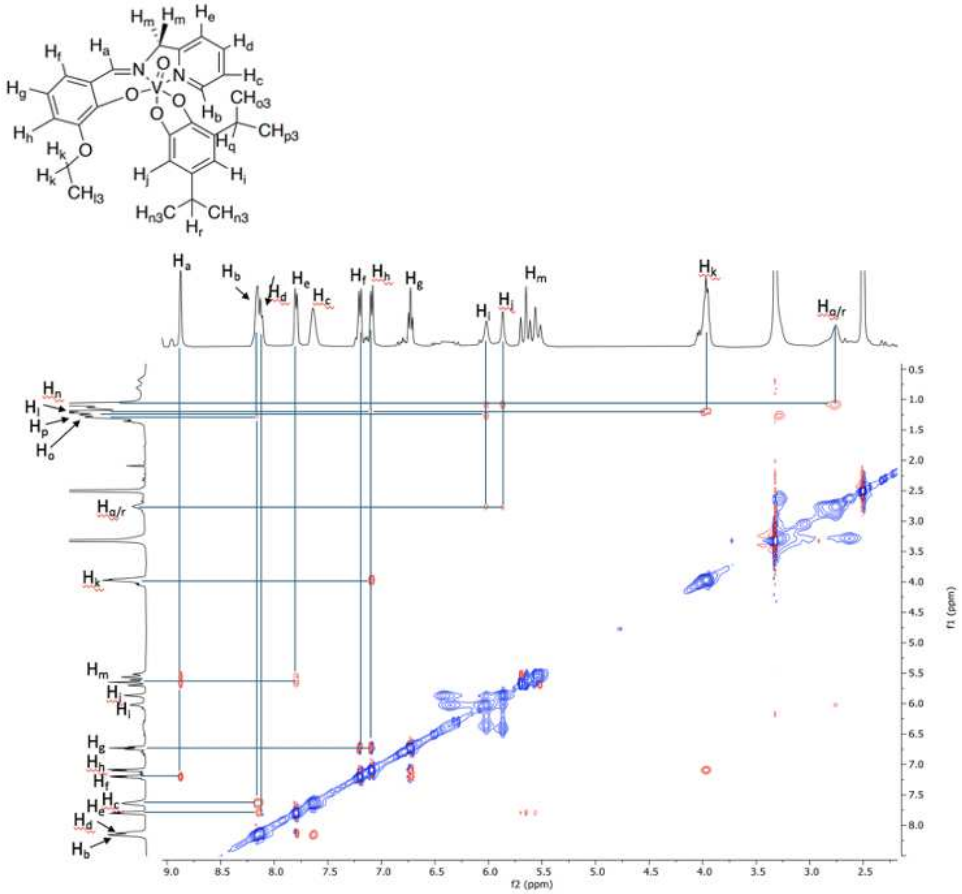

Fig.1.9. NOESY peak assignments of [VO(3-OEtSALIMP)(DIPCAT)].

The 2D spectra of [VO(3-OtSALIMP)(TIPCAT)] (Fig. 1.11), $^1H-^1H$ 2D NOESY, was run in deuterated dimethyl sulfoxide (DMSO).. $^1H-^1H$ 2D NOESY spectra contained key cross peaks that alluded to the major isomer in solution. Similar to the di-isopropyl molecule, H_b had a NOE correlation with H_o of the isopropyl group in the 3rd position of the catechol. Interestingly, the catechol proton (H_i) had a cross peak with Hm but did not see the isopropyl in the 3rd position. This could be due to the isopropyl closest to the pyridine ring residing in a fixed position (farther than 5 Å of length) from the catechol proton. Notably, there was a cross peak between H_k (CH_3 on ethoxy arm) and H_h (proton in Schiff base splitting system). This confirms that the ethoxy arm is oriented upward and closer to the Schiff base than the catechol ligand. Again, the resolution of the alkane region (0.5-2.0 ppm) was compromised due to the overlapping of the isopropyl proton

peaks. This problem holds promise to be amended by using chloroform as the solvent for further NMR spectroscopy.

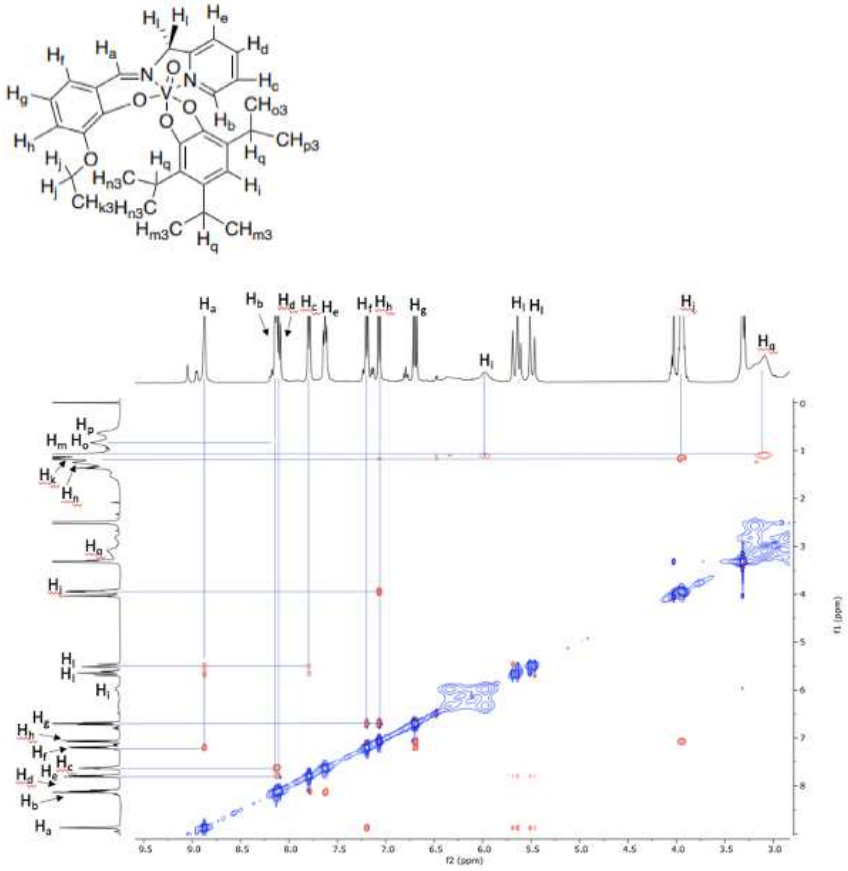

Fig. 1.11. NOESY peak assignments of [VO(3-OEtSALIMP)(TIPCAT)].

1.3.7. Characterization of Vanadium Schiff Base Complexes by UV-Vis Spectroscopy. The UV-Vis show the spectra for the four compounds of interest (Fig. 1.12). The major signals are at 550nm and 900nm. The spectra in DMSO and its stability are shown in addition to the spectra observed in PBS assay solution as a function of time. For [VO(3-tBuHSHED)(TIPCAT)] and [VO(3,5-tBuHSHED)(TIPCAT)], the spectra in DMSO show a slightly lower absorbance compared to the spectra shown after the complexes have been added to the PBS assay solution. This shift is not observed for the other spectra, and the half-life of the other complexes is significantly less.

The relative stabilities of the complexes are compared in Table 1.2, with [VO(3,5-tBuHSHED)(TIPCAT)] and [VO(3,5-tBuHSHED)(TIPCAT)] having the longest lifetimes with half-lives near 24 hr and 48 hr. This is remarkable stability, with complex peaks observed in cell media after 72 hr. Complexes previously synthesized decomposed rapidly, falling apart immediately or within 1 hr. Therefore, these complexes raise questions regarding which is best suited for intratumoral injection, and this remains to be determined.

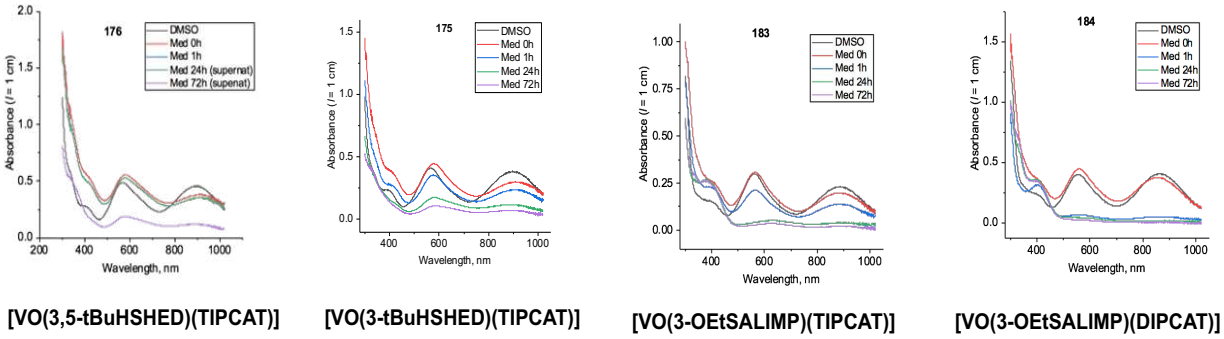

[VO(3,5-tBuHSHED)(TIPCAT)] **[VO(3-tBuHSHED)(TIPCAT)]** **[VO(3-OEtSALIMP)(TIPCAT)]** **[VO(3-OEtSALIMP)(DIPCAT)]**

Fig. 1.12. Decomposition studies of the complexes discussed in this manuscript. The leading compound in terms of stability is [VO(3,5-tBuHSHED)(TIPCAT)], with a determined half-life of the complex is near 48 hours, and some of the complex remaining in solution after 72 hr.

1.3.8. Antiproliferative Activities of Vanadium Schiff Base Complexes. As described previously, experiments were conducted with freshly prepared solutions with the intact Schiff base V(V)-catecholate complexes. Activities were examined initially and after the complexes had been aged in the media for 24 hr to observe decomposition. The experiments enabled determination of the antiproliferative activity of the complexes over time and a better understanding of their stability in culture media. It is critical to see how stable the complexes are over a period of time in biological conditions in order to see their decomposition components. The activity of the complexes containing the TIPCAT and the complex containing DIPCAT were compared to the activity of complexes with previously studied catechol ligands.

The IC_{50} values were measured for T98g in a 72 hr assay of fresh solutions of the complexes and of solutions aged for 24 hr in cell culture media at 310 K (Fig. 1.13). The efficacy of the compounds in terms of IC_{50} value, determined by antiproliferative activity (MTT) assays, are outlined in Table 2. The Table 2 displays the activity in which the complexes were intact initially and after the complexes had been aged in cell media over 72 hr to gain understanding of the toxicity of both the intact complex and the decomposed complex. Thus, the study indicates that the complexes are typically most potent when they are fresh and less potent after they decomposed. The outlier to this pattern is [VO(3,5-tBuHSHED)(TIPCAT)] because it is so stable that it did not decompose to non-toxic ligands after the 72 hr study. The most favorable activity against T98g cells was observed for [VO(3-tBuHSHED)(TIPCAT)] with an IC_{50} value of 1.6 μM in fresh solutions and IC_{50} of 50μM in aged solutions.

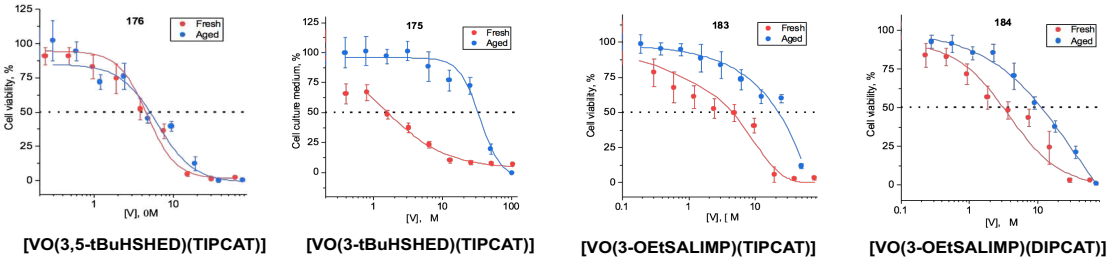

Fig.1.13. Cell viability studies of the complexes described in this manuscript, visualizing both the decomposition of aged and fresh solutions of the complexes in cell culture. The complexes containing the TIPCAT ligand show remarkable efficacy, demonstrating the importance of the modifications of the ligand.

Table 1.2. Comparison of antiproliferative activities of complexes containing tri- and di-isopropyl catechol ligands and those containing di-*tert*-butyl catechol ligands.

Compound	**T98G IC_{50} (μM)(fresh)**	**T98G IC_{50} (μM)(aged)**	**$t_{1/2}$**	**Remaining after 24 hr in media**	**Reference**
[VO(3-tBuHSHED)(TIPCAT)	1.6 ± 0.1	33 ± 3μM	~24hr	yes	This work
[VO(3,5-tBuHSHED)(TIPCAT)	4.7 ± 0.5	5.1 ± 0.6	~48hr	yes	This work
[VO(deaHSHED)(DIPCAT)	5.2 ± 0.7	27 ± 5	<5min	no	This work
[VO(3-OEtSALIMP)(TIPCAT)]	5.0 ± 0.3	22 ± 1	~1hr	no	This work
[VO(3-OEtSALIMP)(DIPCAT)]	3.3 ± 0.7	11 ± 1	<5min	no	This work
[VO(3-OEtSALIMP)(CAT)]	12 ± 2	7.5 ± 1.2	<5min	no	This work
[VO(HSHED)(DTB)]	1.9 ± 0.2	21 ± 1	~5min	no	Murakami, et.al.
[VO(3-OEtSALIMP)(DTB)]	2.6 ± 0.4	12 ± 3	~30min	yes	This work
[VO(3-tBuHSHED)(DTB)]	1.4 ± 0.2	nd	~6hr	no	Manuscript in progress
[VO(3,5-tBuHSHED)(DTB)]	1.5 ± 0.4	nd	~6hr	no	Manuscript in progress

In summary, in comparison to the work that has been previously reported, the new leading complex in terms of stability is [VO(3,5-tBuHSHED)(TIPCAT)], providing valuable insight on how hydrophobic structural modification on the Schiff base backbone in conjunction with the increased hydrophobic bulk on the catecholate ligand grants significant stability improvements to complexes. Next, the leading complex in terms of efficacy and in terms of a candidate for an intratumoral injection is [VO(3-tBuHSHED)(TIPCAT)]. The antiproliferative activity of this complex was far more potent than the others and exhibited a high ratio of aged/fresh IC_{50} ratio, indicating its potential as an intratumoral injection. The [VO_2(3-tBuHSHED)] Schiff base contains a *tert*-butyl group close to the V coordination sphere which increases V catecholate complex stability, and the tri-substituted isopropyl catecholate ligand grants improved stability in comparison to known complexes with sterically hindered ligands such as 3,5-di-*tert*-butylcatechol.

1.4. Conclusions

The treatment of glioblastoma, an aggressive and currently incurable form of brain cancer, remains a significant challenge in the world of medicine today. However, building on previous findings, this work synthesized and characterized catechols and Schiff base vanadium(V) catecholate complexes, focusing on enhancing steric effects and stability. The results indicate that [VO(3-tBuHSHED)(TIPCAT)] exhibits significant antiproliferative activity and prolonged stability in cell culture media in comparison to complexes that have been previously synthesized for this project and that [VO(3,5-tBuHSHED)(TIPCAT)] exhibits significantly higher stability than previously synthesized complexes, making them leading candidates for further investigation. Additionally, the introduction of pyridine-based Schiff bases, specifically [VO_2(3-OEtSALIMP)] has further improved the hydrolytic stability and cellular uptake of vanadium(V) Schiff base complexes.

Future research should continue to explore the structural modifications of Schiff base catecholate ligands to enhance the efficacy of vanadium(V) complexes. Comparative studies with the parent HSHED backbones and tumor-mimetic models will be crucial in advancing these compounds toward clinical applications. Furthermore, ongoing efforts to refine these complexes hold promise for developing effective treatments for glioblastoma and potentially other cancers with similar challenges.

References

[1] Constance Blanchard, 10-year glioblastoma survivor: Get busy living, MD Anderson Cancer Center (2019).

[2] C. Zhang, E.A. Nance, P. Mastorakos, J. Chisholm, S. Berry, C. Eberhart, B. Tyler, H. Brem, J.S. Suk, J. Hanes, Convection enhanced delivery of cisplatin-loaded brain penetrating nanoparticles cures malignant glioma in rats, Journal of Controlled Release 263 (2017) 112–119. https://doi.org/10.1016/j.jconrel.2017.03.007.

[3] J.C. Pessoa, S. Etcheverry, D. Gambino, Vanadium compounds in medicine, Coord Chem Rev 301–302 (2015) 24–48. https://doi.org/10.1016/j.ccr.2014.12.002.

[4] Kate Kostenkova, Kameron Klugh, Debbie C. Crans, Recent Advances of Medicinal Properties of Vanadium Compounds: Cancer and Other Diseases , Metal Ions in Life Sciences (2024).

[5] D.C. Crans, K. Kostenkova, Open questions on the biological roles of first-row transition metals, Commun Chem 3 (2020) 104. https://doi.org/10.1038/s42004-020-00341-w.

[6] Cleave, Crans, The First-Row Transition Metals in the Periodic Table of Medicine, Inorganics (Basel) 7 (2019) 111. https://doi.org/10.3390/inorganics7090111.

[7] A.A. Sharfalddin, I.M. Al-Younis, H.A. Mohammed, M. Dhahri, F. Mouffouk, H. Abu Ali, Md.J. Anwar, K.A. Qureshi, M.A. Hussien, M. Alghrably, M. Jaremko, N. Alasmael, J.I. Lachowicz, A.-H. Emwas, Therapeutic Properties of Vanadium Complexes, Inorganics (Basel) 10 (2022) 244. https://doi.org/10.3390/inorganics10120244.

[8] S. Treviño, A. Díaz, E. Sánchez-Lara, B.L. Sanchez-Gaytan, J.M. Perez-Aguilar, E. González-Vergara, Vanadium in Biological Action: Chemical, Pharmacological Aspects, and Metabolic Implications in Diabetes Mellitus, Biol Trace Elem Res 188 (2019) 68–98. https://doi.org/10.1007/s12011-018-1540-6.

[9] L. Gourdon, K. Cariou, G. Gasser, Phototherapeutic anticancer strategies with first-row transition metal complexes: a critical review, Chem Soc Rev 51 (2022) 1167–1195. https://doi.org/10.1039/D1CS00609F.

[10] K.H. Thompson, J. Lichter, C. LeBel, M.C. Scaife, J.H. McNeill, C. Orvig, Vanadium treatment of type 2 diabetes: A view to the future, J Inorg Biochem 103 (2009) 554–558. https://doi.org/10.1016/j.jinorgbio.2008.12.003.

[11] D. Rehder, The Potentiality Of Vanadium In Medicinal Applications, Future Med Chem 4 (2012) 1823–1837. https://doi.org/10.4155/fmc.12.103.

[12] K. Kostenkova, G. Scalese, D. Gambino, D.C. Crans, Highlighting the roles of transition metals and speciation in chemical biology, Curr Opin Chem Biol 69 (2022) 102155. https://doi.org/10.1016/j.cbpa.2022.102155.

[13] A. Evans, K.A. Kavanagh, Evaluation of metal-based antimicrobial compounds for the treatment of bacterial pathogens, J Med Microbiol 70 (2021). https://doi.org/10.1099/jmm.0.001363.

[14] G.R. Willsky, L.-H. Chi, M. Godzala, P.J. Kostyniak, J.J. Smee, A.M. Trujillo, J.A. Alfano, W. Ding, Z. Hu, D.C. Crans, Anti-diabetic effects of a series of vanadium dipicolinate complexes in rats with streptozotocin-induced diabetes, Coord Chem Rev 255 (2011) 2258–2269. https://doi.org/10.1016/j.ccr.2011.06.015.

[15] H. Sakurai, A New Concept: The Use of Vanadium Complexes in the Treatment of Diabetes Mellitus, The Chemical Record 2 (2002) 237–248. https://doi.org/10.1002/tcr.10029.
[16] R.L. Lucaciu, A.C. Hangan, B. Sevastre, L.S. Oprean, Metallo-Drugs in Cancer Therapy: Past, Present and Future, Molecules 27 (2022) 6485. https://doi.org/10.3390/molecules27196485.
[17] M. Aureliano, N.I. Gumerova, G. Sciortino, E. Garribba, A. Rompel, D.C. Crans, Polyoxovanadates with emerging biomedical activities, Coord Chem Rev 447 (2021) 214143. https://doi.org/10.1016/j.ccr.2021.214143.
[18] M.S. Molinuevo, D.A. Barrio, A.M. Cortizo, S.B. Etcheverry, Antitumoral properties of two new vanadyl(IV) complexes in osteoblasts in culture: role of apoptosis and oxidative stress, Cancer Chemother Pharmacol 53 (2004) 163–172. https://doi.org/10.1007/s00280-003-0708-7.
[19] A. Levina, P.A. Lay, Stabilities and Biological Activities of Vanadium Drugs: What is the Nature of the Active Species?, Chem Asian J 12 (2017) 1692–1699. https://doi.org/10.1002/asia.201700463.
[20] A.A. Sharfalddin, I.M. Al-Younis, H.A. Mohammed, M. Dhahri, F. Mouffouk, H. Abu Ali, Md.J. Anwar, K.A. Qureshi, M.A. Hussien, M. Alghrably, M. Jaremko, N. Alasmael, J.I. Lachowicz, A.-H. Emwas, Therapeutic Properties of Vanadium Complexes, Inorganics (Basel) 10 (2022) 244. https://doi.org/10.3390/inorganics10120244.
[21] D.C. Crans, J.J. Smee, E. Gaidamauskas, L. Yang, The Chemistry and Biochemistry of Vanadium and the Biological Activities Exerted by Vanadium Compounds, Chem Rev 104 (2004) 849–902. https://doi.org/10.1021/cr020607t.
[22] K. Kostenkova, G. Scalese, D. Gambino, D.C. Crans, Highlighting the roles of transition metals and speciation in chemical biology, Curr Opin Chem Biol 69 (2022) 102155. https://doi.org/10.1016/j.cbpa.2022.102155.
[23] V. Ferretti, I. León, An Overview of Vanadium and Cell Signaling in Potential Cancer Treatments, Inorganics (Basel) 10 (2022) 47. https://doi.org/10.3390/inorganics10040047.
[24] A. Levina, D.C. Crans, P.A. Lay, Speciation of metal drugs, supplements and toxins in media and bodily fluids controls in vitro activities, Coord Chem Rev 352 (2017) 473–498. https://doi.org/10.1016/j.ccr.2017.01.002.
[25] R. Zhang, X. Qin, F. Kong, P. Chen, G. Pan, Improving cellular uptake of therapeutic entities through interaction with components of cell membrane, Drug Deliv 26 (2019) 328–342. https://doi.org/10.1080/10717544.2019.1582730.
[26] J.H. Newman, C.B. Chesson, N.L. Herzog, P.K. Bommareddy, S.M. Aspromonte, R. Pepe, R. Estupinian, M.M. Aboelatta, S. Buddhadev, S. Tarabichi, M. Lee, S. Li, D.J. Medina, E.F. Giurini, K.H. Gupta, G. Guevara-Aleman, M. Rossi, C. Nowicki, A. Abed, J.W. Goldufsky, J.R. Broucek, R.E. Redondo, D. Rotter, S.R. Jhawar, S.-J. Wang, F.J. Kohlhapp, H.L. Kaufman, P.G. Thomas, V. Gupta, T.M. Kuzel, J. Reiser, J. Paras, M.P. Kane, E.A. Singer, J. Malhotra, L.K. Denzin, D.B. Sant'Angelo, A.B. Rabson, L.Y. Lee, A. Lasfar, J. Langenfeld, J.M. Schenkel, M.J. Fidler, E.S. Ruiz, A.L. Marzo, J.S. Rudra, A.W. Silk, A. Zloza, Intratumoral injection of the seasonal flu shot converts immunologically cold

tumors to hot and serves as an immunotherapy for cancer, Proceedings of the National Academy of Sciences 117 (2020) 1119–1128. https://doi.org/10.1073/pnas.1904022116.
[27] J. Kamta, M. Chaar, A. Ande, D.A. Altomare, S. Ait-Oudhia, Advancing Cancer Therapy with Present and Emerging Immuno-Oncology Approaches, Front Oncol 7 (2017). https://doi.org/10.3389/fonc.2017.00064.
[28] A. Levina, P.A. Lay, Stabilities and Biological Activities of Vanadium Drugs: What is the Nature of the Active Species?, Chem Asian J 12 (2017) 1692–1699. https://doi.org/10.1002/asia.201700463.
[29] D.C. Crans, L. Henry, G. Cardiff, B.I. Posner, 8. DEVELOPING VANADIUM AS AN ANTIDIABETIC OR ANTICANCER DRUG: A CLINICAL AND HISTORICAL PERSPECTIVE, in: Essential Metals in Medicine: Therapeutic Use and Toxicity of Metal Ions in the Clinic, De Gruyter, 2019: pp. 203–230. https://doi.org/10.1515/9783110527872-008.
[30] L.M.A. Lima, H. Murakami, D.J. Gaebler, W.E. Silva, M.F. Belian, E.C. Lira, D.C. Crans, Acute Toxicity Evaluation of Non-Innocent Oxidovanadium(V) Schiff Base Complex, Inorganics (Basel) 9 (2021) 42. https://doi.org/10.3390/inorganics9060042.
[31] O. Hamid, R. Ismail, I. Puzanov, Intratumoral Immunotherapy—Update 2019, Oncologist 25 (2020) e423–e438. https://doi.org/10.1634/theoncologist.2019-0438.
[32] H.A. Murakami, C. Uslan, A.A. Haase, J.T. Koehn, A.P. Vieira, D.J. Gaebler, J. Hagan, C.N. Beuning, N. Proschogo, A. Levina, P.A. Lay, D.C. Crans, Vanadium Chloro-Substituted Schiff Base Catecholate Complexes are Reducible, Lipophilic, Water Stable, and Have Anticancer Activities, Inorg Chem 61 (2022) 20757–20773. https://doi.org/10.1021/acs.inorgchem.2c02557.
[33] D.C. Crans, J.J. Smee, E. Gaidamauskas, L. Yang, The Chemistry and Biochemistry of Vanadium and the Biological Activities Exerted by Vanadium Compounds, Chem Rev 104 (2004) 849–902. https://doi.org/10.1021/cr020607t.
[34] W. Kaim, B. Schwederski, Non-innocent ligands in bioinorganic chemistry—An overview, Coord Chem Rev 254 (2010) 1580–1588. https://doi.org/10.1016/j.ccr.2010.01.009.
[35] M.S. More, P.G. Joshi, Y.K. Mishra, P.K. Khanna, Metal complexes driven from Schiff bases and semicarbazones for biomedical and allied applications: a review, Mater Today Chem 14 (2019) 100195. https://doi.org/10.1016/j.mtchem.2019.100195.
[36] S. Ren, R. Wang, K. Komatsu, P. Bonaz-Krause, Y. Zyrianov, C.E. McKenna, C. Csipke, Z.A. Tokes, E.J. Lien, Synthesis, Biological Evaluation, and Quantitative Structure−Activity Relationship Analysis of New Schiff Bases of Hydroxysemicarbazide as Potential Antitumor Agents, J Med Chem 45 (2002) 410–419. https://doi.org/10.1021/jm010252q.
[37] J. Manganaro, A. Levina, P.A. Lay, D.C. Crans, Potential Applications of Vanadium-Based Anticancer Drugs for Intratumoral Injections, in: Biosystems in Toxicology and Pharmacology – Current Challenges, MDPI, Basel Switzerland, 2022: p. 10. https://doi.org/10.3390/BiTaP-12783.
[38] K. Kostenkova, A. Levina, D.A. Walters, H.A. Murakami, P.A. Lay, D.C. Crans, Vanadium(V) Pyridine-Containing Schiff Base Catecholate Complexes are Lipophilic, Redox-Active and Selectively Cytotoxic in Glioblastoma (T98G) Cells, Chemistry – A European Journal 29 (2023). https://doi.org/10.1002/chem.202302271.

[39] Kate Kostenkova, John Manganaro, Andrew Bates, Skyler Markham, Kameron Klugh, Heide Murakami, Debbie C. Crans, Vanadium Compounds and Methods of Making and Using Thereof , 10975-043US1, 2023.

[40] E. Griffin, A. Levina, P.A. Lay, Vanadium(V) tris-3,5-di-tert-butylcatecholato complex: Links between speciation and anti-proliferative activity in human pancreatic cancer cells, J Inorg Biochem 201 (2019) 110815. https://doi.org/10.1016/j.jinorgbio.2019.110815.

[41] H. Malke, J. SAMBROCK, E. F. FRITSCH and T. MANIATIS, Molecular Cloning, A Laboratory Manual (Second Edition), Volumes 1, 2 and 3. 1625 S., zahlreiche Abb. und Tab. Cold Spring Harbor 1989. Cold Spring Harbor Laboratory Press. $ 115.00. ISBN: 0-87969-309-6, J Basic Microbiol 30 (1990) 623–623. https://doi.org/10.1002/jobm.3620300824.

[42] P.B. Chatterjee, O. Goncharov-Zapata, L.L. Quinn, G. Hou, H. Hamaed, R.W. Schurko, T. Polenova, D.C. Crans, Characterization of Noninnocent Metal Complexes Using Solid-State NMR Spectroscopy: *o* -Dioxolene Vanadium Complexes, Inorg Chem 50 (2011) 9794–9803. https://doi.org/10.1021/ic200046k.

[43] M. Aureliano, N.I. Gumerova, G. Sciortino, E. Garribba, C.C. McLauchlan, A. Rompel, D.C. Crans, Polyoxidovanadates' interactions with proteins: An overview, Coord Chem Rev 454 (2022) 214344. https://doi.org/10.1016/j.ccr.2021.214344.

[44] D.C. Crans, P.K. Shin, Characterization of Vanadium(V) Complexes in Aqueous Solutions: Ethanolamine- and Glycine-Derived Complexes, J Am Chem Soc 116 (1994) 1305–1315. https://doi.org/10.1021/ja00083a016.

[45] A. Levina, A. Pires Vieira, A. Wijetunga, R. Kaur, J.T. Koehn, D.C. Crans, P.A. Lay, A Short-Lived but Highly Cytotoxic Vanadium(V) Complex as a Potential Drug Lead for Brain Cancer Treatment by Intratumoral Injections, Angewandte Chemie International Edition 59 (2020) 15834–15838. https://doi.org/10.1002/anie.202005458.

[46] D.C. Crans, J.T. Koehn, S.M. Petry, C.M. Glover, A. Wijetunga, R. Kaur, A. Levina, P.A. Lay, Hydrophobicity may enhance membrane affinity and anti-cancer effects of Schiff base vanadium(<scp>v</scp>) catecholate complexes, Dalton Transactions 48 (2019) 6383–6395. https://doi.org/10.1039/C9DT00601J.

[47] T. N. Kocherova, N. O. Druzhkov, A. S. Shavyrin, M. V. Arsenyev, E. V. Baranov, V. A. Kuropatov, V. K. Cherkasov, Isopropyl-substituted o-benzoquinones and oxanthrenequinones. Effect of steric shielding of alkyl substituents on reactivity, Russian Chemical Bulletin 70 (2021) 916–924.

[48] S. Markham, Variations in Pyridine-containing Schiff-base Ligand leads to increased Stability and Biological Activity for an Anticancer Vanadium Catecholate complex, n.d.

[49] S.R. Cooper, Y.B. Koh, K.N. Raymond, Synthetic, structural, and physical studies of bis(triethylammonium) tris(catecholato)vanadate(IV), potassium bis(catecholato)oxovanadate(IV), and potassium tris(catecholato)vanadate (III), J Am Chem Soc 104 (1982) 5092–5102. https://doi.org/10.1021/ja00383a016.

[50] Atomic Physiochemical Parameters for Three Dimensional Structure Directed Quantitative Structure-Activity Relationships., (n.d.).

[51] O. Silakari, P.K. Singh, ADMET tools: Prediction and assessment of chemical ADMET properties of NCEs, in: Concepts and Experimental Protocols of Modelling and Informatics

in Drug Design, Elsevier, 2021: pp. 299–320. https://doi.org/10.1016/B978-0-12-820546-4.00014-3.

[52] S.D. Krämer, H.E. Aschmann, M. Hatibovic, K.F. Hermann, C.S. Neuhaus, C. Brunner, S. Belli, When barriers ignore the “rule-of-five,” Adv Drug Deliv Rev 101 (2016) 62–74. https://doi.org/10.1016/j.addr.2016.02.001.

CHAPTER 2: GASTROINTESTINAL CANCER CELLS WITH Pt-RESISTANCE AND RELATIONSHIP WITH ABERRANT EXPRESSION OF LONG NON-CODING RNAs

2.1. Introduction

Gastrointestinal cancer (GIC) involves a diverse class of tumors that affect the digestive system including cancers of the oral cavity, esophagus, stomach, small intestine, colon, rectum, and anus [1]. According to statistics confirmed by the International Agency for Research on Cancer (IARC), GIC is the leading class of increased cancers, responsible for nearly 25 % of all new cancer diagnoses and for 30 % of cancer-related deaths worldwide [2-5]. For patients with stage I, surgical resection such as regional lymphadenectomy is the frontline treatment, but, at later stages, chemotherapy is involved. National Comprehensive Cancer Network (NCCN), European Society for Medical Oncology (ESMO), European Society for Medical Oncology (ESMO), Japanese, and Chinese guidelines recommended the use of front line drugs such as fluorouracil (5-FU), capecitabine plus cisplatin (CDDP) (Fig. 2.1.), capecitabine plus CDDP, or oxaliplatin (OXA) for the treatment of gastric cancers [6-10] These platinum (Pt)-based drugs are among the most frequently used cancer therapeutic agents [11] and since the discovery of CDDP, the development of various Pt-based drugs such as OXA has improved the efficacy of and decreased the toxicity of CDDP.

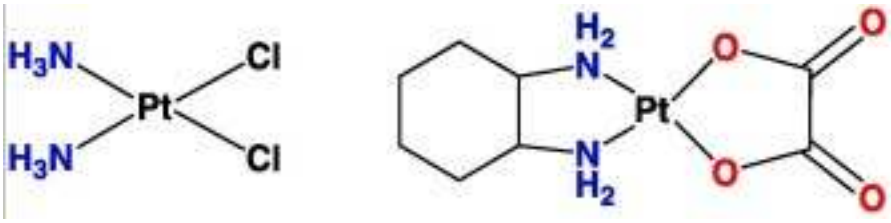

Fig. 2.1. Structures of CDDP (left) and OXA (right).

2.1.1. Metallodrugs and cancer treatment

Metallodrugs contribute to regulation over an extensive range of relevant cellular processes with specificity and selectivity [12-15]. The capability of many metal based drugs to be used as antitumor agents has long been known documented from the 16th century [16]. Many metallodrugs show a differential expression on several proteins involved in cell pathways related to cancer progression, chemoresistance, and cell death [17-23] For example, vanadium complexes with flavonoids and quinolines avoid the FAK activation and inhibit the cell migration and invasion of human osteosarcoma cells reducing the activity of matrix metalloprotease 2 and 9 (MMP-2 and MMP-9). The analysis of interaction shows that the vanadium-clioquinol complex is located adjacent to the activation loop of the kinase domain and its interaction with ATP residues on binding site. A number of different vanadium coordination complexes including polyoxovanadates were found to initiate GPCRs and Tyrosine Kinase receptors signaling through a number of different mechanisms [12-14]. Next, other metal-based drugs such copper-hydrazones compounds impair the cell viability of breast cancer cells, inducing apoptosis through ROS generation. Cancer stem cells, proteasome proteins, and lipid metabolism enzymes are the most important molecular targets related to the anticancer activity of these kind of complexes. The alteration of lipid metabolism is a known aspect in cancer metabolism, meanwhile cancer cells tend to augment several processes such as lipid uptake, lipid storage, or lipogenesis. One of the greatest down-regulated proteins after treatment with these Cu complexes is Lanosterol 14-alpha demethylase (CYP51A1) that catalyzes one of the crucial steps in cholesterol biosynthesis and is usually overexpressed in solid tumors [24]. Therefore, the down-regulation of this protein by a Cu compound is a novel and interesting effect. Other interesting mechanisms described for these Cu compounds are the down-regulation of several proteins that participate in DNA replication. In this way, minichromosome maintenance complex 2, 3 and 5 (MCM2, MCM3, MCM5), ribonucleotide reductase regularoty subunit M2 (RRM2), structural maintenance of

chromosomes 2 (SMC2), and DNA polymerase appear downregulated and confirms the interaction and damage of these complexes over a DNA molecule. P53, a tumor suppressor gene and one of the most important antitumor mechanisms of action, is down-regulating a gain of function mutant (GOF-mutant) in triple negative breast cancer cells for the action of the Cu-hydrazone complexes, suggesting a key molecular target involved in antitumor properties of Cu compounds [23]. Finally, other Pt-based drugs have shown antitumor properties. A Pt-hydroxiquinoline complex exhibits *in vitro* and *in vivo* antitumor properties against human osteosarcoma models. The complex reduces the viability and alters the shape of the spheroids, showing a significant suppression of osteosarcoma tumor growth along 1 month of treatment [19]. Here, it is evident that a multitude of metallo-based drugs have varying biological effects with different cancers, yet we will see that Pt-drugs have the largest effect due to their mechanism of action with DNA and RNA.

The mechanisms of action of Pt-drugs including CDDP and OXA, despite differences in structure, are similar in that they act by forming a coordination complex with guanine bases in DNA to commonly induce a 35–40-degree angle bend in the DNA strands, but as shown in Fig. 2.2, alternative modes of action are possible with a smaller bend and a twist in the strand. All these changes of the DNA strand geometry cause DNA polymerase activity to arrest, inducing cellular apoptosis [25], [26]. As shown in Fig. 2.2, crystal structures are available for numerous Pt-DNA adducts and a representative is shown. This gives insight into the association of the Pt-DNA adduct, including details on where and how the Pt-atom is coordinated to two N atoms on the adjacent G-residues labeled G*, combining the A- and B-type of DNA strong association. A number of different modes of binding have been reported with several proteins, transporters [11], [27-33] and RNA [34], [35] demonstrating a variety of potential binding modes with both the A- and B-DNA helices. It has been proposed that the effects of these drugs are a combination of all the modes of action, including some that do not involve DNA, and most significantly including the interactions of Pt-drug with RNA [28], [29]. In addition to the potential

binding of CDDP to rRNA to inhibit protein synthesis, it has been found that a larger majority of administered Pt-drug is sequestered by RNA rather than DNA, considering the high concentration of RNA in a cell. Because of this sequestration, we have been interested in the mechanisms of these processes and how chemoresistance of metallodrugs including Pt-based drugs develop [36-38]. This mechanism, with RNA's role in interacting with Pt-based drugs, has been suggested to play a key role against chemoresistance and Pt resistance.

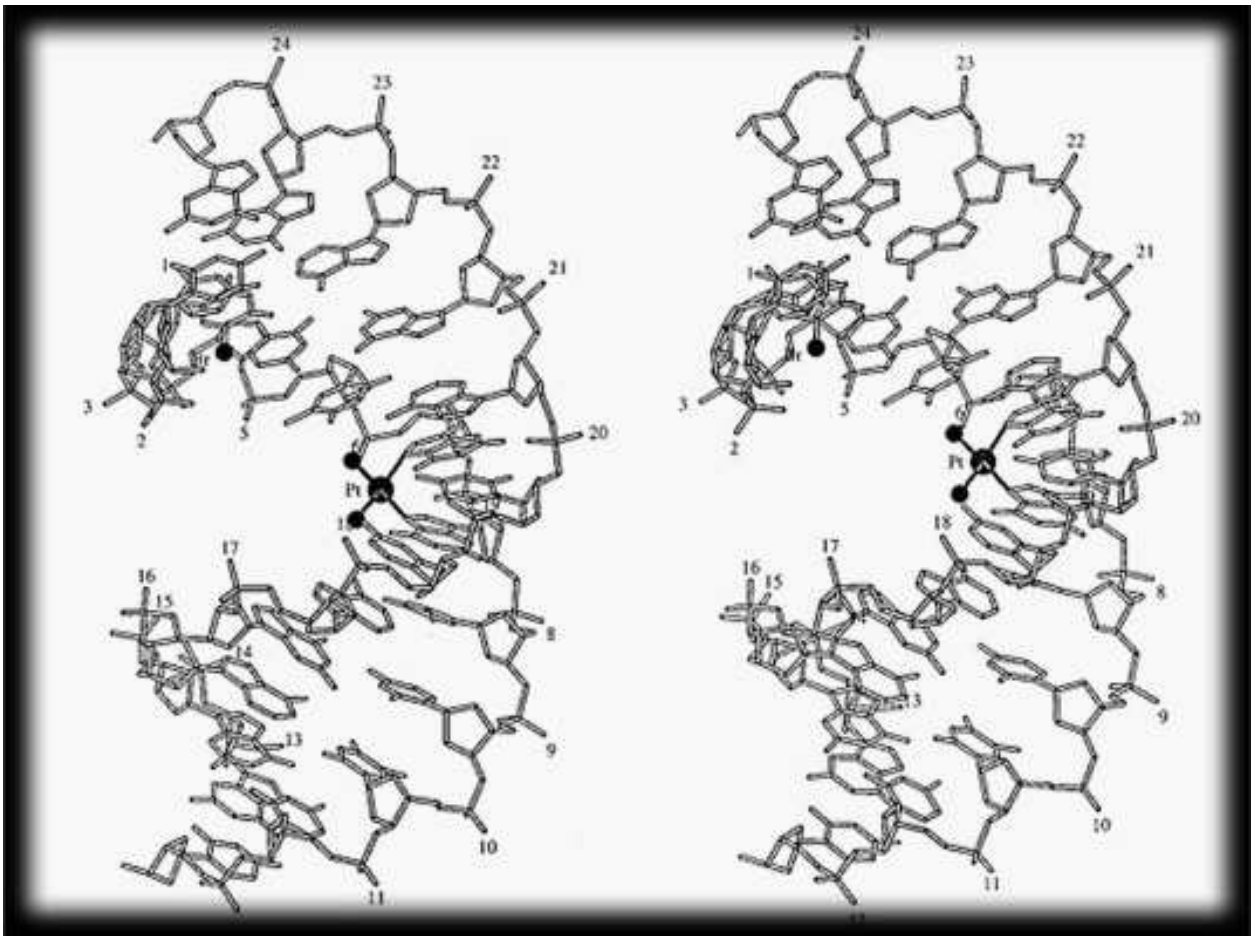

Fig. 2.2. Stereoview of a ball and stick model derived from crystallographic data of the duplex *cis*-platin bound to DNA, d(CCUBrCTG*G*TCTCC),d(GGAGACCAGAGG), where -G*G* is coordinated to the diamino(diaqua)platinum^{2+} complex. Adapted with permission from Ref. [25].

2.1.2. Platinum drugs and chemoresistance

Although the mechanism suggests a strong mode of action for Pt-based drugs acting on DNA and RNA, it is still possible that cancer cells can develop resistance to the chemotherapy.

This resistance is primarily due to several processes, such as augmented expression of certain ATP-binding cassette (ABC) transport proteins, mutations in specific cellular targets, increases in DNA repair, alterations in metabolism that permit cancer cells to evade apoptosis, and increasing the biotransformation of antitumor agents to less efficacious or inactive intermediates [39], [40]. The accumulation of Pt drugs into the cells is necessary to generate cytotoxicity, so diminished influx or increased efflux is at least at partly responsible for Pt resistance. For various years it has been assumed that Pt enters cells by passive diffusion and through gated channels [41]. However, the role of active transport mediated by different carriers becomes prominent to platinum-uptake. Different scientific reports show that solute carrier superfamily (SLCs), copper transporter 1/2, ATP7A and ATP7B, and multidrug resistance protein (MRP, ABCC) show a close relationship between protein expression and Pt chemoresistance [42].

Another mechanism of chemoresistance described for Pt drugs is the GSH redox cycle. Higher expression of glutathione reductase accompanied by lower levels of endogenous reactive oxygen species (ROS) contributes to the CDDP-resistance [43]. The GS-Pt complex catalyzed by glutathione-S-transferase can reach to about 60 % of the intracellular Pt content after 12-h incubation in leukemia cells [44], and the elevated expression of GSH and glutathione-S-transferase are often seen in the resistant-cells [45].

On the other hand, Pt drugs are inactivated by chelating with metallothionein proteins (MTs) that are low-molecular-weight metal-binding proteins, which make MTs become easy targets for Pt to chelate [46]. Tariba *et al* found that metallothionein proteins level is increased in the tumor tissue and in the serum of cancer patients [47].

CDDP can form mono adducts, intrastrand, or interstrand cross-links, but the 1,2-intrastrand crosslinks account for over 90 %. These DNA adducts are the key step for cytotoxicity of Pt drugs since the Pt–DNA complexes influence the structure of DNA double helix [48]. Consequently, it generates replication and transcription inhibition and DNA double-strand breaks (DSBs), followed by the initiation of DNA repair. The increased DNA repair process is considered

noteworthy in Pt-resistance cells [49] with the exception of DNA mismatch repair whose deficiency gives rise to CDDP/carboplatin resistance [50], but has less influence to OXA [51].

Chemoresistance such as this is a challenge that life scientists try to overcome in the quest for curing cancer. Chemoresistance has recently been defined as the ability of cancer cells to evade or to cope with the presence of therapeutics [52]. Hence, chemoresistance includes Pt resistance, which also includes the ability of a cancer to recur withing six months of completion of the chemotherapy protocol [53]. This definition of chemoresistance also includes metabolic deactivation of a particular drug, which results in the decrease of the effective concentration of the active drug. Besides, drug resistance can be existing in tumor cells before chemotherapy, a phenomenon known as acquired drug resistance [54], and is related to many epigenetic events such methylation of DNA and histone modifications. Chemotherapy sensitivity differs from person to person because large interindividual variability exists in the capacity for DNA damage response and its repair [55].

These processes are closely related to the sensitivity to Pt-chemotherapy [56]. Pt-resistance is a sub-category of chemoresistance where the focus is on development of resistance toward Pt-based therapeutics. Since Pt-based drugs are used very frequently as a front-line treatment for GIC cancers, Pt-resistance is a major problem for GIC patients.

2.1.3. Long non-coding RNAs and chemoresistance

Long non-coding RNAs (lncRNAs) have recently been discovered whose dysregulation has been correlated to the development of Pt-chemoresistance. Non-coding RNAs (ncRNAs) are transcripts which do not codify protein and take up roughly 98 % of the human genome [31]. The ncRNAs are abnormally expressed in cancer cells (miRNAs), and they regulate gene expression post-transcriptionally by binding to the untranslated 3′ UTR of their target mRNAs and repressing protein expression [57-60]. LncRNAs are ncRNAs of 200 nucleotides or more, and they are less understood than miRNAs as they exhibit little to no coding potential and, until recently, have been

thought of as “junk” RNA. However, many lncRNAs have now been functionally associated with human diseases, specifically cancer [61-64] Specifically, dysregulation of lncRNAs has been implicated in cancers, with colorectal cancer being one of the most common cancers in which lncRNAs may play a role impacting cellular functions. The processes affected includes induction of angiogenesis, cell proliferation, metastasis induction, resistance to apoptosis, and evasion of tumor suppressors [65-69].

The nature and function of lncRNA is emerging as a novel wide-ranging research field which includes characterization and function of the interactions with macromolecules such as DNA, RNA, and proteins [31]. LncRNAs have now been reported to have crucial regulation activity in biological processes like development, cell differentiation, gene transcription, splicing, and epigenetics [70]. LncRNAs control chemoresistance in cancer through a variety of molecular mechanisms including epithelial-mesenchymal transition (EMT), changes in the tumor microenvironment (TME), epigenetic modification and alterations, multidrug efflux, among others. They may also regulate chemoresistance in cancer through functioning as competitive endogenous RNA [36], [71]. The relationships between lncRNAs and chemoresistance are summarized in Fig. 3.3.

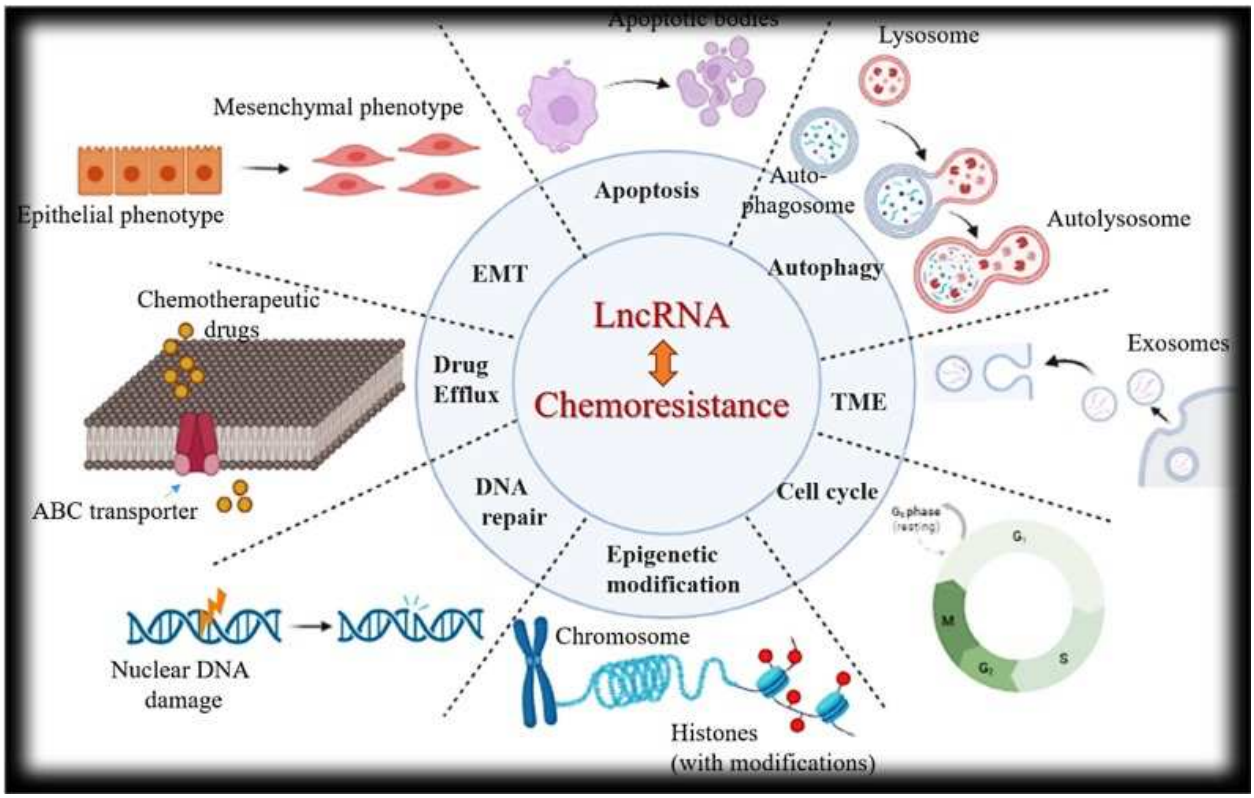

Fig. 3.3. Summary of the relationship between lncRNAs and chemoresistance. Adapted from [72].

2.1.3.1. Long non-coding RNAs and TME

The TME is a complex system comprised of tumor cells, stromal cells, extracellular matrix, and soluble factors such as hormones, cytokines and enzymes. The TME has an important role in the process of tumorigenesis, proliferation, and metastasis but also in the chemotherapeutic efficacy. Exosomes are membrane-derived vesicles originating from endosomal multivesicular bodies (MVBs) and play an essential role in TME. They can transfer useful information from host cells to recipient cells, such as lipids, proteins, and RNAs like lncRNAs. Thus, lncRNAs have been investigated to explore the mechanisms of chemoresistance in different types of tumors [72-77].

Up until now, few studies have addressed the link between exosomal lncRNAs and chemoresistance in different kinds of tumors. For example, it has been reported that exosomes produced by tamoxifen-resistant breast cancer cells containing more lncRNA UCA1 are incorporated into MCF7 cells and then significantly increased tamoxifen resistance in breast

cancer cells [76]. On the other hand, Mao *et al.* have demonstrated that the lncRNA MALAT1 overexpression facilitates ovarian cancer progression through promoting chemoresistance and invasiveness in the TME. Their findings have revealed that the upregulation of MALAT1 suppressed immunity via inhibition of the secretion of the IL-6 and TNF-α cytokines, suggesting reduced cellular apoptosis susceptibility within the immunosuppressive TME [73]. Besides, Xiang and coworkers identified three (CASKIN1, EMR3, and GBP5) novel genes which were linked to the TME and had prognostic significance in Hepatocarcinoma cells, which may be auspicious markers for predicting immunotherapy outcomes [75]. A great number of scientific studies have showed that TME-related lncRNAs are one of the foremost factors to realize precise diagnosis and treatment of lung cancer [78]. Together with various regularoy factors, Cancer Stem Cells (CSCs) are a crucial component of the TME [79]. DUXAP10 is upregulated in lung cancer cells so DUXAP10 knockdown increases the stemness markers (KLF4, KLF5 and Nanog) downregulation, declining the spheroids forming capacity and reducing the number of stem cells in lung cancer cells [80]. Liu and coworkers discovered that HOTAIR could promote CDDP resistance through inducing stem cell-related biomarkers β-catenin and KLF4 [81].

Many reports show the importance of the production of pro-angiogenic factors in TME and the development and tumor progression [82].

Some evidence has shown that lncRNAs act on tumor progression by regulation of VEGF in lung cancer. For instance, Chen et al published that the knockdown of LINC00173.v1 suppresses VEGFA expression, thus attenuating vascular endothelial cell proliferation and migration in lung squamous cell carcinoma cells [83]. Moreover, LINC00667 induces angiogenesis of lung cancer cells and thus results in lung tumor growth and metastasis [84].

2.1.3.2. Long non-coding RNAs and epigenetics

In the last ten years, epigenetic modification has been recognized as a significant contributor on tumor development and progression [85]. Epigenetics refers to heritable alterations in gene expression without alterations in DNA sequence. The epigenetic modifications in tumor progression include chromatin remodeling, DNA methylation, and histone modifications. Several scientific reports show that noncoding RNAs are linked with epigenetic modifications in gastric cancer. For instance, Yang *et al* describe the molecular interactions of histone modifications and noncoding RNAs (ncRNAs) in the pathogenesis of gastric cancer [77]. It is important to mention that ncRNAs are principally classified as lncRNAs (linear, >200 nucleotides), circular RNA (circRNAs, covalently closed continuous loops), and short ncRNAs (linear, <200 nucleotides) [86].

SNHG5 is a lncRNA where expression is aberrantly decreased in gastric cancer. The overexpression of SNHG5 affects the establishment of the NuRD complex by blocking the transference of MTA2 from the cytoplasm to the nucleus, resulting in important upregulation of histone H3 and non-histone p53 acetylation levels, which affects the nucleosome remodeling and the formation of the histone deacetylation complex [87]. Moreover, lncRNA MALAT1 induces EGFL7 protein expression by altering H3 histone acetylation at the region of EGFL7 promoter. MALAT1 stimulates migration and invasion of gastric cancer cell lines through the above mechanism [88]. Besides, several lncRNAs (HOXA11-AS, FEZF1-AS1, Linc01503, HOXD-AS1, PART1, FOXD2-AS1, PCAT-1, HOTAIR) regulate histone methylation and affect different genes and cellular pathways [89], [90], [91]. For example, HOXD-AS1 promotes CDDP resistance in gastric cancer through recruiting EZH2 and upregulating H3K27me3 levels on the region of PDCD4 promoter in this type of cancer cells to epigenetically silence PDCD4 [92]. To regulate histone methylation or acetylation alone, lncRNAs act as molecular scaffolds that bind two or more protein molecules then perform specific biological functions [93]. Sun *et al.* identified gastric cancer-associated lncRNA (GClnc1) whose overexpression is correlated with tumor size, stage,

pathological differentiation, and vascular invasion [94]. GClnc1 can act as a scaffold molecule that recruits the WDR5 and KAT2A complexes to the promoter of SOD2, thereby regulating histone modification and activating transcription of the SOD2 gene.

LUCAT1 (Lung Cancer-Associated Transcript 1), was first identified as smoke-induced and cancer-associated lncRNA1 [95]. The levels of LUCAT-1 were associated with late stage tumor–lymph node metastasis. In addition, LUCAT1 modulates p21 and p57 expression by promoting loci methylation through PRC2 in lung cancer cell lines (A549 and SPC-A1) [96].

2.2. Speciation of CDDP and OXA and their interactions with RNA and DNA under biological conditions

Surgical resection and Pt-based chemotherapy are commonly used to combat cancers and have successfully prolonged overall progression and increased survival of GIC patients [97-99]. CDDP and OXA under physiological conditions undergo a number of reactions pointing to the fact that speciation reactions affect the ability to chelate DNA and the induction of apoptosis is different for each Pt-compound [100], [101]. The conditions and the details of the drug are critical for activity and the large number of effective Pt-based drugs document the importance of these small differences [102], [103]. Details in the speciation reactions such as the presence of chloride ion have a dramatic effect on the nature of the Pt-drug that exists [102] and its stability upon administration [103-105]

Indeed, we and others have shown that differences in media will impact the observed response in biological systems [103]. For example, the presence of protein will depend on the compound and will either enhance or reduce its effects on cell growth. In the same tone, many successes have been reported with different Pt-based drugs [106], although CDDP and OXA still remain the two Pt-compounds used commonly in the clinic [107].

Despite major improvements in the management of GIC patients, resistance to Pt-based drugs remains, and as such, chemoresistance is a main challenge in Pt-chemotherapeutic

GIC therapy. In this paper, we are considering how RNA and Pt-based drugs interact and discuss how such interactions might link to observed chemoresistance of the Pt-drugs. Interactions between metallo-complexes and RNA is a new area of interest, and considering the difference in the fundamental structures of RNA and DNA, the growing data is suggesting that Pt-drugs are binding to RNA as well as binding to DNA.

To begin investigating the mechanism of Pt-based drugs with RNAs, we have identified their role in varying GICs. To begin, oral cavity cancer (OCC) is a subclass of head and neck cancers, in which cancer cells growth in the lining of the lips, mouth, and upper throat, with the most common tumors in this area being squamous cell carcinomas (OSCC) [108]. In this sense, the tongue is the major subsite of origin for squamous cell carcinoma in the oral cavity (tongue squamous cell carcinoma, TSCC [109]. Next, esophageal cancer (EC) is one of the most aggressive and lethal malignant tumors. These kind of tumors are characterized by rapid tumor growth, early metastasis, and with a particularly low response rate to the chemotherapy treatment [110]. Squamous cell carcinoma (ESCC) and esophageal adenocarcinoma, are two major subtypes of EC [111], [112]. Following, in gastric cancer (GC) the cells derived from tumor grow and colonize the wall of the stomach [113], [114]. Finally, in colorectal cancer (CRC) the malignant cells grow in the colon or inner lining of the rectum [115]. Considering all tumor categories in the digestive tract, CRC exhibits the highest incidence and mortality rates. Specifically, CRC is the third most common cancer type in men after lung and prostate cancer, and the second most common cancer type in women after breast cancer [5]. In relation to each of these cancers, the prognosis of GIC patients principally depends on tumor stage and the subsequent response to therapy [8], [116].

To effectively study the relationship between GIC and Pt-resistance, it is critical to look at Pt-based drugs and their interactions with lncRNAs. LncRNAs are now considered to regulate transcription, and several models have been proposed, including lncRNAs as signal and decoy RNAs. Some lncRNAs may serve as a molecular signal to regulate transcription in response to

intra- and extra-cellular stimuli [117]. This point is supported by reported exosomes that contain lncRNA used for cell-to-cell signaling. Decoy lncRNAs may function to limit the availability of small compounds or regulatory factors by presenting 'decoy' binding sites, and may sequester small molecules, transcription factors, catalytic proteins, and even miRNAs to reduce their availability. Specifically, we have identified significant increase and decrease of lncRNA levels in cancer cells treated with CDDP and OXA which will impact negatively in the action of the drugs being the possible causal of chemoresistance. Notable differences in lncRNAs levels and Pt-treated cells have been reported in OCC, EC, GC, and CRC and is the topic of this review.

First, it is critical to understand the speciation of Pt-based drugs and how they interact with DNA and RNA in order to provide a broader scope of understanding Pt-based drug interaction with lncRNAs of varying GICs. While CDDP and OXA are supposed to follow the same general mode of action in which the Pt-compound chelates the DNA, they have different properties and therefore their speciation chemistry differs (Fig. 2.1)[118]. Thus, they convert to different compounds with varying charges in the physiological pH. Speciation chemistry should therefore be considered when investigate their biological effects and their interactions with DNA and RNA.

2.2.1. CDDP speciation and its consequences.

In the case of CDDP, the neutral parent form of the drug is able to cross the cellular membrane, and there are also a number of active uptake and efflux mechanisms that are at play [119], [120]. Upon entering cells, the neutral parent and intact form of the drug (as CDDP) containing two chlorides begins to exchange its chlorine ligands for aqua ligands. After substitution of the chlorine ligand, the two aqua ligands can deprotonate, resulting in diaminoaqua(hydroxy)platinum and diamino(dihydroxy)platinum (Fig. 2.4.) [121], [122].

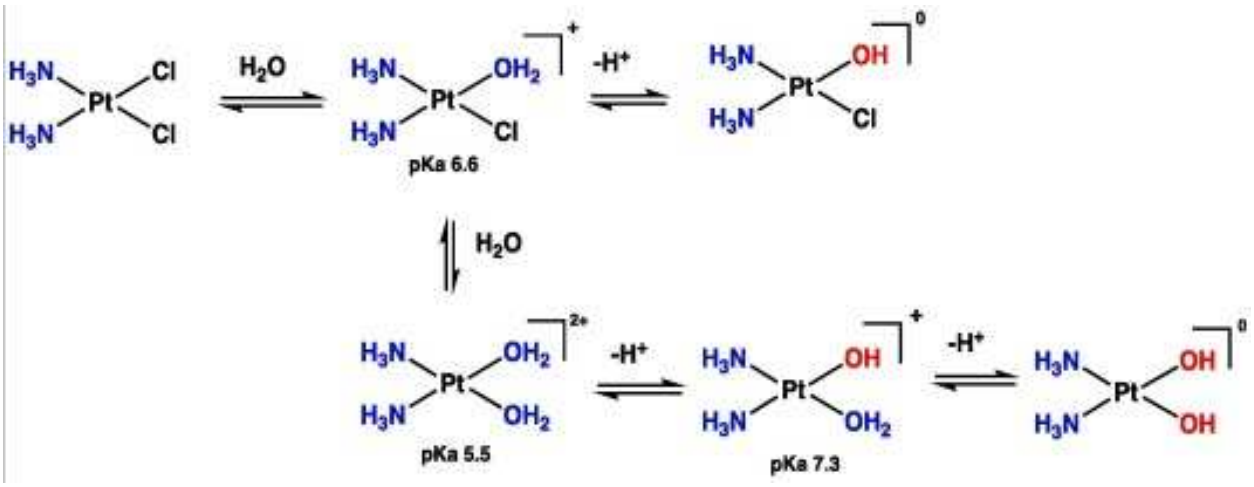

Fig. 2.4. Speciation of CDDP from parent intact form to its positively charged forms (diaminoaqua(hydroxy)platinum and diamino(dihydroxy)platinum.

Since the pKa values of all these partially hydrolyzed CDDP are near 7, their charges can vary, making a large difference for which ones are most readily taken up by the cell. Since CDDP primarily enters the cell through passive diffusion [123], the charges will matter and affect CDDP or hydrolysis products entering the cell. For CDDP, the aquation reaction followed by deprotonation presumably takes place primarily inside of the cell, consistent with the higher concentration of chloride outside the cell (100 mM) compared to the cellular interior (4–12 mM). However, since CDDP is expected to interact with DNA, it or its hydrolysis products will need to pass through the nuclear membrane in addition to the cellular membrane.

In terms of intermediate products resulting from the *in vivo* conversion of CDDP to *cis*-diamino(dihydroxy)platinum(II), the different ligand exchanges that are required result in intermediates which have different chemical properties and reactivity to biological structures. For example, during conversion of CDDP, each of the intermediate products has a different pKa. The first intermediate product, monoaquated CDDP, has a pKa of 6.6, while diaquated CDDP has a pKa of 5.5. The CDDP hydrolysis product with one aqua ligand and one hydroxyl has a pKa of 7.3 as listed in Fig. 2.4. All these derivatives have pKa values around 7, and hence can have two

different charges which is important for transport in the cytoplasm and through the membrane into the nucleus.

The *in vivo* metabolism of CDDP to DNA is difficult to predict with certainty due to variability in drug uptake and conditions of the cellular environment. The presence of different ions or metabolites in the blood affect the ligand exchange of the parent drug; for example, as mentioned above, the conversion of CDDP to *cis*-diamino(dihydroxy)platinum is much slower outside of the cell than inside due to the higher extracellular concentration of the chloride ions [116]. Although it is known that the second chloride is a poorer leaving group than the first, and thus the second nucleophilic substitution reaction (ligand exchange reaction) will be slower, the details of the cellular conditions are not known, so exactly how slow is not clear. Studies have been carried out that show the effects of chloride concentration on speciation. These studies show that with higher concentration of chloride ions there was a significant delay in the hydrolysis of CDDP [124]. Presumably, such studies have contributed to the practice of administering CDDP in solutions high in chloride concentration [104].

2.2.2. OXA speciation and its consequences.

The structure of OXA contains a 1,2-diaminocyclohexane (DACH) ligand and an oxalate group around the central Pt(II) atom as shown Fig. 2.1[125-127]. Speciation reactions of OXA under physiological conditions are similar to those of CDDP, except OXA immediately undergoes aquation reactions upon administration in the blood due to the rapid loss of the oxalate leaving group [128], [129]. This is rapid, non-enzymatic hydrolysis replaces the DACH ligand with aqua ligands and results in a more complex pharmacokinetic profile [128], [129]. The resulting intermediate is deprotonated to form the neutral form of the drug [130]. Additionally, owing to the high concentration of chloride ions outside of the cell, the oxalate leaving group can be replaced by chlorine groups, resulting in a structure that contains chloride ligands as found in CDDP [130], [131].

Although OXA also produces the same type of lesions on DNA as CDDP, its spectrum of activity is different from CDDP, and the cellular resistance profile of OXA is different from that of CDDP [26], [132]. The mechanism for the differences is not fully understood, but it has been suggested that the recognition of platinated DNA adducts of CDDP by the mismatch repair system proteins is different. The mismatch repair proteins may not be able to recognize DNA adducts formed by OXA considering the presence of the large DACH ligand [118], [133].

2.3. Interaction of Pt-drugs with DNA and RNA

Although DNA and RNA both contain G and A bases, there are differences between the 2-deoxyribose sugar in DNA and the ribose sugar in RNA that lead to a small difference of the five-membered sugar ring (see Fig. 2.5a) DNA nucleosides and Fig. 2.5b for RNA nucleosides). The nucleoside bases for DNA and RNA only differ for one of the bases. That is because DNA contains a thymine base and RNA contains an uracil base as shown in Fig. 2.5 [134-136]. These small differences have generally led the community to assume that the interaction of Pt-drugs would be similar between DNA and RNA because the purine bases do not change between the two different structures. However, such an assumption is an oversimplification, because it ignores the 3D structure of the DNA and RNA components in the cells. Perhaps surprisingly, these small differences in 3D structure impact the stability of the double stranded structures that exist under physiological conditions.

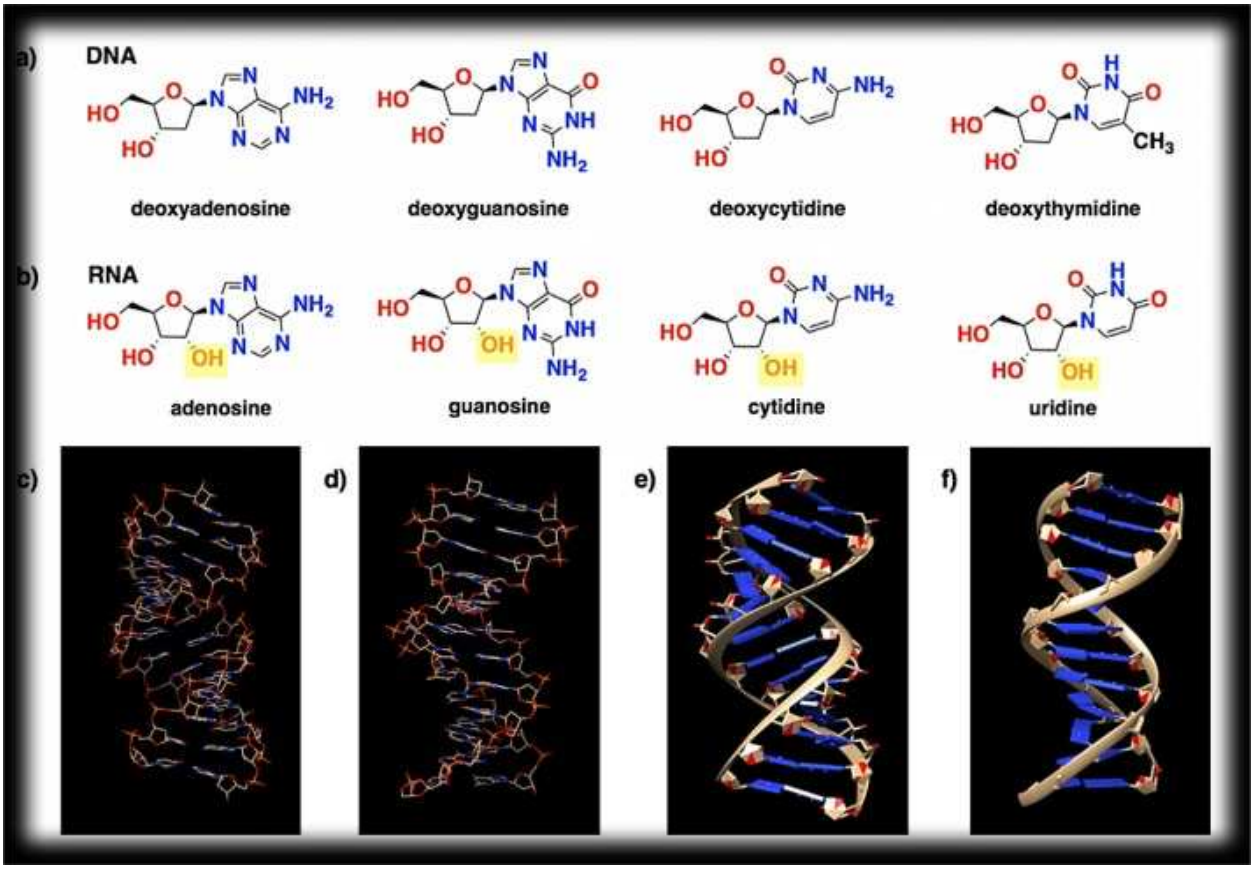

Fig. 2.5. a-f. structural differences of nucleoside base units of a) DNA: deoxyadenosine, deoxyguanosine, deoxycytidine and deoxythymidine; b) RNA: adenosine, guanosine, cytidine and uridine; c) 3d stick model structure of A-RNA [134] d) 3D stick model structure of B-DNA; e) 3D ribbon model structure of A-RNA; f) 3D ribbon model structure of B-DNA [135].

The most stable form of double stranded DNA is B-DNA and the most stable form of the double stranded RNA is A-RNA [136]. These structures are very different, as shown in Fig. 2.5a-f, using both the stick model (Fig. 2.5c and 2.5d) and the ribbon models (Fig. 2.5e and 2.5f). This 3D structural difference can cause a difference in the interaction with Pt-drugs. Furthermore, in addition to these fundamental structural differences, the fact is that DNA is mainly found double stranded under cellular conditions, but RNA is generally found in a single stranded form. The single stranded RNA can form stretches of double stranded RNA, but this happens because the RNA strand folds over on itself. Based on these differences, the interactions between Pt and DNA are likely to be very different from the interactions of Pt and RNA under physiological conditions.

2.3.1. Interaction of Pt-drugs with DNA

Based on the reactions shown in Fig. 2.4, there are several CDDP hydrolysis products that could react with DNA, although it is generally accepted that the highly electrophilic diamino(dihydroxy)platinum is most efficient in crossing the nuclear membrane and undergoes additional S_N2 reactions with the purine bases guanine (G) and adenine (A) on the nuclear DNA. This leads to the final formation of *cis*-$[(NH_3)_2Pt\text{-}DNA]^{2+}$ adducts of which one is shown in Fig. 2.2 [25]. Much work has been done detailing the interaction of the Pt-compounds with DNA, leading to well documented information of these Pt-DNA adducts causing a kink in the DNA, which are generally monitored using UV–vis spectroscopy. Since the binding of the Pt-drug to DNA has been described in X-ray crystal structures, the 26-degree bend in Fig. 2.2 represents a more recent but unusual juxtaposition of an A-like and B-like helical segment of DNA that is clearly demonstrated, and since this geometry or that of other CDDP-DNA adducts is not compatible with repair enzymes, such binding will ultimately arrest DNA polymerase and result in cellular apoptosis [116], [117].

Both CDDP and OXA are highly electrophilic compounds, which allows nucleophilic substitution with the N7 reactive center on purine residues in DNA or RNA. In DNA, when the reaction is undergone with two adjacent G residues, it can form the 1,2-intrastrand cross-links in the purine bases shown in X-ray structures. However, the coordination to DNA does not always result in the intrastrand Pt-GG DNA complex that leads to cellular apoptosis. CDDP and OXA both establish about 65 % intrastrand adducts between two adjacent guanine bases (Pt-GG), 25–30 % intrastrand adducts between adjacent adenine and guanine bases (Pt-AG), and 5–10 % intrastrand adducts of the type Pt-GNG, where N is any of the four bases. The final 1–3 % of the binding of CDDP or OXA to DNA comprises intrastrand adducts between guanine bases on separate pieces of DNA (G-Pt-G). This variation is even more significant when taking into account that of the total concentration of CDDP or OXA administered intravenously to GIC patients, only

1 % of the administered Pt-chemotherapeutic binds to intracellular DNA to induce apoptosis. The remaining 99 % of administered Pt-chemotherapeutic, due to its highly electrophilic nature, binds to other biological structures, which contributes significantly to chemoresistance as well as toxicity of Pt-chemotherapeutics.

2.3.2. Interaction of Pt-drugs with RNA

Pt-drugs were also found to bind to structured RNA from various biological systems and a few representative examples are summarized below [28]. In Fig. 2.6a, the schematic for the crosslinking of Pt in the internal loop of the catalytic core of the U2:U6 spliceosomal RNA (BBD RNA) is shown [137]. This interaction, albeit binding two guanines, is a very different mode of binding than the one observed in most Pt-DNA complexes. The adjacent G's targeted by CDDP in the free and complexed 16S rRNA are shown in contour letters of the helix 24 in *E. Coli* 6S rRNA [138]. CDDP binds to helix 18 of *S. cerevisiae* small ribosomal subunit. However, this site is less prone to platination based on HPLC investigations in structured RNAs [28] or two related Pt derivatives, Oplatin and Kplatin, which only vary in one CH_2 group compared to CDDP and show overall preferential binding to A, AG, or GA in loops or bulges over GG sites in structured RNAs [28], [139]. The Pt-derivative Rplatin, which have an arginine group, displays preferential coordination to a bulge nucleotide. This Pt-derivative favors the interaction of the Tat protein (arginine-rich) with the three-nucleotide bulge region of TAR RNA region. On the other hand, no interaction is observed by CDDP, likely due to electrostatic repulsion. Augmented bulkiness of the cis ligands is exhibited by the different charge distribution and may significantly influence RNA platination profiles, showing that subtle effects will change selectivity. Detailed selection by Pt-derivatives and other metal drugs in different RNAs has previously been described in further detail [28].

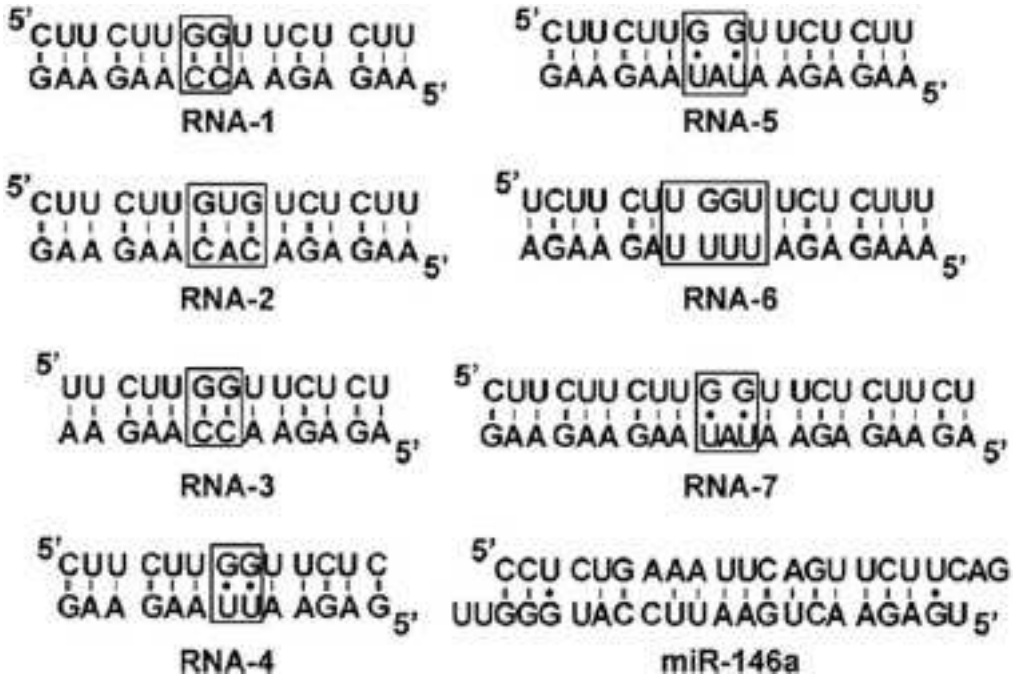

Fig. 2.6. RNA duplexes found to bind to Pt-derivatives; the box indicates the main site the Pt-was binding [28], [140]. This figure was adapted from Ref. [28] with Permission.

Because RNA has a different structure when organized in a double helix, the interaction of Pt-drugs with RNA is not the same, even though many of the interactions with Pt-derivatives also take place with G- and A- residues [34]. For CDDP, based on the fundamental structural similarity between RNA and DNA bases, some interactions may take place with single stranded RNAs, as RNAs also contain G and A bases. The interactions here take place not only between G-G pairings or G-A pairings, but also between G-C and G-U at an even tighter angle than on DNA base pairings (Fig. 2.7). This interaction is particularly plausible because RNA is readily available in the cell, able to act as a scavenger for CDDP and derivatives, attracting the drug before it can reach its intended target of DNA. However, even if the interactions are still taking place with the G and A residues, they are likely to be different from that reported with DNA because of the subtle conformational differences observed for single stranded RNA folded over on itself forming a double helix. Hence, the affinity of these Pt-RNA complexes is much lower and has been much less characterized [34], [35]. Regardless, such interaction will decrease the available Pt-compound and will hence significantly decrease the efficacy of the drug. Although

such dilution of the drug is the result of the metabolism of the drug, it does dilute the effects of Pt-drug and its ability to reach its target.

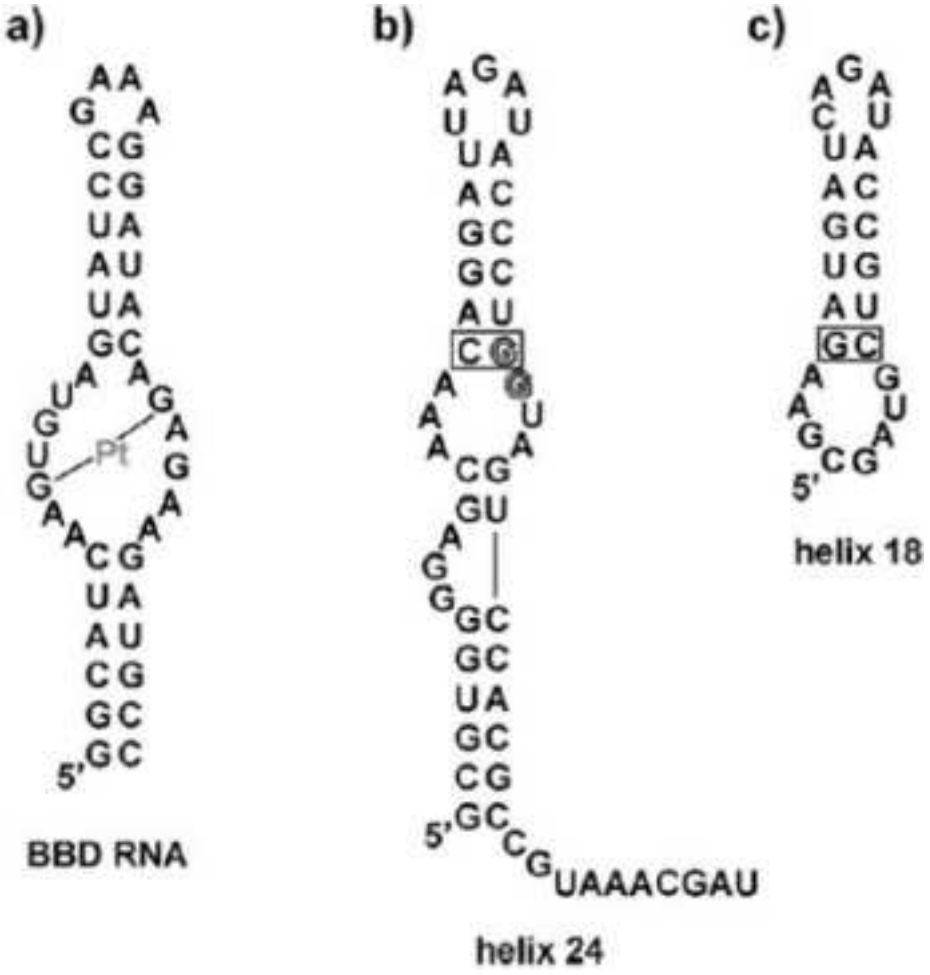

Fig. 2.7. Examples of Pt-structures bound to RNA structures [28]. a) The catalytic core of the U2:U6 spliceosomal RNA (BBD RNA) construct was found to bind Pt [137] b) Pt in CDDP was found to target two consecutive guanines on Helix 24 of the E. coli 16S rRNA both when it is free and coordinated to a protein [138] (c) The secondary structure of helix 18 of S. cerevisiae small ribosomal subunit investigated is found to bind Pt on E. coli and S. cerevisiae RNA [35].

Consequently, lncRNAs have been reported to play a role in Pt-drug chemoresistance. For example, in CRC treated by Pt-based drugs, lncRNAs have been implicated to play a role in altering cellular functions [141-143]. In bone cancer, the regulation of several lncRNAs were altered, affecting important processes like cell signaling, autophagia, apoptosis and metastasis [144]. In addition, there are a number of lncRNAs which exhibit aberrant expression

in GIC patients resistant to CDDP and OXA treatments [145]. Although the nature of the effects is not understood and it may not involve a direct interaction between Pt-drug and RNA, changes in lncRNA expression were reported between patients resistant to Pt-drugs and patients with no resistance to Pt-drugs. Since dysregulation of lncRNAs has been implicated in a wide number of cancers, we summarize here the effects of recently discovered lncRNAs in GIC cancers and specifically those lncRNAs recently discovered and involved in Pt-drug induced chemoresistance of GIC.

2.4. LncRNAs and their potential role in Pt-chemoresistance

Related to the role that lncRNAs play in Pt-drug chemoresistance, there are several biological mechanisms which cells may become resistant to CDDP or OXA. Pt-chemoresistance tends to be mainly mediated through the subsequent mechanisms: regulating drug uptake, increasing DNA damage repair, altering cell cycle regulation, escape of apoptosis, regulation of cellular signaling pathways, promoting EMT, and regulating autophagy induced by therapy (Fig. 2.8).

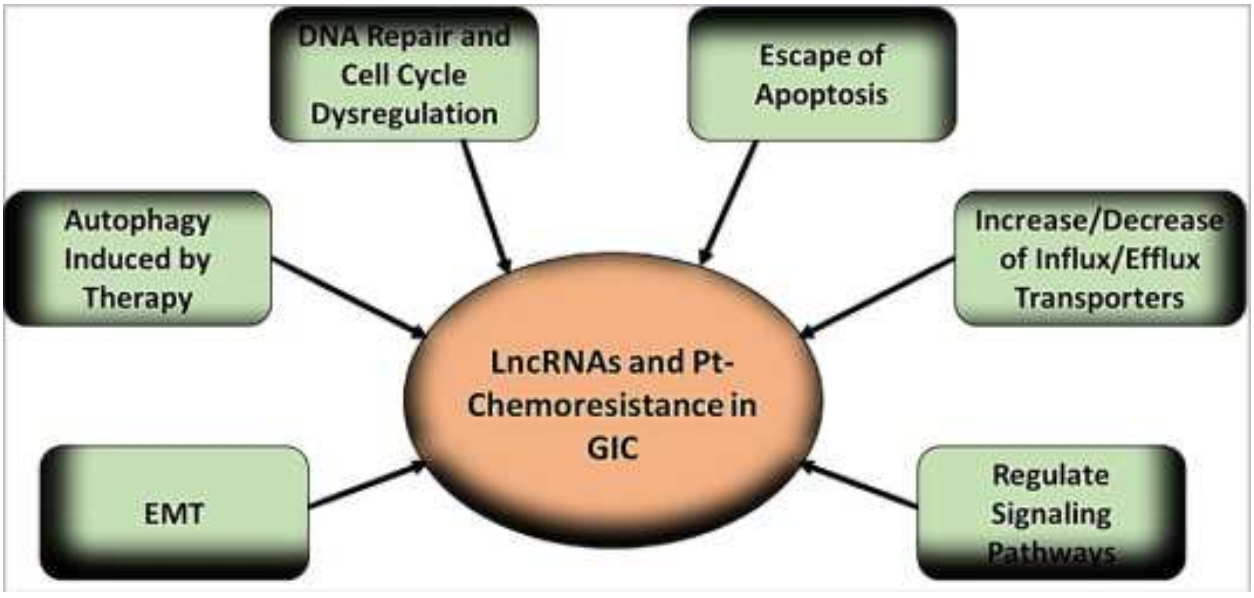

Fig. 2.8. Proposed mechanisms of Pt-chemoresistance in GIC and relationship with dysregulated expression of lncRNAs.

Influx/efflux of Pt drugs. The ABC transporter family regulates the drugs flux across the plasma membrane and its aberrant expression has been associated with chemoresistance [146]. There are 48 genes for ABC transporters in the human genome which are classified into seven subfamilies [147]. In this sense, for instance, lncRNA PVT1 (Plasmacytoma Variant Translocation 1) is an oncogene and has been shown to promote CDDP resistance through increasing the expression of MDR related genes, such us MDR1, MRP, mTOR and HIF-1a in GC cells [148]. Further studies have revealed that ANRIL (antisense noncoding RNA gene at the INK4 locus) knockdown might reverse drug resistance in CDDP-resistant GC cell lines by downregulating MDR-related gene expression, including MDR1 and MRP1 [149].

DNA repair and cell cycle dysregulation. Some lncRNAs contribute to CDDP- resistance via interference in the mechanisms of DNA repair. For example, the loss of lncRNA CRAL (CDDP resistance-associated lncRNA) in GC has been found to inhibit CDDP-induced DNA damage and apoptosis, which would lead to CDDP resistance in GC cells [150]. It has been shown that the level of the γH2AX protein (Phosphorylated histone H2AX) was significantly decreased in the CRAL knockdown GC cells treated with CDDP but increased in the CRAL-overexpressing CDDP-resistant GC.γH2AX and is used as a biomarker of cellular response to DSB (double strand breaks) and thereby, to monitor DNA damage [151].

Some other lncRNAs have been reported to promote CDDP resistance in GIC by regulating transcription factor and protein related to cell cycle progression. The knockdown of the lncRNA CCAT1 (colon cancer-associated transcript 1) combined with CDDP treatment downregulated the expression of cyclin D1 and CDK4 more clearly than CDDP treatment alone, indicating the importance of the CCAT1 expression in CDDP resistance of EC cells [152].

Escape of apoptosis. As CDDP-induced DNA damage causes cell apoptosis, the inhibition of apoptosis may also to be involved in the acquired CDDP resistance. The Bcl-2 family is a key member in mitochondrial apoptosis pathway, which consists of the anti-apoptotic subfamily (such as BCL-2 and BCL-XL), the pro-apoptotic subfamily (BAX and BAK), and the pro-apoptotic BH3-only protein subfamily (such as BAD, BIK) [153]. Several studies have shown that lncRNAs are associated with the CDDP-chemoresistance by regulating Bcl-2 genes in GI cancers. For instance, SNHG5 (Small Nucleolar RNA Host Gene 5) and GHET1 (gastric carcinoma high expressed transcript 1) would promote CDDP resistance in GC through down-regulating BAX and BCL-2 proteins [154], [155]. In addition, various lncRNAs such us UCA1 (urothelial carcinoma associated 1) in GC and OCC or AK022798 in GC, have been associated with CDDP resistance via regulating caspase-3 or caspase-8 [156], [157].

Regulate signaling pathways. Studies over the years have demonstrated that diverse cell signaling pathways are involved in the development of drug resistance [158]. In CRC, as an example, the lncRNA CNRDE (colorectal neoplasia differentially expressed) could promote cell proliferation and chemoresistance to OXA via modulating Wnt/β-catenin signaling [159]. In GC, ZFAS1 (zinc finger antisense 1) and MALAT1 could promote CDDP resistance by activating the Wnt and PI3K/AKT signaling pathway [160], [161]. These Wnt and PI3K-AKT-mTOR signaling pathways are often found to be deregulated in human cancers and are known to contribute to the chemoresistance of cancer cells.

EMT. EMT is a complex and reversible process in which epithelial cells lose their features and gain mesenchymal properties, leading to the cytoskeleton remodeling and contributing to tumor cells migration and metastasis [162]. During the process, epithelial cells lose E-cadherin as an epithelial adhesion molecule and acquire mesenchymal markers such as fibronectin and/or vimentin.

Research findings have revealed that Pt-drug resistance can be, at least partly, caused by EMT [163]. Several EMT-inducing transcription factors, including Snail, Slug, ZEB1 and ZEB2, are well known to be involved in mediating Pt-drug resistance in tumors [164]. Furthermore, there is growing evidence about the role of lncRNAs in regulating those EMT-related signaling pathways and their probable relationship to Pt-drug resistance. For example, the lncRNA PVT1 has been found to be elevated in nearly all GI tumors including GC, EC, OCC and CRC [148], [165], [166]. It has been determined that the increased expression of lncRNA PVT1 conveys in EMT and drug resistance [165], [166].

Autophagy induced by therapy. Autophagy is a highly conserved process in response to environmental stresses such as starvation in which cells start to recycle and degrade macromolecules, including organelles, proteins, carbohydrates, and lipids as an energy supply and for synthesis of vital components [167]. In this process, cellular organelles and components are engulfed by autophagosomes, double-membrane vesicles, for delivery to the lysosome which provides proteases for degradation of autophagosomes contents [168]. The molecular mechanism of autophagy contains several conserved autophagy-related genes (ATGs), such as ATG4, ATG6 (also known as Beclin-1) and ATG12, and LC3 (microtubule-associated protein light chain 3) [169]. Different studies have revealed that autophagy has important roles in development, maintenance, and tumor progression. Recently, autophagy induced by therapy has been shown as a new mechanism of resistance to chemotherapeutic drugs [170]. Several studies have verified that autophagy could act as a protective mechanism against Pt drugs treatment in cancer cells [171]. Notably, increasing evidence has demonstrated that lncRNAs could also promote Pt-drug resistance by regulating signaling pathways related to autophagy. For instance, the lncRNA KCNQ1OT1 (KCNQ1 opposite strand/antisense transcript 1) has been found to generate OXA resistance by up-regulating ATG4B protein and enhancing protective autophagy in CRC [172]. Besides, this lncRNA has also been reported to promote CDDP resistance via

regulating autophagy in OCC [173]. All of these biological mechanisms of resistance can be heavily influenced by aberrant expression of lncRNAs.

2.4.1. Functions contributing to Pt-chemoresistance

The relatively large fraction of administered Pt-chemotherapeutic, then, binds to several intra- and extra-cellular structures. Most notably, highly nucleophilic residues with N- and S-donors are commonly present in cellular macromolecules and metabolites, and due to their electrophilic nature, CDDP and OXA react readily with such functionalities when the surface is exposed on macromolecules. Specific examples of this phenomena include common plasma proteins such as human serum albumin (HSA) and metabolites such as glutathione (GSH). Interaction between Pt-drugs and such functionalities often forms covalent bonds which are not readily broken. Take in account the strong thermodynamic preference of Pt-chemotherapeutics for S-donor ligands and the presence of so many cellular Pt-derivatives in the cytosol, it is hardly surprising that only 1 % of administered CDDP or OXA intercalates with DNA, its intended target. There are countless coordination complexes that may be formed by CDDP or OXA many of which have been well documented [19], [20].

The interactions of CDDP and OXA with cellular RNAs remain one of the most poorly understood interactions of Pt-drugs. Recent research has shown that CDDP is able to inactivate essential RNAs, such as ribosomal, telomeric, and spliceosomal [34]. However, the binding sites and the mechanism of action of CDDP in most RNA molecules remains uncharacterized. A recent study showed that CDDP binds to the 70S ribosome of *T. thermophilus* and it was found that it was able to target the highly conserved mRNA channel and GTPase activating center [34]. This system provides insight beyond its interactions with DNA and shows how CDDP is able to inhibit protein synthesis. It may also explain the efficacy of the Pt-therapeutic despite the low fraction of administered drug.

In studies investigating the potential role of CDDP in inhibiting protein synthesis through binding to ribosomal RNA, it has been found that there is roughly 4–20 fold more Pt accumulation found in the total cellular RNA than total cellular DNA in *S. cerevisiae* [35]. Specifically, the Pt accumulation is observed most with rRNA or total RNA compared to interactions with DNA. Given the recent reports of Pt binding to RNA, it seems reasonable that the mechanism of CDDP action may not simply involve its interactions with DNA to induce cellular apoptosis but involves interactions with RNA. The latter may be particularly prevalent in GIC patients that have developed Pt-chemoresistance. Indeed, the interactions between metal complexes and RNA are so attractive [174] that various forms of RNA can act as “mock” binding sites for metallodrugs, which will serve to decrease available and active drugs from reaching its intended DNA target.

2.5. LncRNAs and Pt-chemoresistance in GIC

In the following sections, Pt-chemoresistance is described in different subgroups of GIC: OCC, EC, GC, and CRC.

2.5.1. LncRNAs and Pt-chemoresistance in OCC

Chemotherapy is an efficient adjuvant treatment for OCC, in particular OSCC, in which the primary treatment strategy is surgery. Though, the progress and development of resistance to Pt-chemotherapeutic drugs hampers the curate effect to a large extent. There have been several lncRNAs associated with CDDP chemoresistance in OSCC, and the observed responses are shown in Table 2.1.

Table 2.1. LncRNAs and CDDP resistance in OCC.

lncRNA	Aberrant expression	CDDP doses	Human Cell lines	Genes and pathways	References
PVT1	+	1–10 μM	SCC9, CAL27 TSCC cell lines	miR-194-5p/HIF1a	[165]

lncRNA	Aberrant expression	CDDP doses	Human Cell lines	Genes and pathways	References
KCNQ1OT1	+	2–10 μM (24 h)	SCC9, CAL27 TSCC cell lines	miR-211-5p/Ezrin/Fak	[175]
	+	2–10 μM (24 h)	SCC9, CAL27 TSCC cell lines	miR-124-3p/TRIM14	[176]
UCA1	+	0,1 – 60 mM (24 h)	SCC9, CAL27 TSCC cell lines	caspase-3, PI3K/Akt	[157]
TUG1	+	0 – 0,1 μg/μl	SCC25, CAL27 TSCC cell lines	miR–133b/CXCR4	[177]
HOXA11-AS	+	0 – 0,1 μg/μl	TSCCA, CAL-27 TSCC cell lines	miR-214-3p/PIM1	[176]
CILA1	+	0 – 0,1 μg/μl	SCC9, CAL27 TSCC cell lines	Wnt/β-catenin	[178]
UCA1	+	0–160 μM (48 h)	Tca8113, TSCCA OSCC cell lines	miR-184/SF1	[157]
lnc-AL355149.1–1	+	0–64 μM (72 h)	HN21B TSCC cell line	n.d	[179]
HOTAIR	–	0 – 0,1 μg/μl	KB, CAL27 cell lines	Autophagy	[180]
lnc-MBL2-4:3	–	0–64 μM (72 h)	HN21B TSCC cell line	n.d	[179]
lnc-IL7R	–	0–64 μM (72 h)	SCC1, SCC4, OSCC3,CAL27 OSCC cell lines	n.d	[181]

*concentrations of CDDP in *in vitro* assays. n.d: not determinate.

As shown in Table 2.1, in most of the observed lncRNAs the aberrant expression is increasing, but a few lnc-MBL2-4:3, HOTAIR and lnc-IL7R, show decreased aberrant expression.

Since CDDP-based chemotherapy has been found to improve the prognosis of patients with OSCC, a well understanding of the molecular mechanisms subjacent the up- or down-regulation of these lncRNAs as a result of Pt-chemotherapy is indispensable and crucial for improving therapeutic outcomes of OSCC patients.

2.5.2. LncRNAs and Pt-chemoresistance in EC

In the last few years, Pt-complexes have gained importance in the clinical treatment of EC [182], [183]. The fundamental mechanisms of drug resistance in EC are not understood but there have been several lncRNAs identified as aberrantly expressed in EC, and there are many lncRNAs such us MALAT1, H19 UCA 1, PVT1 and HOTAIR1 which participate in the development, progression, and chemoresistance of EC [184]. The reported responses in lncRNAs levels in Pt-chemoresistance in EC are shown in Table 2.2**.**

Table 2.2. LncRNAs associated with CDDP resistance in EC.

lncRNA	Aberrant expression	CDDP doses*	Human ESCC cell lines	Genes and pathways	References
TUG1	+	1 μg/ml (48 h)	TE-1	Nrf2, MDR1	[185]
	+	0.1–160 μM (48 h)	ECA109/EC9706	PDCD4/EZH2	[186]
TP73-AS1	+	CDDP	ECA109,EC-1, EC9706, KYSE30, KYSE150	caspase-3	[187]
PCAT1	+	0–20 μM	KYSE30, ECA109	n.d	[188]
FOXD2-AS1	+	CDDP	TE-1	miR-195/Akt/mTOR	[189]
CCAT1	+	0.1–5 μg/ml (48 h)	ECA109, TE-1, KYSE-140, KYSE-70, KYSE-150, KYSE-450	miR-143/PLK1/ BUBR1	[152]

lncRNA	Aberrant expression	CDDP doses*	Human ESCC cell lines	Genes and pathways	References
NMR	+	"0 – 2 μM" (48 h)	KYSE70, KYSE450	NF-κB/ERK pathway	[190]
AFAP1-AS1	+	0.3125–50 μM	KYSE30	n.d	[191]
CASC2	–	5 μM (48 h)	TE-1, EC9706	miR-181a/Akt	[192]
TUSC7	–	0–16 μM (48 h)	EC9706, KYSE30	miR-224/DESC1/EGFR/AKT	[193]

*concentrations of CDDP in *in vitro* assays. n.d: not determinate.

Most of the observed lncRNAs aberrant expression is increasing including TUG1, PCAT1, and CCAT1. However, a few CASC2 and TUSC7 show decreased aberrant expression. The lncRNA TUG1 is also observed to be up-regulated in OCC in addition to EC although the cell signaling pathways involved in its actions are different.

2.5.3. LncRNAs and Pt-chemoresistance in GC

The reported responses in lncRNAs levels in Pt-chemoresistance in GC are shown in Table 2.3.

Table 2.3. LncRNAs associated with CDDP and OXA resistance in GC.

lncRNA	Aberrant expression	Drug doses*	Human GC cell lines	Genes and pathways	References
PVT1	+	1 μg/mL CDDP (24,36,48)	BGC823, SCG7901	MDR1, MRP1, mTOR, HIF-1a	[148]
HOTAIR	+	0–24 μg/mL	SCG7901	miR-126/PI3K/AKT/MRP1,	[194]

lncRNA	Aberrant expression	Drug doses*	Human GC cell lines	Genes and pathways	References
		CDDP (24 h)			
	–	0.004–40 μg/mL CDDP (48 h)	BGC823, SCG7901	miR-34a/PI3K/Akt/Wnt/β-catenin	[141]
UCA1	+	CDDP	SCG7901	miR-27b, Bcl-2, Cleaved caspase-3	[156]
TP73-AS1	+	0–20 μM CDDP (48 h)	BGC823, AGS, GES1	HMGB1	[195]
PCAT1	+	0.1–160 μM (48 h)	SCG7901, BGC223	EZH2, PTEN	[196]
MALAT1	+	CDDP 0–25 μg/mL	SCG7901	miR-23b-3p/ATG12	[160]
	+	0–25 μg/mL CDDP (48 h)	AGS, HGC27	miR-30b/ATG5	[197]
	+	0–256 μM CDDP (24 h)	MGC803	PI3K/AKT	[198]
ANRIL	+	CDDP	BGC823	MDR1, MRP1	[149]
ZFAS1	+	0–40 μM CDDP (96 h)	SCG7901	Wnt/β-catenin, NKD2	[161]
GHET1	+	0.125–16 μg/mL CDDP (48 h)	BGC823, SCG7901	Bax, Bcl-2, MDR1, MRP1	[155]

lncRNA	Aberrant expression	Drug doses*	Human GC cell lines	Genes and pathways	References
BCAR4	+	CDDP	SCG7901	Wnt/β-catenin, Nanog, Klf4 Oct3/4, Sox2, c-Myc	[199]
AK022798	+	10–100 μg/mL (48 h)	SCG7901, BGC223	MRP1, MDR1, Caspase 3/8, Notch1	[200]
DANCR	+	1 μg/mL CDDP (24,36,48, 72 h)	SCG7901, BGC223	MDR1, MRP1	[201]
SNHG5	+	0–25 μg/mL CDDP (48 h) (24,36,48, 72 h)	SCG7901, BGC823 MGC803	Bax, MDR1, MRP1, Bcl-2	[154]
HOTTIP	+	0.01–1000 μM CDDP (48 h)	MGC803, MKN45	miR-218/HMGA1 axis	[202]
	+	CDDP	SCG7901	miR-216a-5p/BCL-2/Beclin1/autophagy	[203]
XLOC_006753	+	2 μg/mL CDDP (48 h)	SCG7901	PI3K/AKT/mTOR	[204]
HOXD-AS1	+	0.1–160 μM CDDP (48 h)	SCG7901, BGC823	EZH2/PDCD4	[205]
FAM84B-AS	+	“Pt drugs”		Apoptosis	[206]
BLACAT1	+	0–60 μM OXA (48 h)	SCG7901, BGC823	ABCB1, MDR1, MRP1, LRP1, miR-361	[207]

lncRNA	Aberrant expression	Drug doses*	Human GC cell lines	Genes and pathways	References
DDX11-AS1	+	0–240 μM OXA (48 h)	MKN45, AGS	miR-326/IRS1	[208]
HULC	–	1 μg/mL CDDP	SCG7901	FoxM1 (autophagy)	[209]
CASC2	–	0–240 μM CDDP (48 h)	SCG7901, BGC823	miR-19a	[210]
CRAL	–	0.4, 0.8 μg/mL CDDP (48 h)	SCG7901, BGC823	miR-505/CYLD/AKT	[150]

*concentrations of CDDP/OXA in *in vitro* assays.

Most of the observed lncRNAs aberrant expression is increasing. Of these, UCA1, PVT1, and PCAT1 show aberrant expression is increasing in other GIC such us OSCC and CRC. A few lncRNAs including HOTAIR, HULC, CASC2, and CRAL show decreased aberrant expression. The lncRNA CASC2 is also observed to decrease in EC in addition to GC, although it involved different genes and different pathways. HOTAIR exhibits a dual behavior in GC cell lines since a low concentration (0.004–40 μg/mL CDDP) are down-regulated in BGC823 and SCG7901 cells.

Nevertheless, after incubation with high concentration (0–24 μg/mL) of CDDP in SCG7901 cells, this lncRNA appears up-regulated. Besides, HOTAIR is down-regulated in OSCC although the cell lines are different and involved different genes and different pathways. Different lncRNAs have been identified to promote tumor growth and chemoresistance in GC. A number of them have been reported to be implicated in resistance to Pt-drugs via regulation of different cell pathways such us mTOR, PTEN, PI3K/AKT, Wnt/β-catenin, among others.

2.5.4. LncRNAs and Pt-chemoresistance in CRC

Currently, Pt-chemotherapeutics, especially OXA, are one of the standard treatments for CRC patients and multiple lncRNAs have been reported to be involved in Pt resistance in CRC. The reported responses in lncRNAs levels in Pt-chemoresistance in CRC are shown in Table 2.4.

Table 2.4. LncRNAs associated with CDDP and OXA resistance in CRC.

LncRNA	Aberrant expression	Drug Doses*	Human CRC cell lines	Genes and pathways	References
PVT1	+	10 μg/mL CDDP (24–96 h)	LoVo, RKO	MDR1, MRP, Bcl-2	[166]
HOTAIR	+	0–3.5 μM CDDP (0–96 h)	Colo205, SW620	miR-203a-3p/Wnt/β-catenin	[211]
KCNQ1OT1	+	0–20 μM OXA (48 h)	HCT116, SW480	mir-34a/ATG4B/ autophagy	[172]
MALAT1	+	0–20 μM OXA (72 h)	HT-29	EZH2	[212]
ANRIL	+	OXA (48 h)	HCT116, SW480	Let-7a/MRP1	[213]
SNHG14	+	CDDP (0,24,48,72 h)	SW480, SW620	miR-186/ATG14/autophagy	[145]
LINC00152	+	0–10 μM OXA (72 h)	SW620, HT29	miR-193a-3p/ERBB4/AKT	[214]
CRNDE	+	0–64 μg/mL OXA (72 h)	SW480, HCT116	miR-181a-5p/Wnt /β-catenin/TCF4	[215]
	+	0–20 μM OXA (48 h)	HCT116	miR-136/E2F1	[216]
CACS15	+	0.01–100 μM OXA (48 h)	HCT116, HT29	miR-145/MRP1 (ABCC1)	[112]
LINC00973	+	2, 20 μM OXA (72 h, 144 h)	HT29, HCT116	n.d	[217]
GIHCG	+	0–60 μg/mL OXA (96 h)	SW480, LoVo	n.d	[218]

LncRNA	Aberrant expression	Drug Doses*	Human CRC cell lines	Genes and pathways	References
LINC00261	–	0–24 μg/mL CDDP (48 h)	SW480	β-catenin/Wnt pathway	[219]
MEG3	–	0–20 μM OXA (72 h)	HT29, SW480	miR-141/PDCD4	[220]

*concentrations of CDDP/OXA in *in vitro* assays. n.d: not determinate.

Most of the observed lncRNAs aberrant expression is increasing. Of these UCA1, PVT1, HOTAIR, MALAT1, and ANRIL show aberrant expression is increasing in other GIC like OSCC and EC. It is important to highlight that MALAT1 is up-regulated in GC in presence of CDDP and the same effects are described in CRC after incubation with OXA suggesting the importance relationship between high expression of MALAT1 and Pt- chemoresistance in GIC. LncRNAs such as HOTAIR show increased aberrant expression in CRC whereas in the aberrant expression levels are decreasing in OCC whilst in GC exhibited a dual behavior depending of concentration of CDDP.

Aberrantly expressed lncRNAs have been suggested to contribute in the development of CRC through regulation of target genes and interaction with nucleic acids and/or secondary structures of proteins [221], [222]. Particularly, dysregulated expression of lncRNAs has been observed to be associated with recurrence, and chemoresistance in CRC.

2.5.5. Comparison of LncRNAs expression in Pt-chemoresistant GIC

The data listed in Table 2.1, Table 2.2, Table 2.3, Table 2.4 were summarized and compared to generate Table 2.5 to demonstrate that aberrant expression of lncRNAs exhibits consistencies in the four different GIC (OSCC, ES, GC and CCR) examined in this work. Considering that different cell lines are expressing these genes and are engaged in different pathways, we pulled the information from Table 2.1, Table 2.2, Table 2.3, Table 2.4 in order to

determine if any lncRNAs are common among the different cancer types and whether the change in gene expressions upon development of Pt-resistance are similar.

Table 2. 5. Aberrant expression of lncRNAs in different GIC related to CDDP and OXA resistance.

LncRNA	OSCC	EC	GC	CCR
PVT-1	+	…	+	+
HOTAIR	–	…	+/-	+
MALAT1	…	…	+	+
KCNQ1OT1	+	…	…	+
ANRIL	…	…	+	+
CASC2	…	–	–	…
PCAT1	…	+	+	…
TP73-AS1	…	+	+	…
UCA1	+	…	+	…
TUG1	+	+	…	…

Although the majority of lncRNAs investigated and listed in Table 2.1, Table 2.2, Table 2.3, Table 2.4 were only observed in one of the four GIC cancers examined, two lncRNAs are observed in three of the four cancers investigated, namely PVT-1 and HOTAIR. PVT-1 is upregulated in all three cancers as expected, and the formation of more PVT-1 lncRNAs would result in more Pt associating with RNA consistent with the general mechanism of Pt-resistance described in this work.

The lncRNA HOTAIR, on the other hand, has increased expression in GC and CCR but decreased expression in OSCC and GC. Expression of HOTAIR shows up and down-regulation depends on type of GIC and the concentration of CDDP used. It controls different genes through sponging and epigenetic mechanisms [223]. This lncRNA favors tumor growth, cell cycle progression, metastasis and it promotes drug and radiation resistance, invasion and migration of

cells, angiogenesis, inflammation, and EMT, while also inhibiting apoptosis by modulating miRNAs. Also, HOTAIR is linked with the immune escape, and oncogenic signaling pathways in several types of cancers [224-226]. For example, HOTAIR modulates CDDP resistance by the modulation of autophagy affecting several proteins like MDR, Beclin-1, and P-glycoprotein (P-gp) expression in endometrial cancer [180]. Also, HOTAIR is up-regulated in CDDP-resistant osteosarcoma tissues and cells. The mechanisms involve an interaction between HOTAIR and MiR-106a-5p and the later downregulation of MiR-106a-5p by HOTAIR [227]. Moreover, HOTAIR increases the migration and proliferation of cervical cancer cells and it facilitates the resistance of these cell lines against CDDP. HOTAIR enhances EMT across the miR-29b/PTEN/PI3K axis in cervical cancer [228].

Down-regulation of CASC2 could be related to Pt-resistance on EC and GC. CASC2 is a lncRNA that has been reported to be downregulated in endometrial and lung cancers as well as the EC, GC, and CRC. This lncRNA has tumor-suppressive actions as the sequestration of oncogenic microRNAs and repression of Wnt/β-catenin signaling [229]. In GC, CASC2 inhibits cell proliferation altering the phosphorylation levels of proteins ERK1/2 and JNK [230]. However, the mechanism by which CASC2 inhibited ERK1/2 and JNK signaling in GC remains unclear. CASC2 expression is meaningly downregulated in CRC tissues and in a series of cancer cell lines (ACO2, SW480, SW620, HCT-116 and HT-29) as compared with non-tumoral tissues and cell lines (CCC-HIE-2 and HER293) [231]. Bioinformatic analysis exposed those three miRNAs (ie, miR-18a/b, miR-4735) contains CASC2-binding sites and the physical interactions between CASC2 and miR-18a were further confirmed. Besides, CASC2 derepresses PIAS3 (a repressor of STAT3 and a target of miR-18a) by sponging miR-18a, which leads to the suppression of genes downstream of STAT3 (eg, c-Myc) [231]. These results showed that CASC2 plays a key role in the carcinogenesis of CRC and may serve as a prognostic biomarker.

The up-regulation of MALAT1 and ANRIL appears in GC and CCR as a possible mechanism of Pt-resistance. However, several other lncRNAs including KCNQ1OT1, PCAT-1, TP73-AS1, UCA-1 and TUGI also are observed in two different cancer types. This would imply that these lncRNAs may be more abundant, and future investigations will document whether they are observed to change gene expression for other cancers.

Due to the absence of specific symptoms at the early stages of GC, most patients are diagnosed at advanced disease stages at which point only poor prognosis generally follow. However, the use of chemotherapy with targeted therapy has prolonged the overall survival and improved patients' life quality and lifespans. The front-line drugs for chemotherapy treatment of GC according to current treatment guidelines include Pt-chemotherapeutics. Nevertheless, as is the case with the other forms of GIC highlighted above, acquired resistance to Pt drugs is a major hurdle to the effective and long-term treatment of GC.

2.6. Conclusions

CDDP and OXA in combination with other drugs are front-line treatments of various GIC, a rapidly growing class of cancers. Due to the metabolism and *in vivo* speciation of CDDP and OXA in addition to the cellular abundance of nucleophilic S- and N-donors, only about 1 % of administered Pt-drug reaches its intended target, cellular DNA. Considering that these Pt-based drugs interact with proteins, metabolites, and RNA in addition to cellular DNA, it has been proposed that the effects of these Pt-drugs is a combination of all the interactions that these drugs engage in, including development of Pt-resistance. It has been proposed that the interactions of CDDP and OXA compounds with RNAs may play a key role in Pt-resistance. However, as we describe in this work, we feel that the possibility that alternative complexes forms should also be considered because Pt-RNA complexes with only one ligand are much less stable compared to the DNA complexes.

In this paper we present a brief overview of the speciation of CDDP and OXA and how these reactions may contribute to some interaction with cellular RNA. Mechanisms for development of Pt-resistance is complex and is likely to involve several proteins, Pt-uptake, and export receptors, TME interaction, epigenetics factors, in addition to mechanisms that may involve RNA. Here we review the response of lncRNAs which are aberrantly expressed in Pt-resistant cell lines of GIC. Since some of the same lncRNAs cause increased expression compared to normal cells, even though different cell lines are tested, varying genes and effected cellular pathways are changed in these different cancers.

PVT-1, MALAT1, and ANRIL appear in GC and CCR as a possible mechanism of Pt-resistance whilst the down-regulation of CASC2 could be related of Pt-resistance on EC and GC. HOTAIR exhibits a dual behavior exhibiting up and down-regulatory effects depending of type GIC and the concentration of CDDP used. Several other LncRNA including KCNQ1OT1, PCAT-1, TP73-AS1, UCA-1, and TUGI are also observed in two different cancer types, so future information obtained testing the presence of these LncRNAs would be of great interest. Indubitably, further understanding of these phenomena will be beneficial to evaluate if these different behaviors can be exploited to begin to develop strategies for use in future therapeutic strategies for GIC patients.

References

[1] Pourhoseingholi, M.A.; Vahedi, M.; Baghestani, A.R. Gastroenterology and Hepatology From Bed to Bench. Asia; an Overview; 2015; Vol. 8.

[2] F. Bray, J. Ferlay, I. Soerjomataram, R.L. Siegel, L.A. Torre, A. Jemal, Global Cancer Statistics 2018, GLOBOCAN estimates of incidence and mortality worldwide for 36 cancers in 185 countries, CA. Cancer J. Clin. (2018) 68, https:// doi.org/10.3322/caac.21492

[3] J. Ferlay, M. Colombet, I. Soerjomataram, C. Mathers, D.M. Parkin, M. Pineros, ˜ Znaor, F. Bray, Estimating the global cancer incidence and mortality in 2018: GLOBOCAN sources and methods, Int. J. Cancer 2019 (2018) 144.

[4] L. Jandorf, Abstract IA18: patient navigation and colorectal cancer screening among African Americans and Latinos, Cancer Epidemiol. Biomarkers Prev. 25 (2016), https://doi.org/10.1158/1538-7755.disp15-ia18.

[5] IARC International Agency for Research in Cancer 2018 .

[6] J. Cheng, M. Cai, X. Shuai, J. Gao, G. Wang, K. Tao, First-line systemic therapy for advanced gastric cancer: a systematic review and network meta-analysis, Ther. Adv. Med. Oncol. 11 (2019).

[7] National Comprehensive Cancer Network. Clinical Practice Guidelines in Oncology. Version 2, 2018.

[8] E.C. Smyth, M. Verheij, W. Allum, D. Cunningham, A. Cervantes, D. Arnold, Gastric cancer: ESMO clinical practice guidelines for diagnosis, treatment and follow-up, Ann. Oncol. 27 (2016), https://doi.org/10.1093/annonc/mdw350.

[9] Japanese Gastric Cancer Association Japanese Gastric Cancer Treatment Guidelines 2018 (5th Edition). Gastric Cancer 2021, 24(1):1-21.

[10] Chinese Society of Clinical Oncology. Chinese Guidelines on the Management of Gastric Cancer . 2018.

[11] S. Rottenberg, C. Disler, P. Perego, The rediscovery of platinum-based cancer therapy, Nat. Rev. Cancer 21 (2021).

[12] K. Kostenkova, D. Althumairy, A. Rajan, U. Kortz, B. Barisas, D.A. Roess, Crans DC polyoxidovanadates [MoVIVV9O28]5- and [H2PtIVVV9O28]5- interact with CHO cell plasma membrane lipids causing aggregation and activation of a G protein-coupled receptor, Front. Chem. Biol. (2023).

[13] N. Samart, D. Althumairy, D. Zhang, D.A. Roess, D.C. Crans, Initiation of a novel mode of membrane signaling: vanadium facilitated signal transduction, Coord. Chem. Rev. 416 (2020). [14] A. Al-Qatati, F.L. Fontes, G. Barisas, D. Zhang, D.A. Roess, D.C. Crans, Raft localization of Type1 fcε receptor and degranulation of RBL-2H3 cells exposed to decavanadate, a structural model for V2O5, Dalt. Trans. 2 (33) (2013) 11912–11920, https://doi.org/10.1039/C3DT50398D.

[15] P.W. Winter, A. Al-Qatati, A.L. Wolf-Ringwall, S. Schoeberl, P.B. Chatterjee, B. G. Barisas, D.A. Roess, D.C. Crans, The anti-diabetic Bis(Maltolato)Oxovanadium (IV) decreases lipid order while increasing insulin receptor localization in membrane microdomains, Dalton Trans. 41 (2012) 6419–6430, https://doi.org/ 10.1039/C2DT30521F.

[16] E.J. Anthony, E.M. Bolitho, H.E. Bridgewater, O.W.L. Carter, J.M. Donnelly, C. Imberti, E.C. Lant, F. Lermyte, R.J. Needham, M. Palau, et al., Metallodrugs are unique: opportunities and challenges of discovery and development, Chem. Sci. 11 (2020) 12888–12917, https://doi.org/10.1039/D0SC04082G.

[17] I. Leon, ´ P. Díez, E. Baran, S. Etcheverry, M. Fuentes, Decoding the anticancer activity of VO-clioquinol compound: the mechanism of action and cell death pathways in human osteosarcoma cells, Metallomics 9 (2017) 891–901, https:// doi.org/10.1039/C7MT00068E.

[18] I.E. Leon, ´ P. Díez, S.B. Etcheverry, M. Fuentes, Deciphering the effect of an oxovanadium(iv) complex with the flavonoid chrysin (VOChrys) on intracellular cell signalling pathways in an osteosarcoma cell line, Metallomics 8 (2016) 739–749, https://doi.org/10.1039/C6MT00045B.
[19] M.C. Ruiz, A. Resasco, A.L. Di Virgilio, M. Ayala, I. Cavaco, S. Cabrera, J. Aleman, I.E. Leon, ´ In vitro and in vivo anticancer effects of two quinoline-platinum(II) complexes on human osteosarcoma models, Cancer Chemother. Pharmacol. 83 (2019) 681–692, https://doi.org/10.1007/S00280-019-03773-X.
[20] M.C. Ruiz, K. Perelmulter, P. Levín, A.I.B. Romo, L. Lemus, M.B. Fogolín, I. E. Leon, ´ A.L. Di Virgilio, Antiproliferative activity of two copper (II) complexes on colorectal cancer cell models: impact on ROS production, apoptosis induction and NF-KB inhibition, Eur. J. Pharm. Sci. 169 (2022), https://doi.org/10.1016/J. EJPS.2021.106092.
[21] L.M. Balsa, P. Quispe, E.J. Baran, M.J. Lavecchia, I.E. Leon, ´ In silico and in vitro analysis of FAK/MMP signaling Axis inhibition by VO-clioquinol in 2D and 3D human osteosarcoma cancer cells, Metallomics 12 (2020) 1931–1940, https:// doi.org/10.1039/d0mt00176g.
[22] L.M. Balsa, V. Ferraresi-Curotto, M.J. Lavecchia, G.A. Echeverría, O.E. Piro, J. García-Tojal, R. Pis-Diez, A.C. Gonzalez-Bar ´ o, ´ I.E. Leon, ´ Anticancer activity of a new copper(II) complex with a hydrazone ligand. Structural and spectroscopic characterization, computational simulations and cell mechanistic studies on 2D and 3D breast cancer cell models, Dalton Trans. 50 (2021) 9812–9826, https:// doi.org/10.1039/D1DT00869B.
[23] L.M. Balsa, M.R. Rodriguez, V. Ferraresi-Curotto, B.S. Parajon-Costa, ´ A. C. Gonzalez-Baro, ´ I.E. Leon, ´ Finding new molecular targets of two copper(II)- hydrazone complexes on triple-negative breast cancer cells using massspectrometry-based quantitative proteomics, Int. J. Mol. Sci. 24 (2023), https:// doi.org/10.3390/IJMS24087531.
[24] M. Kumarakulasingham, P.H. Rooney, S.R. Dundas, C. Telfer, W.T. Melvin, S. Curran, G.I. Murray, Cytochrome P450 profile of colorectal cancer: identification of markers of prognosis, Clin. Cancer Res. 11 (2005), https://doi. org/10.1158/1078-0432.CCR-04-1848.
[25] P.M. Takahara, C.A. Frederick, S.J. Lippard, Crystal structure of the anticancer drug cisplatin bound to duplex DNA, J. Am. Chem. Soc. 118 (1996), https://doi. org/10.1021/ja9625079.
[26] E. Raymond, S. Faivre, J.M. Woynarowski, S.G. Chaney, Oxaliplatin: mechanism of action and antineoplastic activity, Semin. Oncol 25 (1998).
[27] L. Messori, A. Merlino, Cisplatin binding to proteins: a structural perspective, Coord. Chem. Rev. 315 (2016), https://doi.org/10.1016/j.ccr.2016.01.010.
[28] E. Alberti, M. Zampakou, D. Donghi, Covalent and non-covalent binding of metal complexes to RNA, J. Inorg. Biochem. 163 (2016) 278–291, https://doi.org/ 10.1016/J.JINORGBIO.2016.04.021.
[29] A. Kumar Singh, A. Kumar, H. Singh, P. Sonawane, P. Pathak, M. Grishina, J. Pal Yadav, A. Verma, P. Kumar, Metal complexes in cancer treatment: journey so far, Chem. Biodivers. 20 (2023), https://doi.org/10.1002/cbdv.202300061.
[30] L. Cardo, I. Nawroth, P.J. Cail, J.A. McKeating, M.J. Hannon, Metallo supramolecular cylinders inhibit HIV-1 TAR-TAT complex formation and viral replication in cellulo, Sci. Rep. 8 (2018), https://doi.org/10.1038/s41598-018- 31513-3.
[31] F. Arjmand, Z. Afsan, S. Sharma, S. Parveen, I. Yousuf, S. Sartaj, H.R. Siddique, S. Tabassum, Recent advances in metallodrug-like molecules targeting noncoding RNAs in cancer chemotherapy, Coord. Chem. Rev. 387 (2019).
[32] V. Brabec, O. Hrabina, J. Kasparkova, Cytotoxic platinum coordination compounds. DNA binding agents, Coord. Chem. Rev. 351 (2017), https://doi.org/ 10.1016/j.ccr.2017.04.013.

[33] H. Xiao, R. Qi, T. Li, S.G. Awuah, Y. Zheng, W. Wei, X. Kang, H. Song, Y. Wang, Y. Yu, et al., Maximizing synergistic activity when combining RNAi and platinumbased anticancer agents, J. Am. Chem. Soc. 139 (2017), https://doi.org/10.1021/ jacs.6b12108.
[34] S.V. Melnikov, D. Soll, ¨ T.A. Steitz, Y.S. Polikanov, Insights into RNA binding by the anticancer drug cisplatin from the crystal structure of cisplatin-modified ribosome, Nucleic Acids Res. 44 (2016), https://doi.org/10.1093/nar/gkw246.
[35] A.A. Hostetter, M.F. Osborn, V.J. Derose, RNA-pt adducts following cisplatin treatment of saccharomyces cerevisiae, ACS Chem. Biol. 7 (2012) 218–225, https://doi.org/10.1021/CB200279P.
[36] D. Singh, Y.G. Assaraf, R.N. Gacche, Long non-coding RNA mediated drug resistance in breast cancer, Drug Resist. Updat. 63 (2022), https://doi.org/ 10.1016/j.drup.2022.100851.
[37] Z.T. Yao, Y.M. Yang, M.M. Sun, Y. He, L. Liao, K.S. Chen, B. Li, New insights into the interplay between long non-coding RNAs and RNA-binding proteins in cancer, Cancer Commun. 42 (2022), https://doi.org/10.1002/cac2.12254.
[38] X. Zhang, K. Xie, H. Zhou, Y. Wu, C. Li, Y. Liu, Z. Liu, Q. Xu, S. Liu, D. Xiao, et al., Role of non-coding RNAs and RNA modifiers in cancer therapy resistance, Mol. Cancer 19 (2020), https://doi.org/10.1186/s12943-020-01171-z.
[39] L. Norouzi-Barough, M.R. Sarookhani, M. Sharifi, S. Moghbelinejad, S. Jangjoo, R. Salehi, Molecular mechanisms of drug resistance in ovarian cancer, J. Cell. Physiol. 233 (2018), https://doi.org/10.1002/jcp.26289.
[40] T. Nunes, D. Hamdan, C. Leboeuf, M. El Bouchtaoui, G. Gapihan, T.T. Nguyen, S. Meles, E. Angeli, P. Ratajczak, H. Lu, et al., Targeting cancer stem cells to overcome chemoresistance, Int. J. Mol. Sci. 19 (2018), https://doi.org/10.3390/ ijms19124036.
[41] D.P. Gately, S.B. Howell, Cellular accumulation of the anticancer agent cisplatin: a review, Br. J. Cancer 67 (6) (1993) 1171–1176, https://doi.org/10.1038/ bjc.1993.221.
[42] J. Zhou, Y. Kang, L. Chen, H. Wang, J. Liu, S. Zeng, L. Yu, The drug-resistance mechanisms of five platinum-based antitumor agents, Front Pharmacol. 11 (2020), https://doi.org/10.3389/fphar.2020.00343.
[43] Q. Zhu, L. Yu, Z. Qin, L. Chen, H. Hu, X. Zheng, S. Zeng, Regulation of OCT2 transcriptional repression by histone acetylation in renal cell carcinoma, Epigenetics 14 (2019) 791–803, https://doi.org/10.1080/ 15592294.2019.1615354.
[44] T. Ishikawa, F. Ali-Osman, Glutathione-associated cis-diamminedichloroplatinum (II) metabolism and ATP-dependent efflux from leukemia cells. Molecular characterization of glutathione-platinum complex and its biological significance, J. Biol. Chem. 268 (1993) 20116–20125.
[45] S.S. Byun, S.W. Kim, H. Choi, C. Lee, E. Lee, Augmentation of cisplatin sensitivity in cisplatin-resistant human bladder cancer cells by modulating glutathione concentrations and glutathione-related enzyme activities, BJU Int. 95 (2005) 1086–1090, https://doi.org/10.1111/j.1464-410X.2005.05472.x.
[46] T. Kimura, T. Kambe, The functions of metallothionein and ZIP and ZnT transporters: an overview and perspective, Int. J. Mol. Sci. 17 (2016) 336, https://doi.org/10.3390/ijms17030336. [47] B. Tariba, T. Zivkovic, N. Krasnici, V.F. Marijic, M. Erk, M. Gamulin, et al., Serum metallothionein in patients with testicular cancer, Cancer Chemother. Pharmacol. 75 (2015) 813–820, https://doi.org/10.1007/s00280-015-2702-2.
[48] M. Kartalou, J.M. Essigmann, Recognition of cisplatin adducts by cellular proteins, Mutat. Res. 478 (2001) 1–21, https://doi.org/10.1016/s0027-5107(01) 00142-7.
[49] P. Wynne, C. Newton, J.A. Ledermann, A. Olaitan, T.A. Mould, J.A. Hartley, Enhanced repair of DNA interstrand crosslinking in ovarian cancer cells from patients following treatment with platinum-based chemotherapy, Br. J. Cancer 97 (2007) 927–933, https://doi.org/10.1038/sj.bjc.6603973.

[50] A. Sawant, A. Kothandapani, A. Zhitkovich, R.W. Sobol, S.M. Patrick, Role of mismatch repair proteins in the processing of cisplatin interstrand cross-links, DNA Repair (amst.) 35 (2015) 126–136, https://doi.org/10.1016/j. dnarep.2015.10.003.
[51] A. Goodspeed, A. Jean, J.C. Costello, A whole-genome CRISPR screen identifies a role of MSH2 in cisplatin-mediated cell death in muscle-invasive bladder cancer, Eur. Urol. 75 (2019) 242–250, https://doi.org/10.1016/j.eururo.2018.10.040.
[52] G. Yeldag, A. Rice, A. del R. Hern´ andez, Chemoresistance and the selfmaintaining tumor microenvironment, Cancers (Basel) (2018) 10, https://doi. org/10.3390/cancers10120471.
[53] A. Davis, A.V. Tinker, M. Friedlander, “Platinum resistant” ovarian cancer: what is it, who to treat and how to measure benefit? Gynecol. Oncol. (2014) 133, https://doi.org/10.1016/j.ygyno.2014.02.038.
[54] R. Brown, E. Curry, L. Magnani, C.S. Wilhelm-Benartzi, J. Borley, Poised epigenetic states and acquired drug resistance in cancer, Nat. Rev. Cancer (2014) 14, https://doi.org/10.1038/nrc3819.
[55] S. Burdett, J.P. Pignon, J. Tierney, H. Tribodet, L. Stewart, C. Le Pechoux, A. Aup´erin, T. Le Chevalier, R.J. Stephens, R. Arriagada, et al., Adjuvant chemotherapy for resected early-stage non-small cell lung cancer, Cochrane Database Syst. Rev. 2015 (2015), https://doi.org/10.1002/14651858.CD011430.
[56] L. Galluzzi, L. Senovilla, I. Vitale, J. Michels, I. Martins, O. Kepp, M. Castedo, G. Kroemer, Molecular mechanisms of cisplatin resistance, Oncogene (2012) 31, https://doi.org/10.1038/onc.2011.384.
[57] J.J. Chan, H. Tabatabaeian, T.Y. 3’UTR heterogeneity and cancer progression, Trends Cell Biol. 33 (7) (2023) 568–582, https://doi.org/10.1016/j. tcb.2022.10.001.
[58] Y. Wang, Y. Wang, Z. Qin, S. Cai, L. Yu, H. Hu, The role of non-coding RNAs in ABC transporters regulation and their clinical implications of multidrug resistance in cancer, Expert Opin Drug Metab Toxicol. 17 (3) (2021) 291–306, https://doi.org/10.1080/17425255.2021.1887139.
[59] X. Fu, S. Li, M. Jia, B. Xu, L. Yang, R. Ma, H. Cheng, W. Yang, P. Hu, Myogenesis controlled by a long non-coding RNA 1700113A16RIK and Post-transcriptional regulation, Cell Regen. (London, England) 11 (2022), https://doi.org/10.1186/ S13619-022-00114-X.
[60] A. Sadakierska-Chudy, MicroRNAs: diverse mechanisms of action and their potential applications as cancer epi-therapeutics, Biomolecules 10 (2020) 1–21, https://doi.org/10.3390/BIOM10091285.
[61] R.P. Alexander, G. Fang, J. Rozowsky, M. Snyder, M.B. Gerstein, Annotating noncoding regions of the genome, Nat. Rev. Genet. 11 (2010) 559–571.
[62] I.E. Schor, G. Bussotti, M. Male˘s, M. Forneris, R.R. Viales, A.J. Enright, E.E. M. Furlong, Non-coding RNA expression, function, and variation during drosophila embryogenesis, Curr. Biol. 28 (2018) 3547–3561.e9, https://doi.org/ 10.1016/j.cub.2018.09.026.
[63] L. Li, L. Wang, H. Li, X. Han, S. Chen, B. Yang, Z. Hu, H. Zhu, C. Cai, J. Chen, et al., Characterization of LncRNA expression profile and identification of novel LncRNA biomarkers to diagnose coronary artery disease, Atherosclerosis (2018) 275, https://doi.org/10.1016/j.atherosclerosis.2018.06.866.
[64] A. Bhan, P. Deb, N. Shihabeddin, K.I. Ansari, M. Brotto, S.S. Mandal, Histone methylase MLL1 coordinates with HIF and regulate LncRNA HOTAIR expression under hypoxia, Gene 629 (2017) 16–28, https://doi.org/10.1016/j. gene.2017.07.069.
[65] A. Renganathan, E. Felley-Bosco, Long noncoding RNAs in cancer and therapeutic potential, in: Advances in Experimental Medicine and Biology, Springer, New York LLC, 2017, p. 1008.
[66] L.Y.W. Bourguignon, Matrix hyaluronan-CD44 interaction activates MicroRNA and LncRNA signaling associated with chemoresistance, invasion, and tumor progression, Front. Oncol. 9 (2019), https://doi.org/10.3389/fonc.2019.00492.

[67] Y. Rui, M. Hu, P. Wang, C. Zhang, H. Xu, Y. Li, Y. Zhang, J. Gu, Q. Wang, LncRNA HOTTIP mediated DKK1 downregulation confers metastasis and invasion in colorectal cancer cells, Histol. Histopathol. 34 (2019), https://doi.org/10.14670/ HH-18-043.
[68] T. Du, Q. Gao, Y. Zhao, J. Gao, J. Li, L. Wang, P. Li, Y. Wang, L. Du, C. Wang, Long non-coding RNA LINC02474 affects metastasis and apoptosis of colorectal cancer by inhibiting the expression of GZMB, Front Oncol. 11 (2021) 651796, https:// doi.org/10.3389/fonc.2021.651796.
[69] W. Zhang, X. Li, W. Zhang, Y. Lu, W. Lin, L. Yang, Z. Zhang, X. Li, The LncRNA CASC11 promotes colorectal cancer cell proliferation and migration by adsorbing miR-646 and miR-381-3p to upregulate their target RAB11FIP2, Front Oncol. 11 (2021) 657650, https://doi.org/10.3389/fonc.2021.657650.
[70] J. Cao, The functional role of long non-coding RNAs and epigenetics, Biol. Proced. Online 16 (2014).
[71] K. Liu, L. Gao, X. Ma, J.J. Huang, J. Chen, L. Zeng, C.R. Ashby, C. Zou, Z.S. Chen, Long non-coding RNAs regulate drug resistance in cancer, Mol. Cancer (2020) 19, https://doi.org/10.1186/s12943-020-01162-0.
[72] P. Ye, L. Feng, S. Shi, C. Dong, The mechanisms of LncRNA-mediated multidrug resistance and the clinical application prospects of LncRNAs in breast cancer, Cancers 14 (2022) 2101, https://doi.org/10.3390/CANCERS14092101.
[73] T.L. Mao, M.H. Fan, N. Dlamini, C.L. Liu, LncRNA MALAT1 facilitates ovarian cancer progression through promoting chemoresistance and invasiveness in the tumor microenvironment, Int. J. Mol. Sci. 22 (2021), https://doi.org/10.3390/ ijms221910201.
[74] S.C. Gao, M. Di Wu, X.X. Zhang, Y.F. Liu, C.L. Wang, Identification of prognostic melatonin-related LncRNA signature in tumor immune microenvironment and drug resistance for breast cancer, Asian J. Surg. 46 (2023), https://doi.org/ 10.1016/j.asjsur.2023.05.174.
[75] S. Xiang, J. Li, J. Shen, Y. Zhao, X. Wu, M. Li, X. Yang, P.J. Kaboli, F. Du, Y. Zheng, et al., Identification of prognostic genes in the tumor microenvironment of hepatocellular carcinoma, Front. Immunol. 12 (2021), https://doi.org/ 10.3389/fimmu.2021.653836.
[76] C.G. Xu, Y.m.r.y.w.c.w.l., Exosomes mediated transfer of LncRNA UCA1 results in increased tamoxifen resistance in breast cancer cells, Eur. Rev. Med. Pharmacol. Sci. 20 (2016) 4362–4368, https://doi.org/10.12659/msm.900689.
[77] Q. Yang, Y. Chen, R. Guo, Y. Dai, L. Tang, Y. Zhao, X. Wu, M. Li, F. Du, J. Shen, et al., Interaction of NcRNA and epigenetic modifications in gastric cancer: focus on histone modification, Front. Oncol. (2022,) 11, https://doi.org/10.3389/ fonc.2021.822745.
[78] S. Dai, T. Liu, Y.Y. Liu, Y. He, T. Liu, Z. Xu, Z.W. Wang, F. Luo, Long non-coding RNAs in lung cancer: the role in tumor microenvironment, Front Cell Dev Biol. 9 (2022) 795874, https://doi.org/10.3389/fcell.2021.795874.
[79] M. Schwerdtfeger, V. Desiderio, S. Kobold, T. Regad, S. Zappavigna, M. Caraglia, Long non-coding RNAs in cancer stem cells, Transl Oncol. 14 (2021) 101134, https://doi.org/10.1016/j.tranon.2021.101134.
[80] H.-P. Lin, Z. Wang, C. Yang, LncRNA DUXAP10 upregulation and the hedgehog pathway activation are critically involved in chronic cadmium exposure-induced cancer stem cell-like property, Toxicol. Sci. 184 (2021), https://doi.org/10.1093/ toxsci/kfab099.
[81] M.Y. Liu, X.Q. Li, T.H. Gao, Y. Cui, N. Ma, Y. Zhou, G.J. Zhang, Elevated HOTAIR expression associated with cisplatin resistance in non-small cell lung cancer patients, J Thorac Dis. 8 (2016) 3314–3322, https://doi.org/10.21037/ jtd.2016.11.75.
[82] R. Lugano, M. Ramachandran, A. Dimberg, Tumor angiogenesis: causes, consequences, challenges and opportunities, Cell Mol Life Sci. 77 (9) (2020) 1745–1770, https://doi.org/10.1007/s00018-019-03351-7.

[83] Z. Chen, Z. Chen, S. Xu, Q. Zhang, LncRNA SOX2-OT/MIR-30d-5p/PDK1 regulates PD-L1 checkpoint through the mTOR signaling pathway to promote non-small cell lung cancer progression and immune escape, Front Genet. 12 (2021) 674856, https://doi.org/10.3389/fgene.2021.674856.
[84] H. Yang, W. Yang, W. Dai, Y. Ma, G. Zhang, LINC00667 promotes the proliferation, migration, and pathological angiogenesis in non-small cell lung cancer through stabilizing VEGFA by EIF4A3, Cell Biol. Int. 44 (2020) 1671–1680, https://doi.org/10.1002/cbin.11361. [85] S. Ilango, B. Paital, P. Jayachandran, P.R. Padma, R. Nirmaladevi, Epigenetic alterations in cancer, Front. Biosci. (Landmark Ed). 25 (2020) 1058–1109, https://doi.org/10.2741/4847.
[86] D. Li, J. Zhang, J. Li, Role of miRNA sponges in hepatocellular carcinoma, Clin. Chim. Acta Internat. J. Clin. Chem. 500 (2020) 10–19, https://doi.org/10.1016/j.cca.2019.09.013.
[87] L. Zhao, H. Guo, B. Zhou, J. Feng, Y. Li, T. Han, L. Liu, L. Li, S. Zhang, Y. Liu, J. Shi, D. Zheng, Long non-coding RNA SNHG5 suppresses gastric cancer progression by trapping MTA2 in the cytosol, Oncogene. 35 (2016) 5770–5780, https://doi.org/10.1038/onc.2016.110.
[88] Q.J. Deng, L.Q. Xie, H. Li, Overexpressed MALAT1 promotes invasion and metastasis of gastric cancer cells via increasing EGFL7 expression, Life Sci. 157 (2016) 38–44, https://doi.org/10.1016/j.lfs.2016.05.041.
[89] Y.W. Liu, R. Xia, K. Lu, M. Xie, F. Yang, M. Sun, et al., LincRNAFEZF1-AS1 represses P21 expression to promote gastric cancer proliferation through LSD1- mediated H3K4me2 demethylation, Mol Cancer. 16 (2017) 39, https://doi.org/ 10.1186/s12943-017-0588-9.
[90] Z. Ma, X. Gao, Y. Shuai, X. Wu, Y. Yan, X. Xing, et al., EGR1-mediated Linc01503 promotes cell cycle progression and tumorigenesis in gastric cancer, Cell Prolif 54 (2021) 12922, https://doi.org/10.1111/cpr.12922.
[91] Z. Liu, Z. Chen, R. Fan, B. Jiang, X. Chen, Q. Chen, et al., Over-expressed long noncoding RNA HOXA11-AS promotes cell cycle progression and metastasis in gastric cancer, Mol Cancer 16 (2017) 82, https://doi.org/10.1186/s12943-017- 0651-6.
[92] M. Sun, F. Nie, Y. Wang, Z. Zhang, J. Hou, D. He, M. Xie, L. Xu, W. De, Z. Wang, J. Wang, LncRNA HOXA11-AS promotes proliferation and invasion of gastric cancer by scaffolding the chromatin modification factors PRC2, LSD1, and DNMT1, Cancer Res. 76 (2016) 6299–6310, https://doi.org/10.1158/0008-5472.
[93] X. Zhang, W. Wang, W. Zhu, J. Dong, Y. Cheng, Z. Yin, F. Shen, Mechanisms and functions of long non-coding RNAs at multiple regulatory levels, Int J Mol Sci. 20 (2019) 5573, https://doi.org/10.3390/ijms20225573.
[94] T.T. Sun, J. He, Q. Liang, L.L. Ren, T.T. Yan, T.C. Yu, J.Y. Tang, Y.J. Bao, Y. Hu, Y. Lin, D. Sun, Y.X. Chen, J. Hong, H. Chen, W. Zou, J.Y. Fang, LncRNA GClnc1 promotes gastric carcinogenesis and may act as a modular scaffold of WDR5 and KAT2A complexes to specify the histone modification pattern, Cancer Discov. 6 (2016) 784–801, https://doi.org/10.1158/2159-8290.CD-15-0921.
[95] P. Thai, S. Statt, C.H. Chen, E. Liang, C. Campbell, R. Wu, Characterization of a novel long noncoding RNA, SCAL1, induced by cigarette smoke and elevated in lung cancer cell lines, Am J Respir Cell Mol Biol. 49 (2013) 204–211, https://doi.org/10.1165/rcmb.2013-0159RC.
[96] Y. Sun, S.D. Jin, Q. Zhu, L. Han, J. Feng, X.Y. Lu, W. Wang, F. Wang, R.H. Guo, Long non-coding RNA LUCAT1 is associated with poor prognosis in human nonsmall lung cancer and regulates cell proliferation via epigenetically repressing p21 and p57 expression, Oncotarget. 8 (2017) 28297–28311, https://doi.org/ 10.18632/oncotarget.16044.

[97] L. Kelland, The resurgence of platinum-based cancer chemotherapy, Nat. Rev. Cancer 7 (2007) 573–584, https://doi.org/10.1038/nrc2167.
[98] C.A. Rabik, M.E. Dolan, Molecular mechanisms of resistance and toxicity associated with platinating agents, Cancer Treat. Rev. 33 (2007) 9–23, https:// doi.org/10.1016/j.ctrv.2006.09.006.
[99] E. Dudnik, S. Yust-Katz, H. Nechushtan, D.A. Goldstein, A. Zer, D. Flex, T. Siegal, N. Peled, Intracranial response to nivolumab in NSCLC patients with untreated or progressing CNS metastases, Lung Cancer 98 (2016), https://doi.org/10.1016/j. lungcan.2016.05.031.
[100] J. Reedijk, P.H.M. Lohman, Cisplatin: synthesis, antitumour activity and mechanism of action, Pharm. Weekbl. Sci. Ed. (1985) 7.
[101] F. Liu, J. Suryadi, U. Bierbach, Cellular recognition and repair of monofunctionalintercalative platinum-DNA adducts, Chem. Res. Toxicol. 28 (2015), https://doi. org/10.1021/acs.chemrestox.5b00327.
[102] T. Kiss, T. Jakusch, D. Hollender, A. Dornyei, E.A. Enyedy, J.C. Pessoa, H. Sakurai, A. Sanz-Medel, Biospeciation of antidiabetic VO (IV) complexes, Coord. Chem. Rev. 252 (2008) 1153–1162, https://doi.org/10.1016/j.ccr.2007.09.011.
[103] A. Levina, D.C. Crans, P.A. Lay, Speciation of metal drugs, supplements and toxins in media and bodily fluids controls in vitro activities, Coord. Chem. Rev. 352 (2017), https://doi.org/10.1016/j.ccr.2017.01.002.
[104] K.A. Doucette, K.N. Hassell, D.C. Crans, Selective speciation improves efficacy and lowers toxicity of platinum anticancer and vanadium antidiabetic drugs, J. Inorg. Biochem. 165 (2016), https://doi.org/10.1016/j.jinorgbio.2016.09.013.
[105] D.C. Crans, L. Yang, A. Haase, X. Yang, Health benefits of vanadium and its potential as an anticancer agent, Met. Ions Life Sci. 18 (2018).
[106] S. Dilruba, G.V. Kalayda, Platinum-based drugs: past, present and future, Cancer Chemother. Pharmacol. 77 (2016), https://doi.org/10.1007/s00280-016-2976-z.
[107] D.A. Arantseva, E.L. Vodovozova, Platinum-based antitumor drugs and their liposomal formulations in clinical trials, Russ. J. Bioorganic Chem. 44 (2018), https://doi.org/10.1134/S1068162018060031.
[108] M.T. Brands, P.A. Brennan, A.L.M. Verbeek, M.A.W. Merkx, S.M.E. Geurts, Follow-up after curative treatment for Oral squamous cell carcinoma. a critical appraisal of the guidelines and a review of the literature, Eur. J. Surg. Oncol. 44 (2018), https://doi.org/10.1016/j.ejso.2018.01.004.
[109] A. Kolokythas, S. Park, T. Schlieve, K. Pytynia, D. Cox, Squamous cell carcinoma of the Oral tongue: histopathological parameters associated with outcome, Int. J. Oral Maxillofac. Surg. 44 (2015), https://doi.org/10.1016/j.ijom.2015.01.027.
[110] Y. Zhang, Epidemiology of esophageal cancer, World J. Gastroenterol. 19 (2013), https://doi.org/10.3748/wjg.v19.i34.5598.
[111] A.K. Rustgi, H.B. El-Serag, Esophageal carcinoma, N. Engl. J. Med. 371 (2014) 2499–2509, https://doi.org/10.1056/NEJMRA1314530.
[112] R. Gao, C. Fang, J. Xu, H. Tan, P. Li, L. Ma, LncRNA CACS15 contributes to oxaliplatin resistance in colorectal cancer by positively regulating ABCC1 through sponging MiR-145, Arch. Biochem. Biophys. 663 (2019), https://doi.org/ 10.1016/j.abb.2019.01.005.
[113] H. Ashktorab, S.S. Kupfer, H. Brim, J.M. Carethers, Racial disparity in gastrointestinal cancer risk, Gastroenterology 153 (2017).
[114] S. Nagini, Carcinoma of the stomach: a review of epidemiology, pathogenesis, molecular genetics and chemoprevention. world, J Gastrointest. Oncol. 4 (2012), https://doi.org/10.4251/wjgo.v4.i7.156.

[115] E.H. Schreuders, A. Ruco, L. Rabeneck, R.E. Schoen, J.J.Y. Sung, G.P. Young, E. J. Kuipers, Colorectal cancer screening: a global overview of existing programmes, Gut 64 (2015), https://doi.org/10.1136/gutjnl-2014-309086.
[116] R. Glynne-Jones, L. Wyrwicz, E. Tiret, G. Brown, C. Rodel, ¨ A. Cervantes, D. Arnold, Rectal cancer: ESMO clinical practice guidelines for diagnosis, treatment and follow-up, Ann. Oncol. 28 (2017), https://doi.org/10.1093/ annonc/mdx224.
[117] Y. Fang, M.J.R. Fullwood, Functions, and mechanisms of long non-coding RNAs in cancer, Genomics, Proteomics Bioinforma. 14 (2016).
[118] N.D. Eljack, H.Y.M. Ma, J. Drucker, C. Shen, T.W. Hambley, E.J. New, T. Friedrich, R.J. Clarke, Mechanisms of cell uptake and toxicity of the anticancer drug cisplatin, Metallomics 6 (2014), https://doi.org/10.1039/c4mt00238e.
[119] R .A. Alderden, M.D. Hall, T.W. Hambley, The discovery and development of cisplatin, J. Chem. Educ. 83 (2006), https://doi.org/10.1021/ed083p728.
[120] M.A. Fuertes, C. Alonso, J.M. P´erez, Biochemical modulation of cisplatin mechanisms of action: enhancement of antitumor activity and circumvention of drug resistance, Chem. Rev. 103 (2003) 645–662, https://doi.org/10.1021/ cr020010d.
[121] F. Arnesano, G. Natile, Mechanistic insight into the cellular uptake and processing of cisplatin 30 years after its approval by FDA, Coord. Chem. Rev. 253 (2009), https://doi.org/10.1016/j.ccr.2009.01.028.
[122] T. Makovec, Cisplatin and beyond: molecular mechanisms of action and drug resistance development in cancer chemotherapy, Radiol. Oncol. 53 (2019), https://doi.org/10.2478/raon-2019-0018.
[123] W.I. Sundquist, S.J. Lippard, The coordination chemistry of platinum anticancer drugs and related compounds with DNA, Coord. Chem. Rev. 100 (1990) 293–322, https://doi.org/10.1016/0010-8545(90)85013-I.
[124] E. Cvitkovic, Ongoing and unsaid on oxaliplatin: the Hope, Br. J. Cancer 77 (1998), https://doi.org/10.1038/bjc.1998.429.
[125] J.L. Misset, H. Bleiberg, W. Sutherland, M. Bekradda, E. Cvitkovic, Oxaliplatin clinical activity: a review, Crit. Rev. Oncol. Hematol. 35 (2000), https://doi.org/ 10.1016/s1040-8428(00)00070-6.
[126] E. Martinez-Balibrea, A. Martínez-Cardus, A. Gines, V. Ruiz De Porras, C. Moutinho, L. Layos, J.L. Manzano, C. Buges, S. Bystrup, M. Esteller, et al., Tumor-related molecular mechanisms of oxaliplatin resistance, Mol. Cancer Ther. 14 (2015), https://doi.org/10.1158/1535-7163.MCT-14-0636.
[127] S. Mani, M.A. Graham, D.B. Bregman, P. Ivy, S.G.O. Chaney, A review of evolving concepts, Cancer Invest. 20 (2002), https://doi.org/10.1081/cnv-120001152.
[128] G. Sharma, D. Anghore, R. Khare, R.K. Rawal, Oxaliplatin for colorectal cancer therapy: a review, Clin. Cancer Drugs 5 (2018), https://doi.org/10.2174/ 2212697x05666180905094942. [129] Y.S. Kim, S. Shin, M. Cheong, S.S. Hah, Mechanistic insights into in vitro DNA adduction of oxaliplatin, Bull. Korean Chem. Soc. 31 (2010), https://doi.org/ 10.5012/bkcs.2010.31.7.2043. [130] E. Jerremalm, M. Hedeland, I. Wallin, U. Bondesson, H. Ehrsson, Oxaliplatin degradation in the presence of chloride: identification and cytotoxicity of the monochloro monooxalato complex, Pharm. Res. 21 (2004), https://doi.org/ 10.1023/B:PHAM.0000026444.67883.83.
[131] J.M. Woynarowski, S. Faivre, M.C.S. Herzig, B. Arnett, W.G. Chapman, A. V. Trevino, E. Raymond, S.G. Chaney, A. Vaisman, M. Varchenko, et al., Oxaliplatin-induced damage of cellular DNA, Mol. Pharmacol. 58 (2000), https:// doi.org/10.1124/mol.58.5.920.
[132] S.G. Chaney, S.L. Campbell, E. Bassett, Y. Wu, Recognition and processing of cisplatin- and oxaliplatin-DNA adducts, Crit. Rev. Oncol. Hematol. 53 (2005), https://doi.org/10.1016/j.critrevonc.2004.08.008.

[133] E.F. Pettersen, T.D. Goddard, C.C. Huang, G.S. Couch, D.M. Greenblatt, E. C. Meng, T.E. Ferrin, UCSF chimera - a visualization system for exploratory research and analysis, J. Comput. Chem. 25 (2004), https://doi.org/10.1002/ jcc.20084.
[134] Drew, H.R.; Wing, R.M.; Takano, T.; Broka, C.; Tanaka, S.; Itakura, K.; Dickerson, R.E. Structure of a B-DNA Dodecamer: Conformation and Dynamics. Proc. Natl. Acad. Sci. U. S. A. 1981, 78, doi:10.1073/pnas.78.4.2179.
[135] A. P´erez, A. Noy, F. Lankas, F.J. Luque, M. Orozco, The relative flexibility of BDNA and A-RNA duplexes: database analysis, Nucleic Acids Res. 32 (2004), https://doi.org/10.1093/nar/gkh954.
[136] F. Arnesano, M. Losacco, G. Natile, An updated view of cisplatin transport, Eur. J. Inorg. Chem. 2013 (2013), https://doi.org/10.1002/ejic.201300341.
[137] A.A. Hostetter, E.G. Chapman, V.J. DeRose, Rapid cross-linking of an RNA internal loop by the anticancer drug cisplatin, J. Am. Chem. Soc. 131 (2009) 9250–9257, https://doi.org/10.1021/JA809637E.
[138] K. Rijal, C.S. Chow, A new role for cisplatin: probing ribosomal RNA structure, Chem. Commun. (2009), https://doi.org/10.1039/b816633a.
[139] K. Rijal, X. Bao, C.S. Chow, Amino acid-linked platinum(ii) analogues have altered specificity for RNA compared to cisplatin, Chem. Commun. 50 (2014), https://doi.org/10.1039/c3cc49035a.
[140] C. Polonyi, A. Alshiekh, L.A. Sarsam, M. Claus´en, S.K.C. Elmroth, Cisplatininduced duplex dissociation of complementary and destabilized short GGcontaining duplex RNAs, Dalton Trans. 43 (2014) 11941–11949, https://doi.org/ 10.1039/C4DT00213J.
[141] C. Cheng, Y. Qin, Q. Zhi, J. Wang, C. Qin, Knockdown of long non-coding RNA HOTAIR inhibits cisplatin resistance of gastric cancer cells through inhibiting the PI3K/Akt and wnt/β-catenin signaling pathways by up-regulating MiR-34a, Int. J. Biol. Macromol. 107 (2018) 2620–2629, https://doi.org/10.1016/J. IJBIOMAC.2017.10.154.
[142] M. Taheri, M.D. Omrani, S. Ghafouri-Fard, Long non-coding RNA expression in bladder cancer, Biophys. Rev. 10 (2018), https://doi.org/10.1007/s12551-017- 0379-y.
[143] J.K. Dhanoa, R.S. Sethi, R. Verma, J.S. Arora, C.S. Mukhopadhyay, Long noncoding RNA: its evolutionary relics and biological implications in mammals: a review, J Anim. Sci. Technol. 60 (2018), https://doi.org/10.1186/S40781-018- 0183-7.
[144] V.A. Ferretti, I.E. Leon, ´ Long non-coding RNAs in cisplatin resistance in osteosarcoma, Curr. Treat. Options Oncol. 22 (2021).
[145] Y. Han, S. Zhou, X. Wang, E. Mao, L. Huang, SNHG14 stimulates cell autophagy to facilitate cisplatin resistance of colorectal cancer by regulating MiR-186/ATG14 Axis, Biomed. Pharmacother. 121 (2020), https://doi.org/10.1016/j. biopha.2019.109580.
[146] G.L. Beretta, G. Cassinelli, M. Pennati, V. Zuco, L. Gatti, Overcoming ABC transporter-mediated multidrug resistance: the dual role of tyrosine kinase inhibitors as multitargeting agents, Eur J Med Chem. 142 (2017) 271–289, https://doi.org/10.1016/j.ejmech.2017.07.062. [147] Y.L. Sun, A. Patel, P. Kumar, Z.S. Chen, Role of ABC transporters in cancer chemotherapy, Chin J Cancer. 31 (2012) 51–57, https://doi.org/10.5732/ cjc.011.10466.
[148] X.W. Zhang, P. Bu, L. Liu, X.Z. Zhang, J. Li, Overexpression of long non-coding RNA PVT1 in gastric cancer cells promotes the development of multidrug resistance, Biochem. Biophys. Res. Commun. 462 (2015) 227–232, https://doi. org/10.1016/J.BBRC.2015.04.121. [149] W.G. Lan, D.H. Xu, C. Xu, C.L. Ding, F.L. Ning, Y.L. Zhou, L.B. Ma, C.M. Liu, X. Han, Silencing of long non-coding RNA ANRIL inhibits the development of multidrug resistance in gastric cancer cells, Oncol. Rep. 36 (2016), https://doi. org/10.3892/or.2016.4771.
[150] Z. Wang, Q. Wang, G. Xu, N. Meng, X. Huang, Z. Jiang, C. Chen, Y. Zhang, J. Chen, A. Li, et al., The long noncoding RNA CRAL reverses cisplatin resistance via the MiR-

505/CYLD/AKT Axis in human gastric cancer cells, RNA Biol. 17 (2020), https://doi.org/10.1080/15476286.2019.1709296.
[151] V. Valdiglesias, S. Giunta, M. Fenech, M. Neri, S. Bonassi, γH2AX as a marker of DNA double strand breaks and genomic instability in human population studies, Mutat Res. 753 (2013) 24–40, https://doi.org/10.1016/j.mrrev.2013.02.001.
[152] M. Hu, Q. Zhang, X.H. Tian, J.L. Wang, Y.X. Niu, G. Li, LncRNA CCAT1 is a biomarker for the proliferation and drug resistance of esophageal cancer via the MiR-143/PLK1/BUBR1 Axis, Mol. Carcinog. 58 (2019), https://doi.org/10.1002/ mc.23109.
[153] E. Lomonosova, G. Chinnadurai, BH3-only proteins in apoptosis and beyond: an overview, Oncogene. 27 (2008) S2–S, https://doi.org/10.1038/onc.2009.39.
[154] M. Li, Y.Y. Zhang, J. Shang, Y.D. Xu, LncRNA SNHG5 promotes cisplatin resistance in gastric cancer via inhibiting cell apoptosis, Eur. Rev. Med. Pharmacol. Sci. 23 (2019), https://doi.org/10.26355/eurrev_201905_17921.
[155] X. Zhang, P. Bo, L. Liu, X. Zhang, J. Li, Overexpression of long non-coding RNA GHET1 promotes the development of multidrug resistance in gastric cancer cells, Biomed. Pharmacother. 92 (2017), https://doi.org/10.1016/j. biopha.2017.04.111.
[156] Q. Fang, X.Y. Chen, X.T. Zhi, Long non-coding RNA (LncRNA) urothelial carcinoma associated 1 (UCA1) increases multi-drug resistance of gastric cancer via downregulating MiR-27b, Med. Sci. Monit. 22 (2016), https://doi.org/ 10.12659/MSM.900688.
[157] Z. Fang, J. Zhao, W. Xie, Q. Sun, H. Wang, B. Qiao, LncRNA UCA1 promotes proliferation and cisplatin resistance of Oral squamous cell carcinoma by sunppressing MiR-184 expression, Cancer Med. 6 (2017), https://doi.org/ 10.1002/cam4.1253.
[158] M. Wickstrom, ¨ C. Dyberg, J. Milosevic, C. Einvik, R. Calero, B. Sveinbjornsson, ¨ E. Sand´en, A. Darabi, P. Siesjo, ¨ M. Kool, P. Kogner, N. Baryawno, J.I. Johnsen, Wnt/β-catenin pathway regulates MGMT gene expression in cancer and inhibition of wnt signalling prevents chemoresistance, Nat Commun. 6 (2015) 8904, https://doi.org/10.1038/ncomms9904.
[159] P. Han, J.W. Li, B.M. Zhang, et al., The lncRNA CRNDE promotes colorectal cancer cell proliferation and chemoresistance via miR-181a-5p-mediated regulation of wnt/beta-catenin signaling, Mol Cancer. 16 (2017) 9.
[160] H. YiRen, Y. YingCong, Y. Sunwu, L. Keqin, T. Xiaochun, C. Senrui, C. Ende, L. XiZhou, C. Yanfan, Long noncoding RNA MALAT1 regulates autophagy associated chemoresistance via MiR-23b-3p sequestration in gastric cancer, Mol. Cancer 16 (2017), https://doi.org/10.1186/s12943-017-0743-3.
[161] W. Xu, L. He, Y. Li, Y. Tan, F. Zhang, H. Xu, Silencing of LncRNA ZFAS1 inhibits malignancies by blocking wnt/β-catenin signaling in gastric cancer cells, Biosci. Biotechnol. Biochem. 82 (2018) 456–465, https://doi.org/10.1080/ 09168451.2018.1431518.
[162] Y. Huang, W. Hong, X. Wei, The molecular mechanisms and therapeutic strategies of EMT in tumor progression and metastasis, J Hematol Oncol. 15 (2022) 129, https://doi.org/10.1186/s13045-022-01347-8.
[163] X. Duan, M. Luo, J. Li, Z. Shen, K. Xie, Overcoming therapeutic resistance to platinum-based drugs by targeting epithelial-mesenchymal transition, Front Oncol. 12 (2022) 1008027, https://doi.org/10.3389/fonc.2022.1008027.
[164] R. Heery, S.P. Finn, S. Cuffe, S.G. Gray, Long non-coding RNAs: key regulators of epithelial-mesenchymal transition, tumour drug resistance and cancer stem cells, Cancers 9 (2017) 38, https://doi.org/10.3390/cancers9040038.
[165] F. Wang, X. Ji, J. Wang, X. Ma, Y. Yang, J. Zuo, J. Cui, LncRNA PVT1 enhances proliferation and cisplatin resistance via regulating MiR-194-5p/ HIF1a Axis in Oral squamous cell carcinoma, Onco. Targets. Ther. 13 (2020), https://doi.org/ 10.2147/OTT.S232405.

[166] G. Ping, W. Xiong, L. Zhang, Y. Li, Y. Zhang, Y. Zhao, Silencing long noncoding RNA PVT1 inhibits tumorigenesis and cisplatin resistance of colorectal cancer, Am J Transl Res. 10 (2018) 138–149.
[167] S. Liu, S. Yao, H. Yang, et al., Autophagy: regulator of cell death, Cell Death Dis 14 (2023) 648, https://doi.org/10.1038/s41419-023-06154-8.
[168] C.F. Bento, M. Renna, G. Ghislat, C. Puri, A. Ashkenazi, M. Vicinanza, F. M. Menzies, D.C. Rubinsztein, Mammalian autophagy: how does it work? Annu Rev Biochem. 85 (2016) 685–713, https://doi.org/10.1146/annurev-biochem060815-014556.
[169] B. Ravikumar, S. Sarkar, J.E. Davies, M. Futter, M. Garcia-Arencibia, Z.W. GreenThompson, M. Jimenez-Sanchez, V.I. Korolchuk, M. Lichtenberg, S. Luo, D. C. Massey, F.M. Menzies, K. Moreau, U. Narayanan, M. Renna, F.H. Siddiqi, B. R. Underwood, A.R. Winslow, D.C. Rubinsztein, Regulation of mammalian autophagy in physiology and pathophysiology, Physiol Rev. 90 (2010) 1383–1435, https://doi.org/10.1152/physrev.00030.2009.
[170] L. Galluzzi, E.H. Baehrecke, A. Ballabio, P. Boya, J.M. Bravo-San Pedro, F. Cecconi, A.M. Choi, C.T. Chu, P. Codogno, M.I. Colombo, et al., Molecular definitions of autophagy and related processes, EMBO J. 36 (2017) 1811–1836, https://doi.org/10.15252/embj.201796697. [171] M.A. Taylor, B.C. Das, S.K. Ray, Targeting autophagy for combating chemoresistance and radioresistance in glioblastoma, Apoptosis. 23 (2018) 563–575, https://doi.org/10.1007/s10495-018-1480-9.
[172] Y. Li, C. Li, D. Li, L. Yang, J. Jin, B. Zhang, LncRNA KCNQ1OT1 enhances the chemoresistance of oxaliplatin in colon cancer by targeting the MiR-34a/ATG4B pathway, Onco. Targets. Ther. 12 (2019) 2649–2660, https://doi.org/10.2147/ OTT.S188054.
[173] C.Y. Qiao, T.Y. Qiao, H. Jin, L.L. Liu, M.D. Zheng, Z.L. Wang, LncRNA KCNQ1OT1 contributes to the cisplatin resistance of tongue cancer through the KCNQ1OT1/ miR-124-3p/TRIM14 axis, Eur Rev Med Pharmacol Sci. 24 (2020) 200–212, https://doi.org/10.26355/eurrev_202001_19912.
[174] E. Alberti, M. Zampakou, D. Donghi, Covalent and non-covalent binding of metal complexes to RNA, J. Inorg. Biochem. 163 (2016), https://doi.org/10.1016/j. jinorgbio.2016.04.021.
[175] S. Zhang, H. Ma, D. Zhang, S. Xie, W. Wang, Q. Li, Z. Lin, Y. Wang, LncRNA KCNQ1OT1 regulates proliferation and cisplatin resistance in tongue cancer via MIR-211-5p mediated ezrin/fak/src signaling, Cell Death Dis. 9 (2018), https:// doi.org/10.1038/s41419-018-0793-5.
[176] X. Wang, H. Li, J. Shi, Lncrna Hoxa11-as promotes proliferation and cisplatin resistance of Oral squamous cell carcinoma by suppression of Mir-214-3p expression, Biomed Res. Int. 2019 (2019), https://doi.org/10.1155/2019/ 8645153.
[177] K. Zhang, H. Zhou, B. Yan, X. Cao, TUG1/MiR-133b/CXCR4 Axis regulates cisplatin resistance in human tongue squamous cell carcinoma, Cancer Cell Int. 20 (2020), https://doi.org/10.1186/s12935-020-01224-9.
[178] Z. Lin, L. Sun, S. Xie, S. Zhang, S. Fan, Q. Li, W. Chen, G. Pan, W. Wang, B. Weng, Z. Zhang, B. Liu, J. Li, Chemotherapy-induced long non-coding RNA 1 promotes metastasis and chemo-resistance of TSCC via the wnt/β-catenin signaling pathway, Mol Ther. 26 (6) (2018) 1494–1508.
[179] W. Gao, J.Y.W. Chan, T.S. Wong, Long non-coding RNA deregulation in tongue squamous cell carcinoma, Biomed Res. Int. 2014 (2014), https://doi.org/ 10.1155/2014/405860. [180] M.Y. Sun, J.Y. Zhu, C.Y. Zhang, M. Zhang, Y.N. Song, K. Rahman, L.J. Zhang, H. Zhang, Autophagy regulated by LncRNA HOTAIR contributes to the cisplatininduced resistance in endometrial cancer cells, Biotechnol. Lett. 39 (2017), https://doi.org/10.1007/s10529-017-2392-4.

[181] L. Ding, J. Ren, D. Zhang, Y. Li, X. Huang, J. Ji, Q. Hu, H. Wang, Y. Ni, Y. Hou, The TLR3 agonist inhibit drug efflux and sequentially consolidates low-dose cisplatin-based chemoimmunotherapy while reducing side effects, Mol. Cancer Ther. 16 (2017), https://doi.org/10.1158/1535-7163.MCT-16-0454.
[182] J. Chen, T. Su, Y. Lin, B. Wang, J. Li, J. Pan, C. Chen, Intensity-modulated radiotherapy combined with paclitaxel and platinum treatment regimens in locally advanced esophageal squamous cell carcinoma, Clin. Transl. Oncol. 20 (2018), https://doi.org/10.1007/s12094-017-1734-y.
[183] Y. Akiyama, T. Iwaya, F. Endo, T. Chiba, T. Takahara, K. Otsuka, H. Nitta, K. Koeda, M. Mizuno, Y. Kimura, et al., Investigation of operative outcomes of thoracoscopic esophagectomy after triplet chemotherapy with docetaxel, cisplatin, and 5-fluorouracil for advanced esophageal squamous cell carcinoma, Surg. Endosc. 32 (2018), https://doi.org/10.1007/s00464-017-5688-5. [184] C. Yang, K. Chen, Long non-coding RNA in esophageal cancer: a review of research Progress, Pathol. Oncol. Res. 28 (2022), https://doi.org/10.3389/ PORE.2022.1610140.
[185] Z. Zhang, R. Xiong, C. Li, M. Xu, M. Guo, LncRNA TUG1 promotes cisplatin resistance in esophageal squamous cell carcinoma cells by regulating Nrf2, Acta Biochim. Biophys. Sin. (shanghai) 51 (2018), https://doi.org/10.1093/abbs/ gmz069.
[186] C. Xu, Y. Guo, H. Liu, G. Chen, Y. Yan, T. Liu, TUG1 confers cisplatin resistance in esophageal squamous cell carcinoma by epigenetically suppressing PDCD4 expression via EZH2, Cell Biosci. 8 (2018), https://doi.org/10.1186/s13578-018- 0260-0.
[187] W. Zang, T. Wang, Y. Wang, X. Chen, Y. Du, Q. Sun, M. Li, Z. Dong, G. Zhao, Knockdown of long non-coding RNA TP73-AS1 inhibits cell proliferation and V.A. Ferretti et al. Coordination Chemistry Reviews 509 (2024) 215791 17 induces apoptosis in esophageal squamous cell carcinoma, Oncotarget 7 (2016), https://doi.org/10.18632/oncotarget.6963.
[188] Q. Zhen, L.N. Gao, R.F. Wang, W.W. Chu, Y.X. Zhang, X.J. Zhao, B.L. Lv, J.B. Liu, LncRNA PCAT-1 promotes tumour growth and chemoresistance of oesophageal cancer to cisplatin, Cell Biochem. Funct. 36 (2018) 27–33, https://doi.org/ 10.1002/cbf.3314.
[189] H. Liu, J. Zhang, X. Luo, M. Zeng, L. Xu, Q. Zhang, H. Liu, J. Guo, L. Xu, Overexpression of the long noncoding RNA FOXD2-AS1 promotes cisplatin resistance in esophageal squamous cell carcinoma through the MiR-195/Akt/ MTOR Axis, Oncol. Res. 28 (2020), https://doi.org/10.3727/ 096504019X15656904013079.
[190] Y. Li, J. Li, M. Luo, C. Zhou, X. Shi, W. Yang, Z. Lu, Z. Chen, N. Sun, J. He, Novel long noncoding RNA NMR promotes tumor progression via NSUN2 and BPTF in esophageal squamous cell carcinoma, Cancer Lett. 430 (2018), https://doi.org/ 10.1016/j.canlet.2018.05.013. [191] X.L. Zhou, W.W. Wang, W.G. Zhu, C.H. Yu, G.Z. Tao, Q.Q. Wu, Y.Q. Song, P. Pan, Y.S. Tong, High expression of long non-coding RNA AFAP1-AS1 predicts chemoradioresistance and poor prognosis in patients with esophageal squamous cell carcinoma treated with definitive chemoradiotherapy, Mol. Carcinog. 55 (2016), https://doi.org/10.1002/mc.22454.
[192] D. Zhu, Y. Yu, Y. Qi, K. Wu, D. Liu, Y. Yang, C. Zhang, S. Zhao, Long non-coding RNA CASC2 enhances the antitumor activity of cisplatin through suppressing the akt pathway by inhibition of MiR-181a in esophageal squamous cell carcinoma cells, Front. Oncol. 9 (2019), https://doi.org/10.3389/fonc.2019.00350.
[193] Z.W. Chang, Y.X. Jia, W.J. Zhang, L.J. Song, M. Gao, M.J. Li, R.H. Zhao, J. Li, Y. L. Zhong, Q.Z. Sun, et al., LncRNA-TUSC7/MIR-224 affected chemotherapy resistance of esophageal squamous cell carcinoma by competitively regulating DESC1, J. Exp. Clin. Cancer Res. 37 (2018), https://doi.org/10.1186/s13046- 018-0724-4.
[194] J. Yan, Y. Dang, S. Liu, Y. Zhang, G. Zhang, LncRNA HOTAIR promotes cisplatin resistance in gastric cancer by targeting MiR-126 to activate the PI3K/AKT/MRP1 genes, Tumor Biol. 37 (2016), https://doi.org/10.1007/s13277-016-5448-5.

[195] J. Peng, Si-TP73-AS1 suppressed proliferation and increased the chemotherapeutic response of GC cells to cisplatin, Oncol. Lett. 16 (2018) 3706–3714, https://doi.org/10.3892/OL.2018.9107.
[196] H. Li, X. Ma, D. Yang, Z. Suo, R. Dai, C. Liu, PCAT-1 contributes to cisplatin resistance in gastric cancer through epigenetically silencing PTEN via recruiting EZH2, J. Cell. Biochem. 121 (2020), https://doi.org/10.1002/jcb.29370.
[197] Z. Xi, J. Si, J. Nan, LncRNA MALAT1 potentiates autophagy-associated cisplatin resistance by regulating the MicroRNA-30b/Autophagy-related gene 5 Axis in gastric cancer, Int. J. Oncol. 54 (2019) 239–248, https://doi.org/10.3892/ IJO.2018.4609.
[198] Q. Dai, T. Zhang, C. Li, LncRNA MALAT1 regulates the cell proliferation and cisplatin resistance in gastric cancer via PI3K/AKT pathway, Cancer Manag. Res. 12 (2020), https://doi.org/10.2147/CMAR.S243796.
[199] L. Wang, Q. Chunyan, Y. Zhou, Q. He, Y. Ma, Y. Ga, X. Wang, BCAR4 increase cisplatin resistance and predicted poor survival in gastric cancer patients, Eur. Rev. Med. Pharmacol. Sci. (2017) 21.
[200] Q. Hang, R. Sun, C. Jiang, L.Y. Notch, 1 promotes cisplatin-resistant gastric cancer formation by upregulating LncRNA AK022798 expression, Anticancer. Drugs 26 (2015), https://doi.org/10.1097/CAD.0000000000000227.
[201] Y.D. Xu, J. Shang, M. Li, Y.Y. Zhang, LncRNA DANCR accelerates the development of multidrug resistance of gastric cancer, Eur. Rev. Med. Pharmacol. Sci. 23 (2019), https://doi.org/10.26355/eurrev_201904_17554.
[202] J. Wang, B. Lv, Y. Su, X. Wang, J. Bu, L. Yao, Exosome-mediated transfer of LncRNA HOTTIP promotes cisplatin resistance in gastric cancer cells by regulating HMGA1/MiR-218 Axis, Onco. Targets. Ther. 12 (2019) 11325–11338, https://doi.org/10.2147/OTT.S231846.
[203] R. Zhao, X. Zhang, Y. Zhang, Y. Zhang, Y. Yang, Y. Sun, X. Zheng, A. Qu, Y. Umwali, Y. Zhang, HOTTIP predicts poor survival in gastric cancer patients and contributes to cisplatin resistance by sponging MiR-216a-5p, Front. Cell Dev. Biol. 8 (2020), https://doi.org/10.3389/fcell.2020.00348.
[204] L. Zeng, Q. Liao, Z. Zou, Y. Wen, J. Wang, C. Liu, Q. He, N. Weng, J. Zeng, H. Tang, et al., Long non-coding RNA xloc_006753 promotes the development of multidrug resistance in gastric cancer cells through the PI3K/AKT/MTOR signaling pathway, Cell. Physiol. Biochem. 51 (2018) 1221–1236, https://doi. org/10.1159/000495499.
[205] Y. Ye, S. Yang, Y. Han, J. Sun, L. Xv, L. Wu, L. Ming, HOXD-AS1 confers cisplatin resistance in gastric cancer through epigenetically silencing PDCD4 via recruiting EZH2, Open Biol. 9 (2019), https://doi.org/10.1098/rsob190068.
[206] Y. Zhang, Q. Li, S. Yu, C. Zhu, Z. Zhang, H. Cao, J. Xu, Long non-coding RNA FAM84B-AS promotes resistance of gastric cancer to platinum drugs through inhibition of FAM84B expression, Biochem. Biophys. Res. Commun. 509 (2019), https://doi.org/10.1016/j.bbrc.2018.12.177.
[207] X. Wu, Y. Zheng, B. Han, X. Dong, Long noncoding RNA BLACAT1 modulates ABCB1 to promote oxaliplatin resistance of gastric cancer via sponging MiR-361, Biomed. Pharmacother. 99 (2018), https://doi.org/10.1016/j. biopha.2018.01.130.
[208] W. Song, Y. Qian, M.H. Zhang, H. Wang, X. Wen, X.Z. Yang, W.J. Dai, The long non-coding RNA DDX11-AS1 facilitates cell progression and oxaliplatin resistance via regulating MiR-326/IRS1 Axis in gastric cancer, Eur. Rev. Med. Pharmacol. Sci. 24 (2020) 3049–3061, https://doi.org/10.26355/EURREV_202003_20669.
[209] L. Xin, Q. Zhou, Y.W. Yuan, L.Q. Zhou, L. Liu, S.H. Li, C. Liu, METase/LncRNA HULC/FoxM1 reduced cisplatin resistance in gastric cancer by suppressing autophagy, J. Cancer Res. Clin. Oncol. 145 (2019), https://doi.org/10.1007/ s00432-019-03015-w.

[210] Y. Li, S. Lv, H. Ning, K. Li, X. Zhou, H. Xv, H. Wen, Down-regulation of CASC2 contributes to cisplatin resistance in gastric cancer by sponging MiR-19a, Biomed. Pharmacother. 108 (2018), https://doi.org/10.1016/j.biopha.2018.09.181.
[211] Z. Xiao, Z. Qu, Z. Chen, Z. Fang, K. Zhou, Z. Huang, X. Guo, Y. Zhang, LncRNA HOTAIR is a prognostic biomarker for the proliferation and chemoresistance of colorectal cancer via MiR-203a-3p-mediated wnt/ß-catenin signaling pathway, Cell. Physiol. Biochem. 46 (2018), https://doi.org/10.1159/000489110.
[212] P. Li, X. Zhang, H. Wang, L. Wang, T. Liu, L. Du, Y. Yang, C. Wang, MALAT1 is associated with poor response to oxaliplatin-based chemotherapy in colorectal cancer patients and promotes chemoresistance through EZH2, Mol. Cancer Ther. 16 (2017), https://doi.org/10.1158/1535-7163.MCT-16-0591.
[213] Z. Zhang, L. Feng, P. Liu, W. Duan, ANRIL promotes chemoresistance via disturbing expression of ABCC1 by regulating the expression of let-7a in colorectal cancer, Biosci. Rep. 38 (2018), https://doi.org/10.1042/ BSR20180620.
[214] B. Yue, D. Cai, C. Liu, C. Fang, D. Yan, Linc00152 functions as a competing endogenous RNA to confer oxaliplatin resistance and holds prognostic values in colon cancer, Mol. Ther. 24 (2016), https://doi.org/10.1038/mt.2016.180.
[215] Peng Han, Jing-Wen Li, Bo-Miao Zhang, Jia-Chen Lv, Yong-Min Li, Gu Xin-Yue, Yu Zhi-Wei, Yun-He Jia, Xue-Feng Bai, Li Li, Yan-Long Liu, Bin-Bin Cui, et al., The LncRNA CRNDE promotes colorectal cancer cell proliferation and chemoresistance via MiR-181a-5p-mediated regulation of wnt/β-catenin signaling, Mol. Cancer 16 (2017), https://doi.org/10.1186/s12943-017-0583-1.
[216] H. Gao, X. Song, T. Kang, B. Yan, L. Feng, L. Gao, L. Ai, X. Liu, J. Yu, H. Li, Long noncoding RNA CRNDE functions as a competing endogenous RNA to promote metastasis and oxaliplatin resistance by sponging MiR-136 in colorectal cancer, Onco. Targets. Ther. 10 (2017), https://doi.org/10.2147/OTT.S116178.
[217] O.L. Zinovieva, E.N. Grineva, M.M. Prokofjeva, D.S. Karpov, A.O. Zheltukhin, G. S. Krasnov, A.V. Snezhkina, A.V. Kudryavtseva, P.M. Chumakov, T.D. Mashkova, et al., Expression of long non-coding RNA LINC00973 is consistently increased upon treatment of colon cancer cells with different chemotherapeutic drugs, Biochimie 151 (2018), https://doi.org/10.1016/j.biochi.2018.05.021.
[218] X. Jiang, Q. Li, S. Zhang, C. Song, P. Zheng, Long noncoding RNA GIHCG induces cancer progression and chemoresistance and indicates poor prognosis in colorectal cancer, Onco. Targets. Ther. 12 (2019), https://doi.org/10.2147/OTT. S192290.
[219] Z.K. Wang, L. Yang, L.L. Wu, H. Mao, Y.H. Zhou, P.F. Zhang, G.H. Dai, Long noncoding RNA LINC00261 sensitizes human colon cancer cells to cisplatin therapy, Braz. J. Med Biol. Res. 51 (2018), https://doi.org/10.1590/1414-431x20176793.
[220] H. Wang, H. Li, L. Zhang, D. Yang, Overexpression of MEG3 sensitizes colorectal cancer cells to oxaliplatin through regulation of MiR-141/PDCD4 Axis, Biomed. Pharmacother. 106 (2018), https://doi.org/10.1016/j.biopha.2018.07.131.
[221] N. Chen, D. Guo, Q. Xu, M. Yang, D. Wang, M. Peng, Y. Ding, S. Wang, J. Zhou, Long non-coding RNA FEZF1-AS1 facilitates cell proliferation and migration in colorectal carcinoma, Oncotarget 7 (2016), https://doi.org/10.18632/ oncotarget.7168.
[222] Z. Zhang, C. Zhou, Y. Chang, Z. Zhang, Y. Hu, F. Zhang, Y. Lu, L. Zheng, W. Zhang, X. Li, X. Li, Long non-coding RNA CASC11 interacts with HnRNP-K and activates the WNT/B-catenin pathway to promote growth and metastasis in colorectal cancer, Cancer Lett. 376 (1) (2016) 62–73.
[223] C. Zhu, X. Wang, Y. Wang, K. Wang, Functions and underlying mechanisms of LncRNA HOTAIR in cancer chemotherapy resistance, Cell Death Discov. 8 (2022), https://doi.org/10.1038/s41420-022-01174-3.

[224] S. Biswas, B. Feng, S. Chen, J. Liu, E. Aref-Eshghi, J. Gonder, V. Ngo, B. Sadikovic, S. Chakrabarti, The long non-coding RNA HOTAIR is a critical epigenetic mediator of angiogenesis in diabetic retinopathy, Investig. Ophthalmol. Vis. Sci. 62 (2021), https://doi.org/10.1167/IOVS.62.3.20.
[225] Z. Miao, J. Ding, B. Chen, Y. Yang, Y. Chen, HOTAIR overexpression correlated with worse survival in patients with solid tumors, Minerva Med. 107 (2016).
[226] Z. Wei, L. Chen, L. Meng, W. Han, L. Huang, A. Xu, LncRNA HOTAIR promotes the growth and metastasis of gastric cancer by sponging MiR-1277-5p and upregulating COL5A1, Gastric Cancer 23 (2020), https://doi.org/10.1007/ s10120-020-01091-3.
[227] J. Guo, D. Dou, T. Zhang, B. Wang, HOTAIR promotes cisplatin resistance of osteosarcoma cells by regulating cell proliferation, invasion, and apoptosis via MiR-106a-5p/STAT3 Axis, Cell Transplant. 29 (2020), https://doi.org/10.1177/ 0963689720948447.
[228] W. Zhang, Q. Wu, Y. Liu, X. Wang, C. Ma, W. Zhu, LncRNA HOTAIR promotes chemoresistance by facilitating epithelial to mesenchymal transition through MiR-29b/PTEN/PI3K signaling in cervical cancer, Cells Tissues Organs 211 (2022), https://doi.org/10.1159/000519844.
[229] X. Yu, H. Zheng, G. Tse, L. Zhang, W.K.K. Wu, CASC2: an emerging tumoursuppressing long noncoding RNA in human cancers and melanoma, Cell Prolif. 51 (2018).
[230] P. Li, W.J. Xue, Y. Feng, Q.S. Mao, Long non-coding RNA CASC2 suppresses the proliferation of gastric cancer cells by regulating the MAPK signaling pathway, Am. J. Transl. Res. 8 (2016).
[231] G. Huang, X. Wu, S. Li, X. Xu, H. Zhu, X. Chen, The long noncoding RNA CASC2 functions as a competing endogenous RNA by sponging MiR-18a in colorectal cancer, Sci. Rep. 6 (2016), https://doi.org/10.1038/srep26524.

APPENDIX A1: MTT ASSAYS OF VANADIUM(V) SCHIFF BASE COMPLEXES

As described in the body of this work, MTT assays were performed for efficacy studies of the complexes. The figure below displays the images of the colorimetric technique from the laboratory (Fig. A1.1).

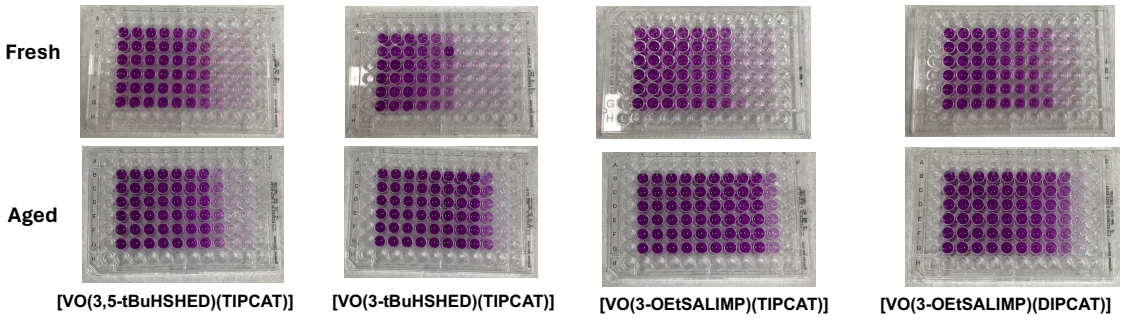

Fig. A1.1. Images of MTT assays for complexes mentioned in the body of this manuscript. The intensity of the purple color relates to the number of viable cells in each well. From these assays, we can gauge an IC_{50} value and obtain a ratio of the aged/fresh complex efficacy.

APPENDIX A2: COMPARISON OF ANTIPROLIFERATIVE ACTIVITIES OF VANADIUM(V) COMPLEXES WITH A COBALT SCHIFF BASE COMPLEX

A project that was worked on in tandem to the work in chapter 1 was to investigate the prospect of using other metals as the core of the Schiff base complexes to observe reactivity in comparison to vanadium-based complexes. The metal chosen for these investigations was cobalt because it is also a first-row transition metal with similar properties as vanadium. Due to difficulties with purification, only one complex was successfully synthesized. This complex, $[Co(MeOHSHED)_2][NO_3]$, was relatively stable in cell media but exhibited very low toxicity (fresh IC_{50}>100μM). The complex is not reported in the main body of this work because it does not contribute significantly to the overarching story, but it is included here because it is a new complex for the purpose of anti-cancer activity. More studies should be conducted with varying Co Schiff bases or Schiff bases with other first row transition metals to fully understand the impact of a different metal on stability and efficacy.

LIST OF ABBREVIATIONS

BBB	Blood-brain barrier
HSHED	N-(salicylideneaminato)-N′-(2-hydroxyethyl)-1,2-ethanediamine
DTB	3,5-di-*tert*-butyl catechol
SALIMP	N-(salicylideneaminato)-2-(2-aminomethylpyridine)
SALIEP	N-(salicylideneaminato)-2-(2-aminoethylpyridine)
TIPCAT	3,4,6-tri-isopropyl catechol
DIPCAT	3,5-di-isporopyl catechol
T98g	Glioblastoma cell lines
TBAP	tetra-*n*-butylammonium perchlorate
ACAC	acetylacetonate
DEA	Diethylamine
DAD	3,5-di-adamantyl catechol
TMS	Tetramethyl silane
tBu	*tert*-butyl
TBU	3-*tert*-butyl catechol
CAT	catechol
DMSO	Dimethyl sulfoxide
MTT	(3-(4,5-dimethylthiazol-2-yl)-2,5-diphenyltetrazolium bromide
ABC, ATP	binding cassette (transporter family)
ADR	adryamicin
AFAP1-AS1	actin filament-associated protein 1 antisense RNA 1
ANRIL	antisense non-coding RNA gene at the INK4 locus
ATGs	autophagy-related genes
BCAR4	breast cancer anti-estrogen resistance 4
BLACAT1	bladder cancer-associated transcript 1
CASC15	lncRNA cancer susceptibility candidate 15
CASC2	cancer susceptibility 2
CCAT1	colon cancer-associated transcript 1
CCND1	cyclin D1
CDDP	cisplatin
CILA1	chemotherapy-induced long non-coding RNA 1
CRAL	cisplatin resistance-associated lncRNAs
CRC	colorectal cancer
CRNDE	Colorectal neoplasia differentially expressed
CXCR4	cysteine-X-cysteine chemokine receptor 4
CYLD	cylindromatosis
DANCR	differentiation antagonizing non-protein coding RNA
DDX11-AS1	long non-coding RNA DDX11 antisense RNA 1
DESC1	differentially expressed in squamous cell carcinoma 1
EC	esophageal cancer
ESCC	esophageal squamous cell carcinoma

EZH2	Enhancer of zeste homolog 2
FAM84B-AS	family with Sequence Similarity 84 Member B- antisense lncRNA
FOXD2-AS1	FOXD2 adjacent opposite strand RNA 1
GC	gastric cancer
GHET1	gastric carcinoma high expressed transcript 1
GIC	gastrointestinal cancer
GIHCG	lncRNA gradually increased during hepatocarcinogenesis
GOF mutant	Gain of function mutant
HIF-1ª	hypoxia-inducible factor 1ª
HMGA1	High-mobility group A1
HOTAIR	HOX transcript antisense intergenic RNA
HOTTIP	HOXA transcript at the distal tip
HOXA11-AS	homeobox A11- HOXA11- antisense RNA
HOXD-AS1	HOXD cluster antisense RNA 1
HULC	highly up-regulated in liver cáncer
IRS1	Insulin receptor substrate 1
KCNQ1OT1	KCNQ1 opposite strand/antisense transcript 1
LINC00261	is a long intergenic non-coding RNA 00261
LINC00973	long intergenic non-coding RNA 00973
Lnc-IL7R	long non-coding interleukin 7 receptor
lncRNAs	long non-coding RNAs
MALAT1	Metastasis associated lung adenocarcinoma transcript 1
MDR	multidrug resistance
MEG3	maternally expressed 3
miRNAs	micro RNAs
MMP	matrix metalloproteases
MMCC	minichromosome maintenance complex component
MRP	multidrug resistance protein
mTOR	mammalian Target of Rapamycin
NF-Kb	Nuclear factor kappa B
NKD2	naked cuticle homolog 2, NKD Inhibitor of WNT Signaling Pathway 2
NMR	NSUN2 methylated lncRNA
Nrf2	nuclear factor (erythroid-derived 2)-like 2
OCC	oral cavity cancer
OSCC	oral squamous cell carcinoma
OXA	oxaliplatin
PCAT1	prostate cancer-associated transcript 1
PDCD4	Programmed Cell Death 4
PLK1	polo-like kinase 1
PRC2	polycomb repressive complex 2
PVT1	Plasmacytoma Variant Translocation 1
P53	tumor suppressor gene
RRM2	ribonucleotide reductase regularotory subunit M2
SF1	splicing factor 1

SMC2	structural maintanance of chromosomes 2
SNHG14	Small nucleolar RNA host gene 14
SNHG5	Small Nucleolar RNA Host Gene 5
TCF4	transcription factor 4
TP73	AS1 lncRNA P73 antisense RNA 1T
TRIM14	tripartite motif-containing 14
TSCC	tongue squamous cell carcinoma
TUG1	taurine up-regulated 1
TUSC 7	tumor suppressor candidate 7
UCA1	urothelial carcinoma associated 1
ZEB1	Zinc finger E-box-binding homeobox 1
ZEB2	Zinc finger E-box-binding homeobox 2
ZFAS1	zinc finger antisense